

# **A USER-FRIENDLY APPROACH FOR MODELING AIR DISPERSION OF CHEMICALS IN INDUSTRIAL FACILITIES**

Prepared by

Stephen G. Zemba, Ph.D. and Steven J. Luis

NIOSH Grant 1 R43 OH03009-01

September 28, 1993

1993 Cambridge Environmental Inc.  
58 Charles St., Cambridge MA 02141  
All rights reserved

  
**Cambridge Environmental Inc**

---

58 Charles Street Cambridge, Massachusetts 02141  
617-225-0810 617-225-0813 FAX



<b>REPORT DOCUMENTATION PAGE</b>	1. REPORT NO.	2.	3. Recipient's Accession No.
4. Title and Subtitle A User-Friendly Approach for Modeling Air Dispersion of Chemicals in Industrial Facilities			5. Report Date 1993/09/28
			6.
7. Author(s) Zemba, S. G., and S. J. Luis			8. Performing Organization Rept. No.
9. Performing Organization Name and Address Cambridge Environmental, Inc., Cambridge, Massachusetts			10. Project/Task/Work Unit No.
			11. Contract (C) or Grant(G) No. (C) (G) R43-OH-03009
12. Sponsoring Organization Name and Address			13. Type of Report & Period Covered
			14.
15. Supplementary Notes			
<p>16. Abstract (Limit: 200 words) Algorithms developed to model airborne concentrations of hazardous chemicals in large indoor spaces in which the pollutants are not uniformly distributed were described. The approach used involved dividing the indoor space being studied into a network of rectangular volumes called parallelepipeds. A volume element modeling the first order differential equation integrating the mass of the pollutant in the volume representative of each parallelepiped was described. The influence of physical processes such as contaminant emission, local air supply and exhaust, and chemical removal due to reaction and deposition was evaluated. Exchange elements specified the rates of air transfer between adjacent volume elements and these elements were used to generate interconnected grids for modeling pollutant dispersion. The authors conclude that this model is useful in determining the causes of indoor air pollution in situations in which adequate ventilation data are available.</p>			
<p>17. Document Analysis a. Descriptors</p> <p>b. Identifiers/Open-Ended Terms NIOSH-Publication, NIOSH-Grant, Grant-Number-R43-OH-03009, End-Date-07-31-1993, Grants-other, Mathematical-models, Indoor-air-pollution, Ventilation-systems, Air-quality, Industrial-environment</p> <p>c. COSATI Field/Group</p>			
18. Availability Statement	19. Security Class (This Report)	21. No. of Pages 138	
	22. Security Class (This Page)	22. Price	



## Contents

List of Abbreviations .....	iv
List of Figures .....	v
List of Tables .....	ix
1 Significant Findings .....	1-1
2 Abstract .....	2-1
3 Introduction .....	3-1
3.1 Background .....	3-1
3.2 Dimensional units .....	3-2
3.3 Organization of the report .....	3-3
4 Theoretical Development .....	4-1
4.1 Well-mixed rectangular volume .....	4-1
4.2 Time-averaging .....	4-4
4.3 Multiple volumes .....	4-5
5 SIMULINK™ Environment .....	5-1
5.1 SIMULINK™: A general description .....	5-1
5.2 SIMULINK™ main library .....	5-2
5.3 Examples of SIMULINK™ elements .....	5-2
5.4 SIMULINK™ elements developed for indoor air modeling .....	5-4
5.4.1 The Volume element .....	5-4
5.4.2 The Exchange element .....	5-7
5.4.3 Emission elements .....	5-10
5.4.3.1 Solvent evaporation from a rectangular tank .....	5-10
5.4.3.2 Volatile organic emission from coil coating operations .....	5-13
5.4.3.3 Vapor release from a ruptured tank .....	5-14
5.4.4 Time-averaging element .....	5-17
5.5 SIMULINK™ simulations .....	5-18
6 Applications .....	6-1
6.1 Illustrative examples .....	6-1
6.1.1 Two-volume example .....	6-1



6.1.2	Eight-volume example	6-4
6.2	Indoor Ozone Modeling	6-7
6.2.1	Physical setting	6-8
6.2.2	Ozone sources and reaction	6-9
6.2.3	SIMULINK™ model of indoor ozone dispersion	6-10
6.2.4	Ozone modeling simulations	6-10
6.2.4.1	Simulation with only an outdoor source	6-11
6.2.4.2	Simulation with both an indoor and outdoor source	6-12
6.3	Hoover Universal case study	6-15
6.3.1	Description of Hoover Universal facility	6-16
6.3.2	Model formulation	6-17
6.3.3	Estimation of TDI emission rates	6-18
6.3.4	Analysis of measured concentrations of TDI in air	6-20
6.3.5	Modeling simulation for the Hoover Universal case study	6-21
6.3.6	Implications of the Hoover Universal modeling application	6-22
7	Conclusions and Recommendations for Further Development	7-1
8	References	8-1
Appendix A: NIOSH Measurements of 2,4- and 2,6-Toluene diisocyanate (TDI)		A-1

Acknowledgments

Present and Future Publications

## List of Abbreviations

<u>Abbreviation</u>	<u>Meaning</u>
atm	atmosphere(s)
cfm	cubic feet per minute
Conc.	concentration
EPA	Environmental Protection Agency
fpm	feet per minute
ft, ft <sup>2</sup> , ft <sup>3</sup>	foot(feet), square feet, and cubic feet, respectively
g	gram(s)
gal	gallon(s)
hr	hour(s)
in	inch(es)
K	degree(s) Kelvin
kcal	kilocalorie(s)
kg	kilogram(s)
lb	pound(s)
m, m <sup>2</sup> , m <sup>3</sup>	meter(s), square meters, and cubic meters, respectively
mg	milligrams
min	minute(s)
NIOSH	National Institute of Occupational Safety and Health
Pa	Pascals
ppb	parts per billion
s	second(s)
Std. Dev.	standard deviation
TDI	toluene diisocyanate
U.S.	United States



## List of Figures

Figure 4.1	Well-mixed rectangular volume. . . . .	4-9
Figure 4.2	Pollutant concentration predicted by Equation (4.4) for $C_0 = 0$ . . . . .	4-10
Figure 4.3	Pollutant concentration predicted by Equation (4.5) for $C_0 = 0.5 \text{ g/m}^3$ . . . . .	4-11
Figure 4.4	Pollutant concentration predicted by Equation (4.4) for $C_0 = 0.5 \text{ g/m}^3$ . . . . .	4-12
Figure 4.5	Periodic emission function in which pollutant emissions are on and off for alternating one-hour periods . . . . .	4-13
Figure 4.6	Time-dependent pollutant concentration profile that results from periodic emissions (Figure 4.5) with constant ventilation and initial concentration $C_0 = 0$ . . . . .	4-14
Figure 4.7	Time-averaged concentration [Equation (4.7), (dashed curve)] compared with the instantaneous solution [Equation (4.4) (solid curve)], $C_0 = 0$ . . . . .	4-15
Figure 4.8	Comparison of time-averaged [Equation (4.7), (dashed curve)] and instantaneous concentrations [Equation (4.4), (solid curve)], $C_0 = 0.5 \text{ g/m}^3$ . . . . .	4-16
Figure 4.9	Comparison of time-averaged [Equation (4.8), (dashed curve)] and instantaneous solutions [Equation (4.5) (solid curve)], $C_0 = 0.5 \text{ g/m}^3$ . . . . .	4-17
Figure 4.10	Schematic of a two-volume system with direct and constant flow-through ventilation $Q$ , emission in Volume 1, and no emission in Volume 2 . . . . .	4-18
Figure 4.11	Air pollutant concentrations in Volumes 1 (solid) and 2 (dashed) predicted by Equations (4.13) and (4.14), respectively . . . . .	4-19
Figure 5.1	SIMULINK™ elements used in the analyses . . . . .	5-19
Figure 5.2	SIMULINK™ elements developed for indoor air modeling applications . . . . .	5-20
Figure 5.3	Block diagram for the Volume element . . . . .	5-21
Figure 5.4	Conventions used to connect two Volume elements with an Exchange element . . . . .	5-22
Figure 5.5	Block diagram for the Exchange element . . . . .	5-23
Figure 5.6	Examples of the calculation of volume flux rates for use in Exchange elements . . . . .	5-24
Figure 5.7	Emissions from a rectangular tank . . . . .	5-25
Figure 5.8	Emissions from a coil-coating operation . . . . .	5-26
Figure 5.9	Example of the simultaneous use of a lookup table and default override option as implemented in the Coil coating Emission element . . . . .	5-27
Figure 5.10	Vapor release from a ruptured tank . . . . .	5-28
Figure 5.11	Time-averaging element . . . . .	5-29
Figure 6.1	Volume element for Volume 1 of the two-volume example (see Figure 4.10 for a schematic of the two-volume system) . . . . .	6-31
Figure 6.2	Exchange element connecting Volumes 1 and 2 of the two-volume example (see Figure 4.10 for a schematic of the two-volume system) . . . . .	6-32
Figure 6.3	Volume element for Volume 2 of the two-volume example (see Figure 4.10 for a schematic of the two-volume system) . . . . .	6-33

Figure 6.4	SIMULINK™ block diagram of the two-volume example . . . . .	6-34
Figure 6.5	Pollutant concentrations in Volumes 1 and 2. Solid, dotted, dashed, and dash-dotted lines indicate concentrations in Volume 1 (instantaneous), Volume 1 (time-averaged), Volume 2 (instantaneous), and Volume 2 (time-averaged), respectively. . . . .	6-35
Figure 6.6	Periodic emission element with constant emission for one-hour in a two-hour cycle. This element, when reduced to icon form, is substituted into the Volume 1 element (shown in Figure 6.1). . . . .	6-36
Figure 6.7	Concentrations under periodic emissions (Time On:Time Off = 1:1). Solid, dotted, dashed, and dash-dotted lines indicate the concentrations in Volume 1 (instantaneous), Volume 1 (time-averaged), Volume 2 (instantaneous), and Volume 2 (time-averaged). . . . .	6-37
Figure 6.8	Periodic emission element with constant emission of one-hour in a six-hour period. This element, when reduced to icon form, is substituted into the Volume 1 element (shown in Figure 6.1). . . . .	6-38
Figure 6.9	Concentrations under periodic emissions (Time On:Time Off = 1:4). Solid, dotted, dashed, and dash-dotted lines indicate the concentrations in Volume 1 (instantaneous), Volume 1 (time-averaged), Volume 2 (instantaneous), and Volume 2 (time-averaged). . . . .	6-39
Figure 6.10	Topological diagram of a two-dimensional eight-volume system. . . . .	6-40
Figure 6.11	Two-dimensional air flow streamlines obtained from potential flow theory. Air is assumed to enter the room in Volumes 1, 3, 5, and 8, and exit the room from Volumes 6 and 7. . . . .	6-41
Figure 6.12	Cross-boundary air fluxes derived from integration of the streamlines shown in Figure 6.11. . . . .	6-42
Figure 6.13	SIMULINK™ block diagram representation of the eight-volume system. The numbering and connection of Volume elements is consistent with Figure 6.10. . . . .	6-43
Figure 6.14	Modeled air pollutant concentrations in Volumes 1, 2, 3, 4 of the eight-volume example; Volume 1 line is solid, Volume 2 is dashed, Volume 3 is dotted, Volume 4 is dash-dot. . . . .	6-44
Figure 6.15	Modeled air pollutant concentrations in Volumes 5, 6, 7, 8 of the eight-volume example; Volume 5 line is solid, Volume 6 is dashed, Volume 7 is dotted, Volume 8 is dash-dot. . . . .	6-45
Figure 6.16	Schematic of room (overhead view) showing the locations of a photocopier (ozone source), an air supply, air exhaust to the outdoors, and the subdivisions used for modeling . . . . .	6-46
Figure 6.17	SIMULINK™ diagram of the ozone model application . . . . .	6-47
Figure 6.18	Block diagram of Volume 1 that houses the photocopier emission element . .	6-48

Figure 6.19	Simulation of ozone concentrations ( $\mu\text{g}/\text{m}^3$ ) as a function of time with no indoor source of ozone generation. Outdoor air containing $200 \mu\text{g}/\text{m}^3$ of ozone enters the room, which is free of ozone initially, in Volume 3. Time-dependent ozone concentrations in Volumes 1, 2, 3, and 4 are represented by the solid, dotted, dashed, and dash-dotted curves, respectively. . . . .	6-49
Figure 6.20	Simulation of time-averaged ozone concentrations ( $\mu\text{g}/\text{m}^3$ ) as a function of time with no internal source of ozone generation. Curves depict time-averages of the concentration profiles of Figure 6.19. Time-averaged ozone concentrations in Volumes 1, 2, 3, and 4 are represented by the solid, dotted, dashed, and dash-dotted curves, respectively. . . . .	6-50
Figure 6.21	Photocopier emission element that produces step function output as a function of time . . . . .	6-51
Figure 6.22	Emission rate of ozone (g/hr) from copier operation over the two-hour simulation period. The lower (dashed) and upper (solid) profiles model average ( $259 \mu\text{g}/\text{min}$ ) and maximum ( $1350 \mu\text{g}/\text{min}$ ) rates, respectively. . . . .	6-52
Figure 6.23	Simulation of ozone concentrations ( $\mu\text{g}/\text{m}^3$ ) as a function of time with both internal and external sources. Outdoor air containing $200 \mu\text{g}/\text{m}^3$ of ozone enters the room, which is free of ozone initially, in Volume 3, and ozone is also emitted in Volume 1 by a copier at the assumed average rate of $259 \mu\text{g}/\text{min}$ . Time-dependent ozone concentrations in Volumes 1, 2, 3, and 4 are represented by the solid, dotted, dashed, and dash-dotted curves, respectively. . . . .	6-53
Figure 6.24	Time-averaged ozone concentrations ( $\mu\text{g}/\text{m}^3$ ) as a function of time with both internal and external sources. Time-averages are constructed from the time-dependent profiles depicted in Figure 6.23. Time-dependent ozone concentrations in Volumes 1, 2, 3, and 4 are represented by the solid, dotted, dashed, and dash-dotted curves, respectively. . . . .	6-54
Figure 6.25	Simulation of ozone concentrations ( $\mu\text{g}/\text{m}^3$ ) as a function of time with both internal and external sources. Outdoor air containing $200 \mu\text{g}/\text{m}^3$ of ozone enters the room, which is free of ozone initially, in Volume 3, and ozone is also emitted in Volume 1 by a copier at the assumed maximum rate of $1350 \mu\text{g}/\text{min}$ . Time-dependent ozone concentrations in Volumes 1, 2, 3, and 4 are represented by the solid, dotted, dashed, and dash-dotted curves, respectively. . . . .	6-55
Figure 6.26	Time-averaged ozone concentrations ( $\mu\text{g}/\text{m}^3$ ) as a function of time with both internal and external sources. Time-averages are constructed from the time-dependent profiles depicted in Figure 6.26. Time-dependent ozone concentrations in Volumes 1, 2, 3, and 4 are represented by the solid, dotted, dashed, and dash-dotted curves, respectively. . . . .	6-56
Figure 6.27	Floor plan of the Hoover Universal Plant. Adapted from Boeniger (1986). . .	6-57

Figure 6.28	Control volumes used to model the Hoover Universal Plant . . . . .	6-58
Figure 6.29	SIMULINK™ block diagram model of the Hoover Universal Plant. Volume numbers correspond to the control volumes in Figure 6.28. . . . .	6-59
Figure 6.30	Simulation of TDI concentrations in air ( $\mu\text{g}/\text{m}^3$ ) as a function of time in Volume elements 1, 2, 2a, 3, and 4. The TDI concentration is assumed to be zero in each Volume at the beginning of the simulation. Time-dependent concentration profiles in Volumes 1, 2, and 4 are represented by the solid, dashed, and dash-dotted curves, respectively. The modeled concentrations for Volumes 2a and 3 are zero over the entire simulation. . . . .	6-60
Figure 6.31	Simulation of TDI concentrations in air ( $\mu\text{g}/\text{m}^3$ ) as a function of time in Volume elements 5, 6, 7, and 8. The TDI concentration is assumed to be zero in each Volume at the beginning of the simulation. Time-dependent concentration profiles in Volumes 5, 6, 7, and 8 are represented by the solid, dashed, dotted, and dash-dotted curves, respectively. . . . .	6-61
Figure 6.32	Simulation of TDI concentrations in air ( $\mu\text{g}/\text{m}^3$ ) as a function of time in Volume elements 9, 10, and 11. The TDI concentration is assumed to be zero in each Volume at the beginning of the simulation. Time-dependent concentration profiles in Volumes 9, 10, and 11 are represented by the solid, dashed, and dotted curves, respectively. . . . .	6-62
Figure 6.33	Comparison of instantaneous (solid curve) and time-averaged (dashed curve) concentration profiles predicted for Volume 5 of the Hoover Universal application. . . . .	6-63

## List of Tables

Table 6.1	Steady-state concentrations for the indoor ozone demonstration problem . . .	6-15
Table 6.2	Air flow and emission rate coefficients assumed for the eight-volume example . . . . .	6-23
Table 6.3	Dimensions of SIMULINK™ control volumes . . . . .	6-24
Table 6.4	Allocation of ventilation airflows of general ventilation system to SIMULINK™ elements . . . . .	6-25
Table 6.5	Velocities, cross-sectional areas, and air fluxes across control volume boundaries for the Hoover Universal case study . . . . .	6-26
Table 6.6	Summary of NIOSH air sampling data used . . . . .	6-27
Table 6.7	Statistical summary of NIOSH data used in the study . . . . .	6-29
Table 6.8	Measured and predicted air concentrations for Hoover Universal case study . . . . .	6-30
Table A.1	Measurements of 2,4- and 2,6-Toluene Diisocyanate [from Boeniger (1986)] . . . . .	A-2



## 1 Significant Findings

The approaches developed herein demonstrate a methodology to model air pollutant dispersion in indoor environments in which pollutant concentrations are subject to spatial and/or temporal variability. Estimates of pollutant concentrations can then be used to derive estimates of exposure to airborne contaminants. Specific types of problems to which the modeling techniques can be applied include:

- **Estimation of pollutant concentrations in industrial facilities**  
Typical indoor air models assume that pollutants are uniformly distributed throughout entire rooms. Many industrial facilities, however, contain large, open floorplans in which pollutant concentrations may vary considerably. The indoor air modeling elements developed in this research can be used to divide an air space into an arbitrary number of volumes. Sources of pollutant emissions may be placed within one or more volumes, and the volumes are connected by the specification of air flow and ventilation data. A simulation of pollutant dispersion can then be used to investigate (1) differences in pollutant concentrations among volumes (spatial variability) and (2) changes in pollutant concentrations with time (temporal variability).
- **Retrospective modeling of industrial hygiene studies**  
Direct measurements have been the traditional approach to the investigation of air pollutant hazards in the workplace. Although modeling should not and cannot supplant measurements, it can provide insight in some cases. The retrospective modeling of industrial hygiene surveys is an area in which the indoor air modeling algorithms can be applied to existing data to investigate the basic factors responsible for pollutant dispersion. An example of such an application is detailed in the body of this report. Similar applications may be of assistance to epidemiological investigations.
- **Evaluation of ventilation strategies**  
Given knowledge of the performance of various ventilation strategies and their effect on air flow patterns in enclosures, the indoor air dispersion algorithms can be applied to test the effectiveness of ventilation strategies in dispersing contaminants. Such evaluations can suggest areas in which pollutant emissions should be reduced or additional controls should be added. Also, the model predictions can be used to identify uncertainties that may require further empirical investigation.
- **Integration into basic research projects**  
Even at a basic level, many indoor air dispersion problems rapidly become complex, such that a complete understanding of contaminant movement may demand prohibitively detailed measurements. In some cases, however, it may be possible and advantageous

to combine the elemental modeling techniques with limited measurements to investigate the basic features that govern pollutant dispersion.



## 2 Abstract

→ Current indoor air pollution models typically assume that contaminants are mixed throughout individual rooms. In general, this assumption is valid only if air movement is sufficient to disperse the pollutant. In this research, algorithms have been developed to model airborne concentrations of hazardous chemicals in large indoor spaces in which pollutants are not uniformly distributed. SIMULINK™, a user-friendly software package for simulating dynamic systems, has been applied to simulate indoor air dispersion of contaminants. The modeling approach consists of dividing the indoor space into an interconnected network of rectangular volumes (parallelepipeds). Each parallelepiped is represented by a volume element, which models the first-order differential equation that integrates the mass of the pollutant contained in the volume. A variety of physical processes are included that influence the concentrations of pollutants in each volume, including contaminant emission, local air supply and exhaust, and chemical removal due to reaction and deposition. The output of the volume element is the concentration (mass divided by volume) of the pollutant, and inputs are the concentrations and airflows that are exchanged with adjacent volumes. Exchange elements are used to specify the rates of air transfer between adjacent volume elements. Volume and exchange elements can be used to generate interconnected grids to model pollutant dispersion. In addition, emission elements that model the generation and release of a pollutant may be placed within volume elements. Development and application of volume, exchange, and emission elements are detailed in the body of the report. The element techniques are best applied to problems in which ventilation data are adequate to characterize air flow patterns within the indoor environment. In such situations, the modeling approach can be useful in assessing the causes of indoor air pollution in industrial facilities, as an aid to the design of ventilation systems designed to reduce the levels of pollutants in indoor settings, and other applications in which information is desired concerning the distribution of a pollutant in an enclosed space. We emphasize, however, that this and all modeling approaches are constrained by uncertainties and the quality/representativeness of input data, and as a general rule should not be used to supplant direct measurements of indoor air quality.



### 3 Introduction

This report describes a research effort entitled *Air Dispersion of Chemicals in Industrial Facilities*, which has been funded by the U.S. Department of Health and Human Services under the Small Business Innovative Research Program (NIOSH Grant 1 R43 OH03009-01). The ultimate goal of the research study is to develop user-friendly software algorithms to model air pollutant dispersion in large indoor spaces in which contaminants are unevenly distributed. Such models could be used in conjunction with monitoring programs to identify potential workplace hazards and to facilitate the design of control systems that minimize worker exposure to hazardous chemicals.

The objective of this Phase I study is to identify, develop, and demonstrate interactive software algorithms that model the concentrations of air pollutants in indoor settings. Software requirements included flexibility, ease of application, and the ability to incorporate relevant physical processes such as chemical reactions. Further development (if undertaken) will incorporate and expand the research to produce a general purpose algorithm to predict air pollutant concentrations in large indoor spaces.

#### 3.1 Background

Theory of the fate and transport of airborne contaminants in well-mixed indoor settings is well-developed, since many important processes are first order and are amenable to relatively simple mathematical modeling. In many manufacturing settings, however, the air spaces of interest are large and the distribution of contaminants can vary greatly depending upon the layout of the building, the locations at which pollutants are released or generated, the effectiveness of ventilation, and other factors that influence contaminant movement.

This report describes an approach to modeling the fate and transport of air contaminants in large indoor air spaces such as those frequently found in industrial settings in which the transport and dispersion of contaminants can be complex. The approach circumvents the limiting assumption of homogeneous mixing throughout the entire space by breaking the air space into smaller volumes, each of which itself is well-mixed, and considers the relationships and interactions between volumes.

Two processes dominate the dispersion of contaminants. The first, advection-driven transport, results from the bulk transport of contaminants by large-scale movement of the transporting media such as water or air. The second, dispersion-driven transport, results from molecular diffusion of contaminants due to concentration gradients and mechanical dispersion due to small-scale variations (turbulence) in the large-scale advective flowfield.

These two processes are described mathematically by the advection-diffusion equation. A key element to the evaluation of the advection-diffusion equation is the advective flowfield, which for unrestricted fluid flow is described by the Navier-Stokes equation. Strictly, the advection-diffusion equation is linked to the Navier-Stokes equation, since the fluid flow can be influenced by density gradients induced by heterogeneous contaminant distributions. Simultaneous solution of the two equations is difficult, if not impossible, in most cases. Typically, however, differences in fluid density are small, and the equations can be treated as uncoupled. In this case, the advective velocities needed in the advection-diffusion equation may be determined by solving the Navier-Stokes equation independently. Nonlinearity and limitations on the treatment of turbulence, however, make even the solution of the Navier-Stokes equation impractical in most cases.

Due to the limited scope of the Phase I study, limitations on the ability to predict advective flow fields are not addressed herein. Rather, the air flow patterns that drive contaminant dispersal are assumed to be known, either from measurements, intuitive assumption, or the design of the air handling system. Thus, the approach developed herein is not complete, but is one of a series of tools that can be integrated into a larger modeling framework that considers both airflow patterns and contaminant dispersion. The approach applies user-friendly software that enables the user to evaluate a large region in which a pollutant is not uniformly distributed by (1) dividing the space into a series of well-mixed volumes and (2) establishing and solving the set of relationships that govern contaminant transport and dispersion throughout the larger region.

### 3.2 Dimensional units

The variables and parameters used in subsequent chapters are typically dependent upon dimensional units. Two issues are of importance in addressing units for air pollutant modeling. First, pollutant concentrations in air may be expressed on a molar basis (e.g., parts per billion [ppb]) or on a mass basis (e.g., micrograms per cubic meter [ $\mu\text{g}/\text{m}^3$ ]). Except for references to ambient pollutant standards, a mass-based convention is used exclusively in this report because it is more amenable to the control volume/mass conservation methodologies that serve as the foundation of the modeling study.

The second issue relates to the choice of units. Both metric and English units are in common usage in the United States, with various disciplines emphasizing different conventions. As such, this report does not use a single, uniform set of units throughout. Rather, different sets of units are used in various settings to emphasize that the choice of units is arbitrary, subject to the requirement that consistency be maintained within an application, i.e., the units of parameters used in equations must balance and agree with each other. As such, unit conversion factors are applied where necessary and appropriate, and the dimensions of all variables are indicated clearly.

### 3.3 Organization of the report

Chapter 4 provides the theoretical development for our approach, including discussion and examples of the governing equation for predicting the pollutant concentration in a single, well-mixed volume, time-averaging, and the treatment of systems of volumes. Chapter 5 introduces the interactive software used to implement our approach, leading to the development of modeling elements that represent the processes that determine pollutant concentrations in indoor air. Chapter 6 contains examples of how the interactive software is used to model indoor air pollutant dispersion, including a case study application based on data from a NIOSH Industrial Hygiene report. Finally, Chapter 7 summarizes our research findings and suggests avenues for further development of our approach.

A large number of figures are referenced in subsequent chapters. For convenience, all figures for a given chapter are located at the end of the chapter. Tables, which are less numerous, are either included within the text or follow the end of the relevant chapter of the report, as appropriate.



## 4 Theoretical Development

We begin by introducing the control volume concept, which is the fundamental basis of our approach. After a discussion of time-averaging, the control volume concept is extended to systems of control volumes. Several examples are provided for illustration. These examples serve two purposes. First, they provide a background and framework for the model development in Chapter 5. Second, the examples are characterized by analytical, or known, solutions that can be used as benchmark problems for the generalized model algorithms developed in subsequent chapters.

### 4.1 Well-mixed rectangular volume

The foundation of our approach is a rectangular volume of arbitrary size in which a pollutant is assumed to be present in all parts at a uniform concentration because of sufficient air movement within the volume. As a result, the volume is said to be well-mixed. An example of such a volume is shown schematically in Figure 4.1. Air and pollutant fluxes into and out of the volume are represented by arrows. Inside the box, several chemical and physical processes can occur that are assumed to affect the contaminant concentration uniformly throughout the box. These processes include emission, reaction, and deposition of chemicals within the volume. Chemical emissions include source terms within the volume such as releases that result from industrial processes or accidental spills. Chemical reactions include the decay (or creation) of a contaminant that occurs either spontaneously or from reaction with other chemicals present in the volume. Deposition includes reactions with or at surfaces that some airborne chemicals are known to undergo; this term may be used to model first-order desorption/adsorption processes.

Chemical concentrations in such a well-mixed volume can be described by:<sup>1</sup>

$$\frac{d(cV)}{dt} = E - \alpha c + Q_{in} c^* \quad (4.1)$$

where  $c$  is the chemical concentration in the volume ( $\text{g}/\text{m}^3$ ),  
 $V$  is the volume of the rectangular box ( $\text{m}^3$ ),  
 $t$  is time (hr),

---

<sup>1</sup> Units are assigned to each variable for the purpose of illustration. The choice of units is somewhat arbitrary throughout this document and in model application; the only requirement is that a consistent set of units be applied so that air flows, concentrations, and mass emission rates are expressed in units of volume/time, mass/volume, and mass/time, respectively, and that conversion factors be included as necessary to maintain correct unit dimensions.

$E$  is the emission rate of chemical within the volume (g/hr),  
 $\alpha$  is the rate of chemical loss from the volume (sink term) ( $\text{m}^3/\text{hr}$ ),  
 $Q_{\text{in}}$  is the rate of air transferred into the volume from external sources ( $\text{m}^3/\text{hr}$ ),  
 and  $c$  is the average chemical concentration in external sources (weighted by the rates of volume flow) ( $\text{g}/\text{m}^3$ ).

The sink term,  $\alpha$ , can be expressed as:

$$\alpha = Q_{\text{out}} + k_{\text{bulk}} V + k_{\text{surf}} A \quad (4.2)$$

where  $Q_{\text{out}}$  is the rate at which air exits the control volume ( $\text{m}^3/\text{hr}$ ),  
 $k_{\text{bulk}}$  is the rate of reaction of chemical within control volume (1/hr),  
 $k_{\text{surf}}$  is the rate of surface reaction or deposition of chemical within control volume ( $\text{m}/\text{hr}$ ), often called the deposition velocity,  
 and  $A$  is the surface area available for deposition or chemical reaction ( $\text{m}^2$ ).

As written, equations (4.1) and (4.2) combine to form a linear first-order differential equation.<sup>2</sup> The solution of Equation (4.1) for a single volume is straightforward for simple boundary conditions and constant coefficients. For example, if it is assumed that the volume is constant, that air entering the volume from an external source is uncontaminated and that the only chemical loss from the volume is due to air exchange, Equation (4.1) reduces to:

$$\frac{dc}{dt} + \frac{Q_{\text{out}}}{V} c = \frac{E}{V} \quad (4.3)$$

For an initial concentration  $C_0$ , the solution is:

$$c = C_0 + \left( \frac{E}{Q_{\text{out}}} - C_0 \right) \left( 1 - e^{-\frac{Q_{\text{out}}}{V} t} \right) \quad (4.4)$$

This expression describes exponential growth from an initial concentration of  $C_0$  to a steady-state value of  $E/Q_{\text{out}}$ . If the emission rate is set to zero, Equation (4.4) is simplified to:

---

<sup>2</sup> Nonlinearities could easily be included, however, especially in the reaction and deposition terms. Additionally, the modeling approach is developed for a single chemical species. Systems of linked equations, however, can be easily postulated by developing a mass-balance equation separately for each chemical species.



$$c = C_0 e^{-\frac{Q_{out}}{V} t} \quad (4.5)$$

This expression describes exponential decay from an initial concentration of  $C_0$  to an ultimate concentration of zero.

For purposes of illustration, we have assumed the following parameter values:

$$\begin{aligned} E &= 100 \text{ g/hr} \\ V &= 100 \text{ m}^3 \\ Q_{out} &= 100 \text{ m}^3/\text{hr} \end{aligned}$$

Air concentrations predicted by Equation (4.4) are plotted in Figure 4.2 for an initial concentration ( $C_0$ ) of zero. The air concentration increases exponentially, approaching its asymptotic value of  $1 \text{ g/m}^3$  ( $E/Q_{out}$ ) after about five hours. Air concentrations predicted by Equation (4.5) for an initial concentration of  $0.5 \text{ g/m}^3$  are plotted in Figure 4.3. Since there is no emission source in this case, the solution decays exponentially, beginning at the initial concentration of  $0.5 \text{ g/m}^3$  and asymptotically approaching zero after about five hours. Figure 4.4 shows predicted air concentrations for Equation (4.4) with an initial concentration of  $0.5 \text{ g/m}^3$ . The solution is similar to that shown in Figure 4.2, approaching the same asymptotic value of  $1 \text{ g/m}^3$  after about five hours, except that the time-dependent concentration begins at a value of  $0.5 \text{ g/m}^3$  instead of zero.

These solutions are only valid for cases in which the sources and sinks are of constant strength. Given the nature of industrial processes, it may be necessary to predict air concentrations due to sources that vary with time. As long as other coefficients remain constant in time, the linear nature of the governing equations allows the use of the principle of superposition to add individual solutions, and thereby provide solutions to more complex, time-dependent emission problems. For example, emissions could occur periodically, according to the function:

$$\begin{array}{lllll} E = 100 \text{ g/hr} & \text{for} & 0 \leq t < 1; & 2 \leq t < 3; & 4 \leq t < 5; & \text{etc;} \\ E = 0 & \text{for} & 1 \leq t < 2; & 3 \leq t < 4; & 5 \leq t < 6; & \text{etc.} \end{array}$$

In this case, air concentrations during periods in which emissions occur could be described by Equation (4.4). Equation (4.5) could be used to describe air concentrations during periods in which no emissions occur. If emissions occur for every other hour for an hour as described above and shown in Figure 4.5, the previous parameter values and Equations (4.4) and (4.5) yield the solution plotted in Figure 4.6. The resulting sawtooth pattern is characteristic of systems in which intermittent emissions occur. The pollutant concentration increases when the emission source is active and decreases when the source is dormant. After an initial transient response, a

periodic pattern emerges, centered roughly about a concentration of  $0.5 \text{ g/m}^3$ , which is half the value for the case of continuous emissions (Figure 4.2 and Figure 4.4) and consistent with the fact that the source emits half of the time.

## 4.2 Time-averaging

The danger presented by an air pollutant depends upon its concentration, persistence, and mode of action. Some pollutants can cause deleterious health effects in humans in very short times, while other pollutants may lead to cumulative health risk over long periods. For example, carbon monoxide poisoning can occur within minutes, while the risk from exposure to a carcinogen may accumulate over an entire lifetime. Moreover, exposure to some chemicals may be dangerous over differing time periods. For example, the same chemical may cause intoxication at high concentrations and lead to chronic health effects at low concentrations. For these reasons, exposure calculations should be consistent with the time period associated with adverse effects. Instantaneous concentrations are appropriate for evaluating very short-term hazards, while for long-term risks in which cumulative exposure is important, it is often useful to compute time-averaged air contaminant concentrations.

Time-averaged model predictions are also appropriate to compare with air concentrations measured over long periods of time, such as personal breathing space samples taken over the course of a work day. The average concentration can be determined by integrating the instantaneous concentration with respect to time and dividing by the total time. This can be expressed as:

$$c_{\text{avg}} = \frac{\int_0^T c \, dt}{\int_0^T dt} = \frac{1}{T} \int_0^T c \, dt \quad (4.6)$$

where  $t$  represents time,  
 $T$  is the upper limit of the time period of integration, defined from  $0 \leq t \leq T$ ,  
 $c$  is the time-dependent concentration,  
 and  $c_{\text{avg}}$  is the time-averaged concentration.

Equation (4.6) can be applied to the examples of Section 4.1. For the case of a source of constant strength and an initial concentration of zero averaged over the time period  $T$ , Equation (4.4) can be integrated to yield:

$$c_{avg} = \frac{E}{Q} + \frac{1}{T} \left( \frac{E}{Q_{out}} - C_0 \right) \frac{V}{Q_{out}} \left( e^{-\frac{Q_{out}}{V} T} - 1 \right) \quad (4.7)$$

Figure 4.7 shows both the instantaneous (solid curve) and time-averaged (dashed curve) air concentrations. The initial concentration is assumed to be zero and parameter values are the same as those reported in Section 4.1. Note that the time-averaged concentration, plotted as a function of the period of integration ( $T$ ), evolves more slowly with time than the instantaneous concentration because it must integrate a history of lower values into its average. If plotted for very long times, the time-averaged concentration would asymptotically approach the steady-state (maximum) concentration of  $1 \text{ g/m}^3$ . Figure 4.8 shows air pollutant concentration profiles for the case of  $C_0 = 0.5 \text{ g/m}^3$ . Again, the time-averaged concentration (dashed curve) approaches the asymptotic (steady-state) value more slowly than the instantaneous concentration (solid curve).

The time-averaged expression for Equation (4.5) is:

$$c_{avg} = \frac{1}{T} \frac{C_0 V}{Q_{out}} \left[ 1 - e^{-\frac{Q_{out}}{V} T} \right] \quad (4.8)$$

Figure 4.9 illustrates the instantaneous and time-averaged air pollutant concentration profiles [Equations (4.5) and (4.8), respectively] as a function of time using the example parameter values described in section 4.1. In this case, since the instantaneous concentration (solid curve) decays with time, the time-averaged concentration profile (dashed curve) also decreases with time (or period of integration). Again, however, the time-averaged concentration approaches the steady-state concentration of zero more slowly than does the instantaneous concentration profile because the time-averaged concentration remembers the higher concentrations that occur at early times.

### 4.3 Multiple volumes

The modeling of large indoor air spaces in which air is not well-mixed requires a more elaborate approach than that discussed in Section 4.1. In this section, we develop a technique in which multiple volumes of the type described in Section 4.1 are connected to one another.<sup>3</sup> Effectively,

<sup>3</sup> Other techniques are also possible. An alternative approach involves the discretization of the governing differential equations using either finite difference or finite element algorithms. Our approach, however, maintains a flexible, easy-to-apply framework that is consistent with physical

we assume that air is well-mixed locally within volumes, but that contaminant concentrations can differ between volumes. The extension from a single volume to multiple volumes requires accounting for fluxes across control volume boundaries. These boundary fluxes are easily incorporated into the governing differential equation [an extension of Equation (4.1)], which is written for a single control volume  $j$ :

$$\frac{d(c_j V_j)}{dt} = E_j - \alpha_j c_j + \sum_{\substack{i=1 \\ i \neq j}}^n Q_{i \rightarrow j} c_i \quad (4.9)$$

where  $c_j$  is the chemical concentration in control volume  $j$  ( $\text{g}/\text{m}^3$ ),  
 $V_j$  is the physical volume of control volume  $j$  ( $\text{m}^3$ ),  
 $E_j$  is the emission rate into control volume  $j$  ( $\text{g}/\text{hr}$ ),  
 $\alpha_j$  is the rate of chemical loss within control volume  $j$  (sink term) ( $\text{m}^3/\text{hr}$ ),  
 $n$  is the number of volumes that border volume  $j$ ,  
 $i$  is a subscript that refers to one of the  $n$  volumes that border volume  $j$ ,  
 $Q_{i \rightarrow j}$  is the rate of air exchange from control volume  $i$  into control volume  $j$  ( $\text{m}^3/\text{hr}$ ),  
 and  $c_i$  is the chemical concentration in control volume  $i$  ( $\text{g}/\text{m}^3$ ).

Equation (4.9) must be written independently for each control volume of the system. The sink term  $\alpha_j$  is further defined to be:

$$\alpha_j = \sum_{\substack{i=1 \\ i \neq j}}^n Q_{i \leftarrow j} + k_{\text{bulk } j} V_j + k_{\text{surf } j} A_j \quad (4.10)$$

where  $Q_{i \leftarrow j}$  is the rate of air exchange from control volume  $j$  to an external sink or control volume  $i$  ( $\text{m}^3/\text{hr}$ ),  
 $k_{\text{bulk } j}$  is the rate of reaction of the chemical within control volume  $j$  ( $1/\text{hr}$ ),  
 $k_{\text{surf } j}$  is the rate of surface reaction of deposition velocity of the chemical within control volume  $j$  ( $\text{m}/\text{hr}$ ),  
 and  $A_j$  is the area in control volume  $j$  on which the chemical reacts or deposits ( $\text{m}^2$ ).

Since Equation (4.9) must be solved for each control volume of the system, the solution becomes much more difficult as the number of volumes and the degree of interconnectedness increases. We will return to a treatment of this problem in Section 6.1.2. Before doing so, however, we demonstrate a simple case that can be solved analytically. For purposes of illustration, we

---

intuition. In the limit of very small volumes, our approach should yield identical results to numerical solutions on refined computational grids.

consider a system consisting of two control volumes in which air is exchanged in one direction only and a contaminant is released only in Volume 1. A diagram of this system is shown in Figure 4.10.

If no reaction or deposition of the contaminant occurs and the air exchange rate for each volume is the same, the governing equations for the two volumes are:<sup>4</sup>

$$\frac{d(c_1 V)}{dt} = E_1 - Q c_1 \quad (4.11)$$

$$\frac{d(c_2 V)}{dt} = -Q c_2 + Q c_1 \quad (4.12)$$

The solution to Equation (4.11) is unchanged from that for the single volume example in Section 4.1, Equation (4.4). Using the notation for multiple volumes and assuming the initial concentration in Volume 1 is zero, the time-dependent concentration is given by:

$$c_1 = \frac{E_1}{Q} \left( 1 - e^{-\frac{Q}{V}t} \right) \quad (4.13)$$

Assuming an initial concentration of zero in Volume 2 as well, the solution to Equation (4.12) integrates the solution for Volume 1 [Equation (4.13)], and is expressed as:

$$c_2 = \frac{E}{Q} \left[ 1 - \left( 1 + \frac{Q}{V}t \right) e^{-\frac{Q}{V}t} \right] \quad (4.14)$$

Assuming the previously defined set of parameter values (section 4.1), the solutions to Equations (4.13) and (4.14) are shown in Figure 4.11. The concentration in Volume 2 can be seen to lag behind that in Volume 1, although it does reach the same asymptotic (steady-state) value. The reason for this result is apparent in the structure of Equation (4.14): at later times, the exponential term goes to zero and the concentration in the volume is simply the emission rate divided by the air exchange rate, which is the same as the steady-state concentration for Volume 1 [Equation (4.14)]. Mathematically, the delayed response of Volume 2 results from the moderation of the

---

<sup>4</sup> For simplicity, the subscripts on volume flowrates have been dropped in Equations (4.11) and (4.12). In this case,  $Q_{1 \rightarrow 2} = Q_{2 \leftarrow 1} = Q$ .

exponential term by the  $(1 + Qt/V)$  term in Equation (4.14), which is also responsible for the parabolic behavior of the concentration profile at very early times.<sup>5</sup>

Equation (4.14) can be generalized to express the air concentration in the  $n^{\text{th}}$  control volume in a series of control volumes in which emissions occur only in the first, and  $Q$  and  $V$  are equal in each control volume (that is, a straight-through flow is maintained through a series of volumes, such as can be expected in flow within a long duct):

$$c_n = \frac{E}{Q} \left[ 1 - \left( \sum_{k=0}^{n-1} \frac{1}{k!} \left( \frac{Q}{V} t \right)^k \right) e^{-\frac{Q}{V} t} \right] \quad (4.15)$$

It can be seen that the concentration in any volume approaches the ratio of the emission rate and the air exchange rate at large times.

The previous example solutions [Equations (4.14) and (4.15)] are based on the assumption that there is no return flow of air. In many practical applications, this assumption is not valid. Air is often recirculated between volumes due to complex air flow patterns that are typical of practical settings. In such cases, the system of governing equations becomes more complex and analytical solutions become impractical. The application of SIMULINK™ with the control volume approach, as described in the next chapter and demonstrated in Chapter 6, is especially well-suited to these cases.

---

<sup>5</sup> This parabolic behavior can be demonstrated using a power series expansion of Equation (4.14).

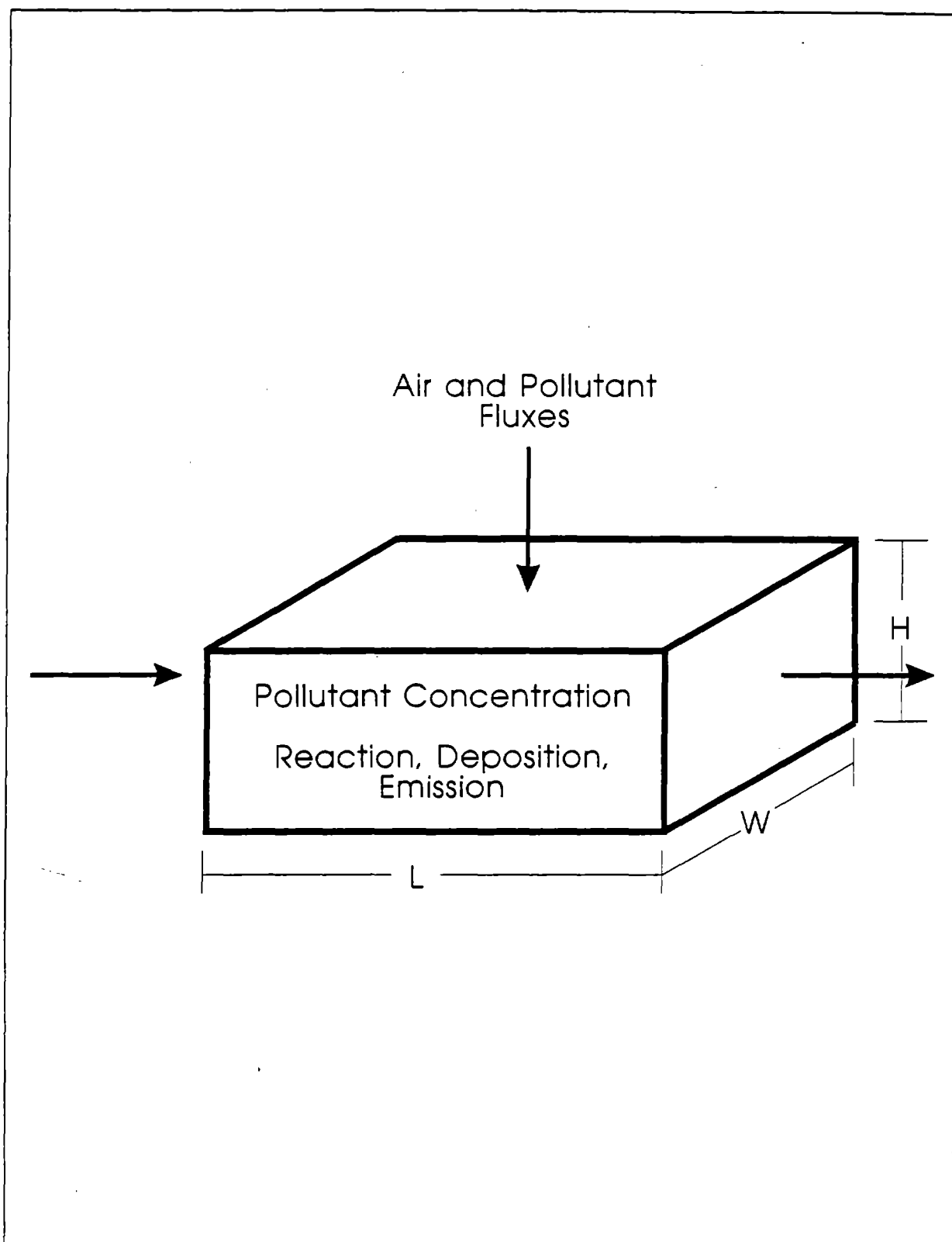


Figure 4.1 Well-mixed rectangular volume.

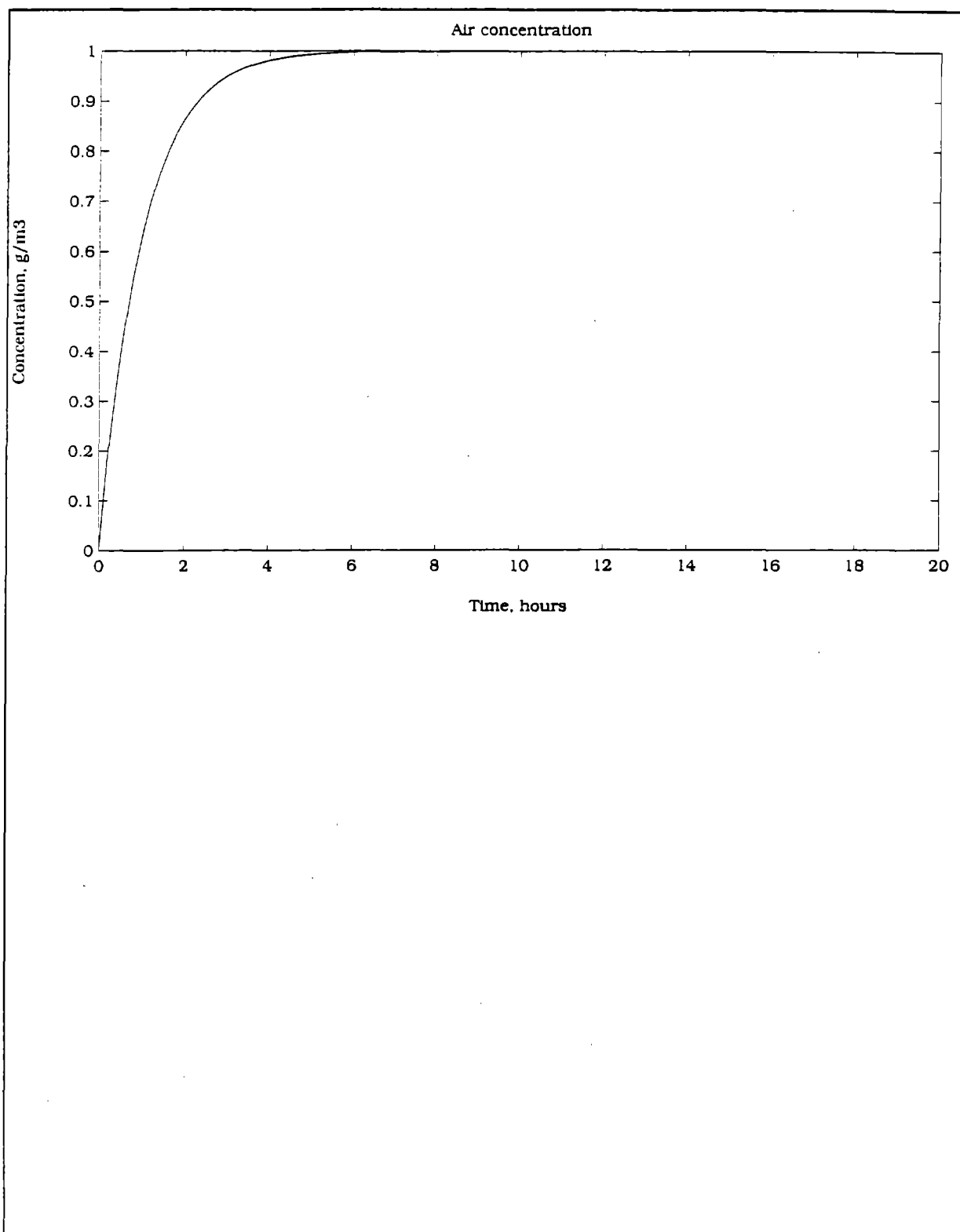


Figure 4.2 Pollutant concentration predicted by Equation (4.4) for  $C_0 = 0$



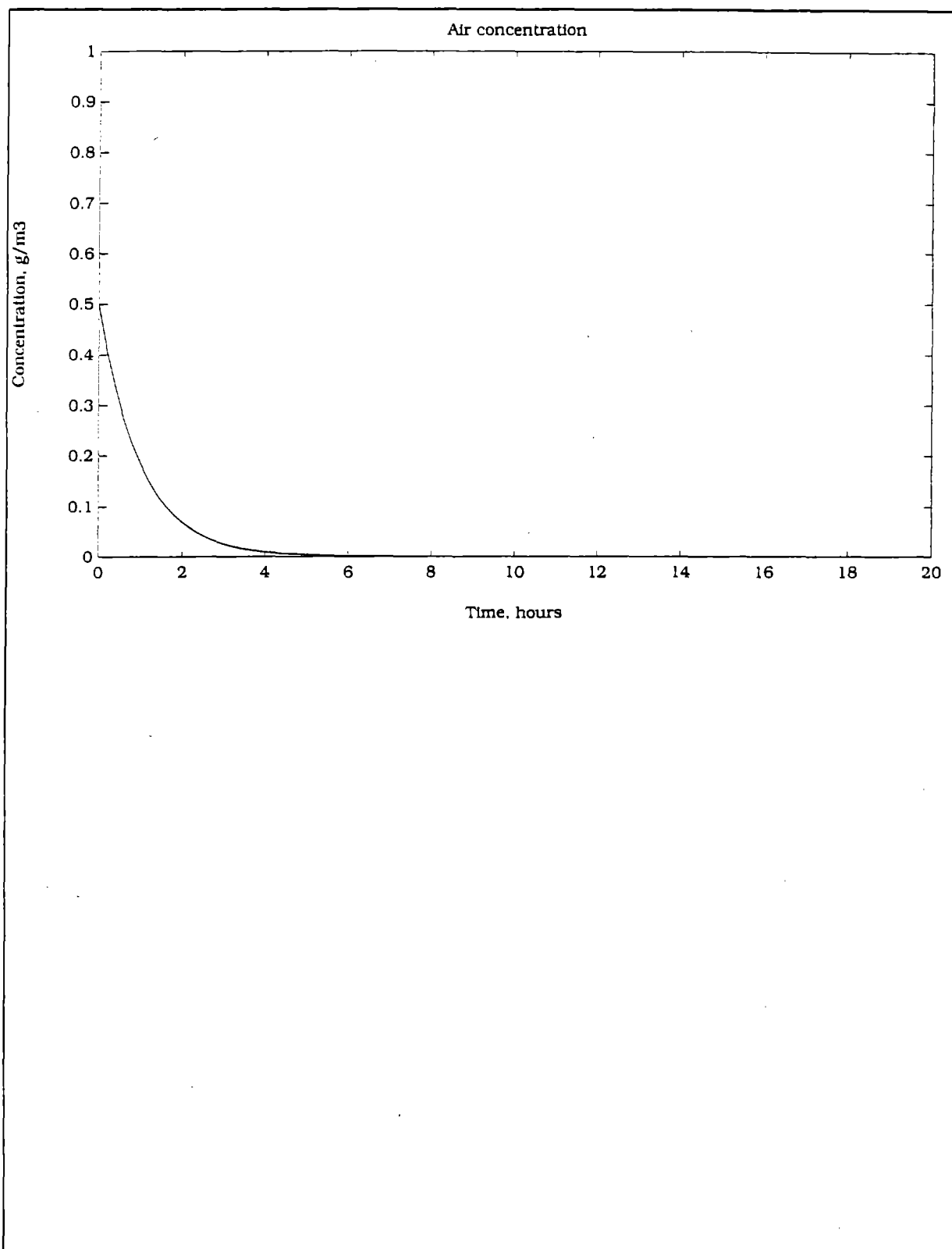


Figure 4.3 Pollutant concentration predicted by Equation (4.5) for  $C_0 = 0.5 \text{ g/m}^3$

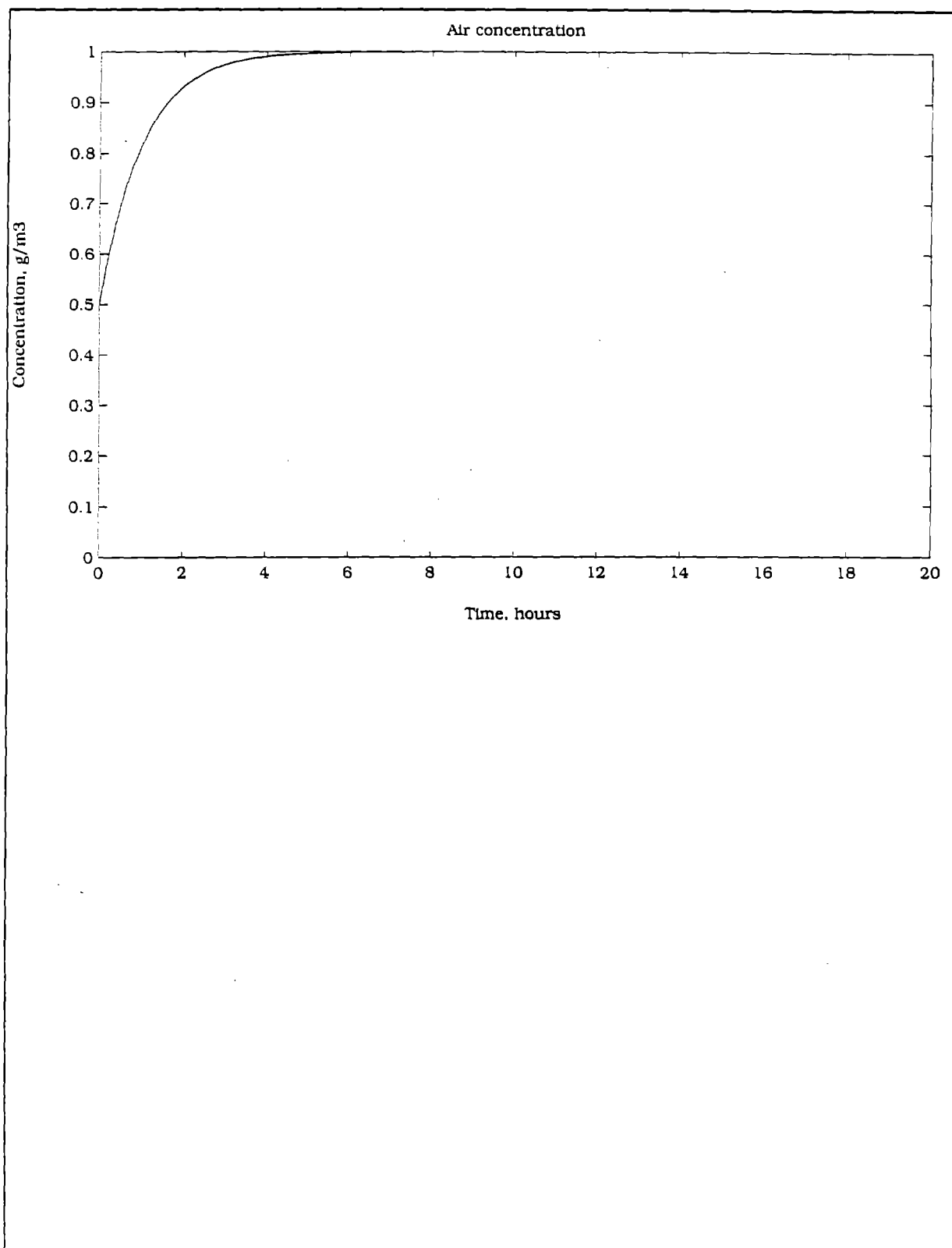


Figure 4.4 Pollutant concentration predicted by Equation (4.4) for  $C_0 = 0.5 \text{ g/m}^3$

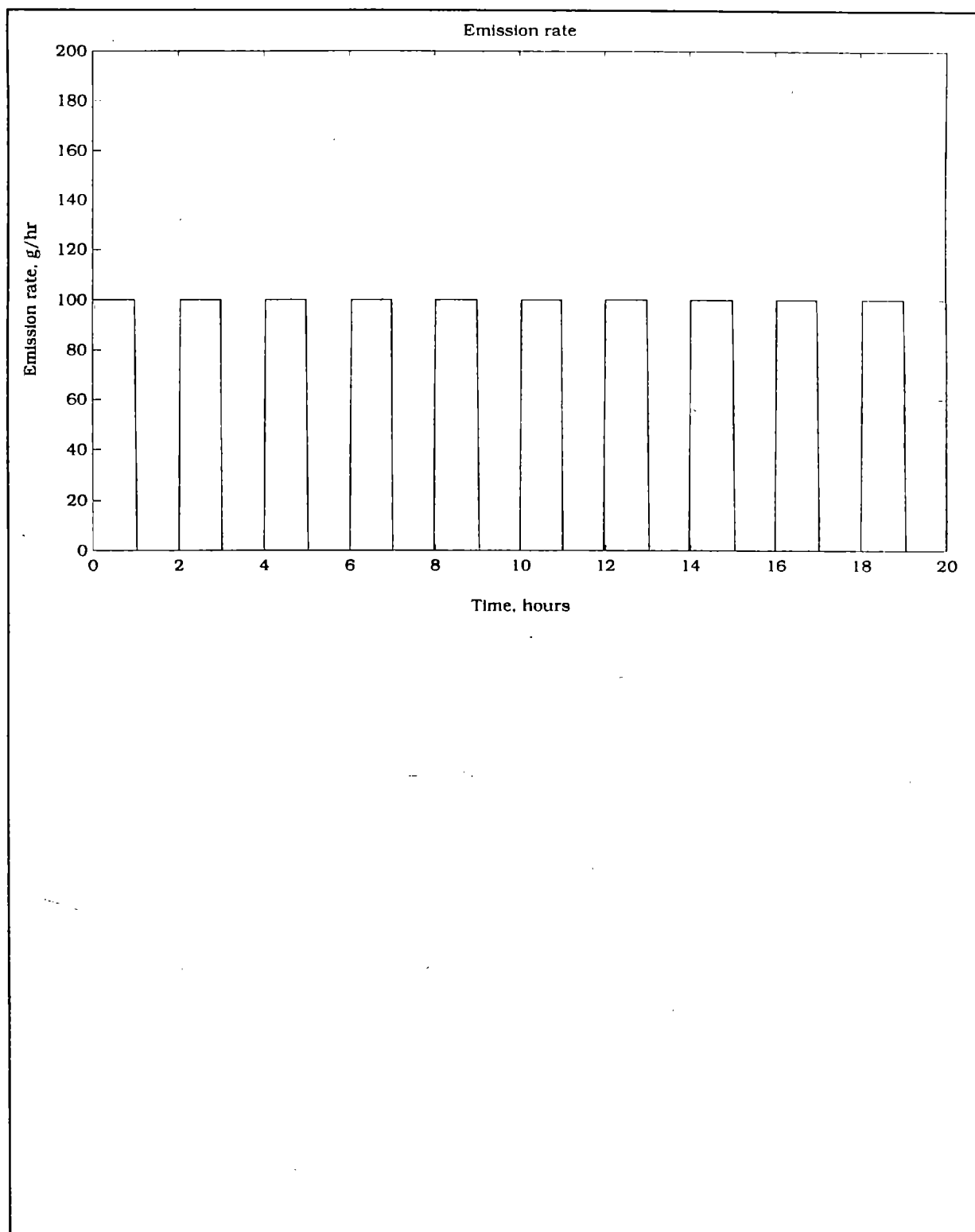


Figure 4.5 Periodic emission function in which pollutant emissions are on and off for alternating one-hour periods

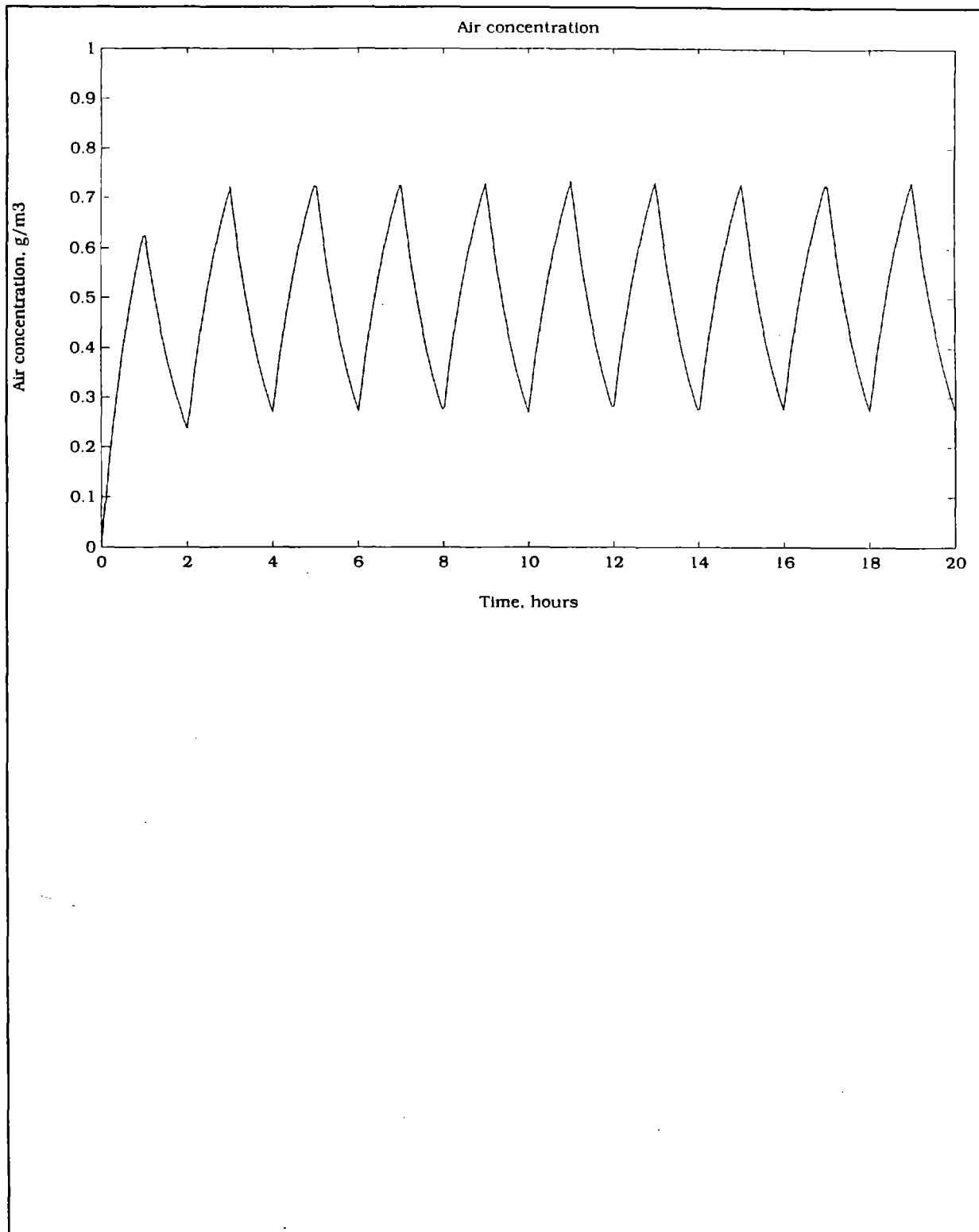


Figure 4.6 Time-dependent pollutant concentration profile that results from periodic emissions (Figure 4.5) with constant ventilation and initial concentration  $C_0 = 0$

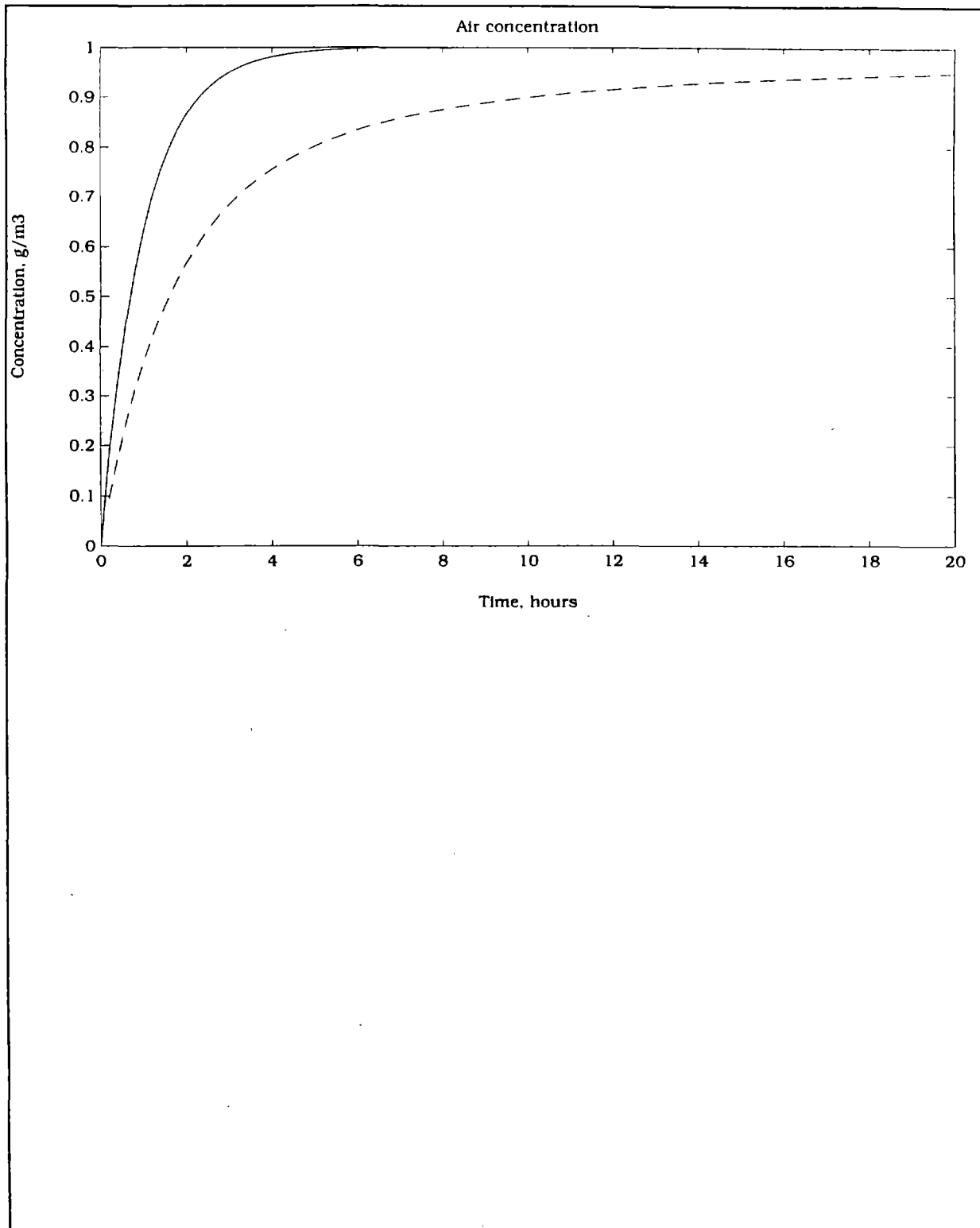


Figure 4.7 Time-averaged concentration [Equation (4.7), (dashed curve)] compared with the instantaneous solution [Equation (4.4) (solid curve)],  $C_0 = 0$

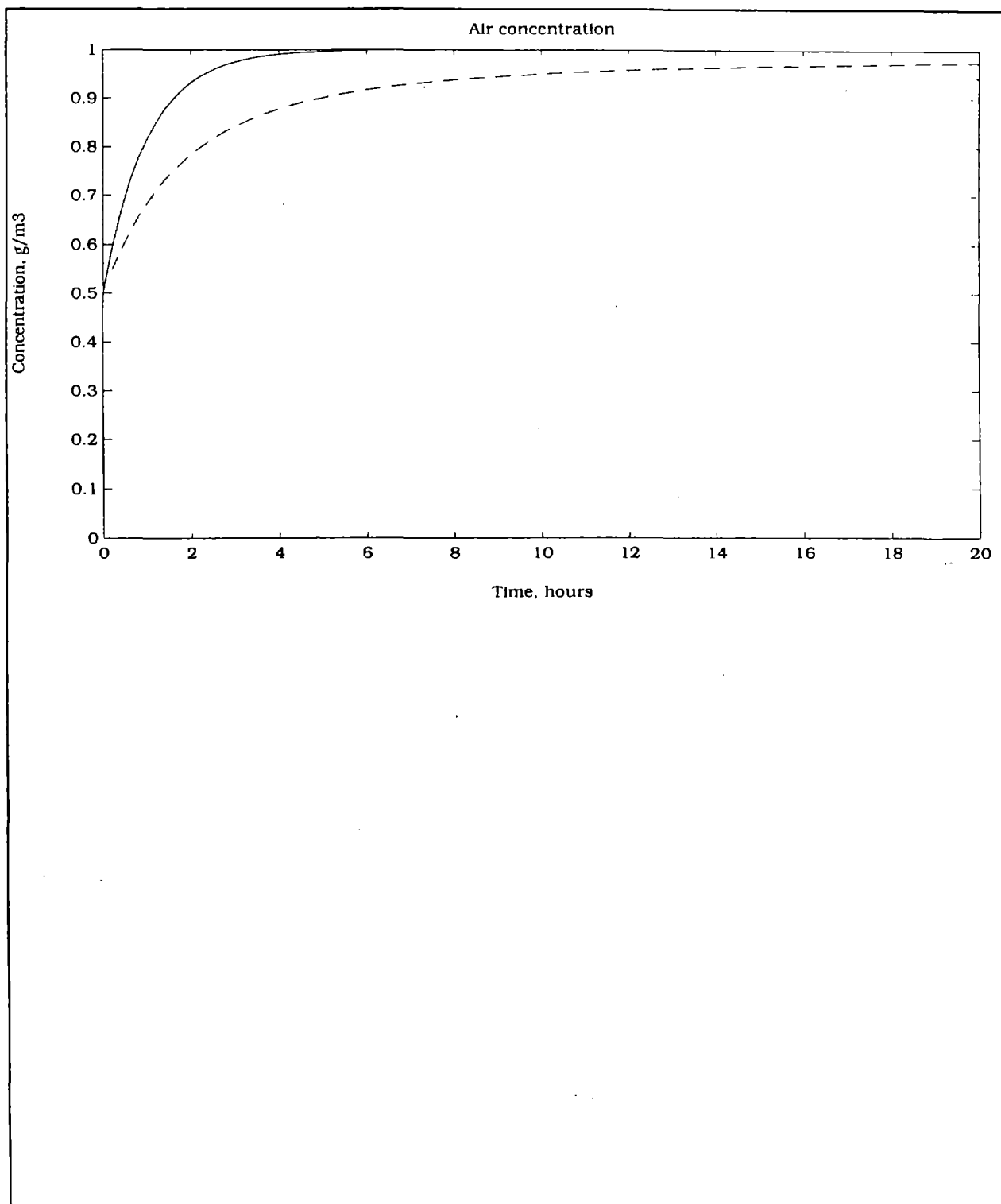


Figure 4.8 Comparison of time-averaged [Equation (4.7), (dashed curve)] and instantaneous concentrations [Equation (4.4), (solid curve)],  $C_0 = 0.5 \text{ g/m}^3$

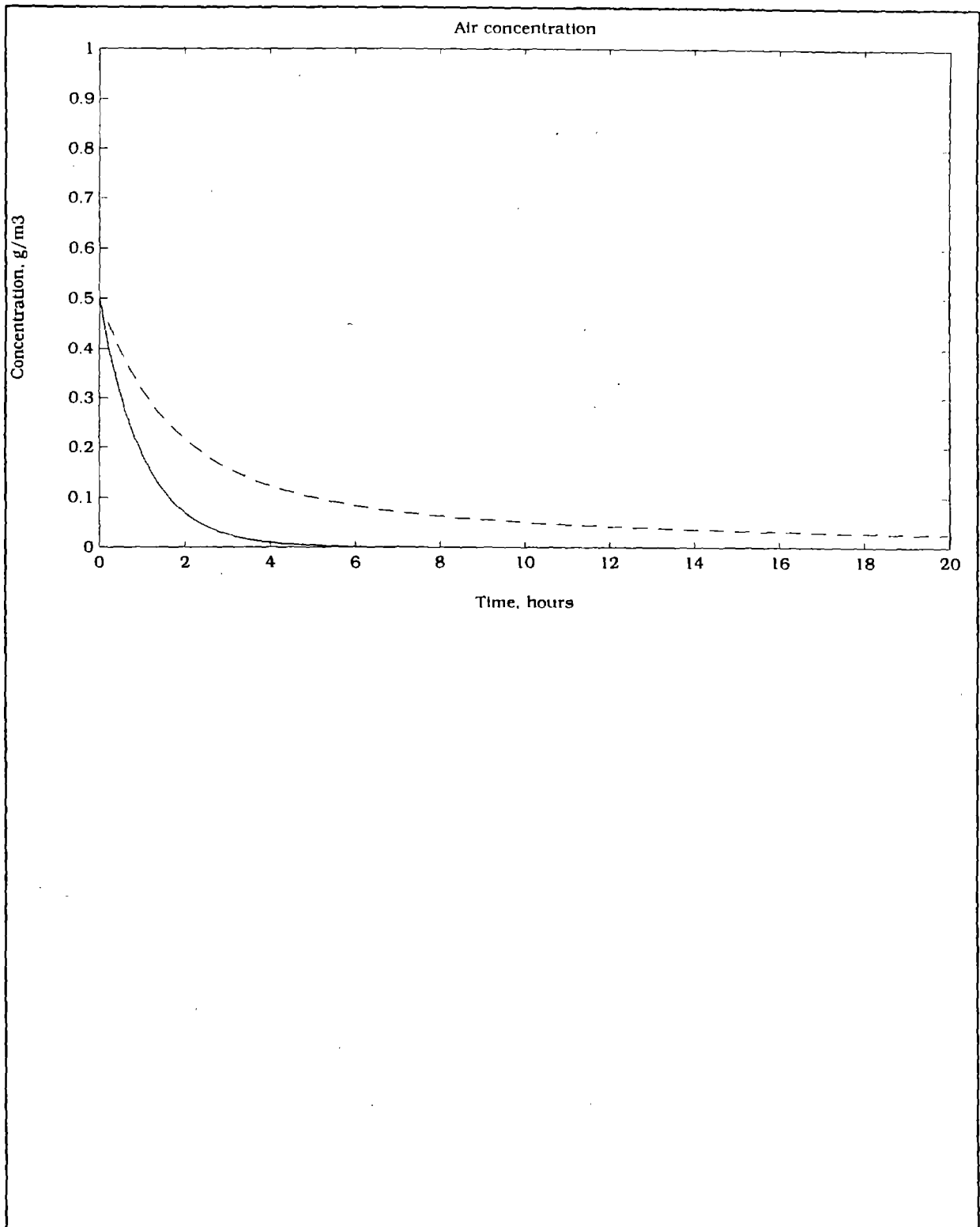


Figure 4.9 Comparison of time-averaged [Equation (4.8), (dashed curve)] and instantaneous solutions [Equation (4.5) (solid curve)],  $C_0=0.5 \text{ g/m}^3$

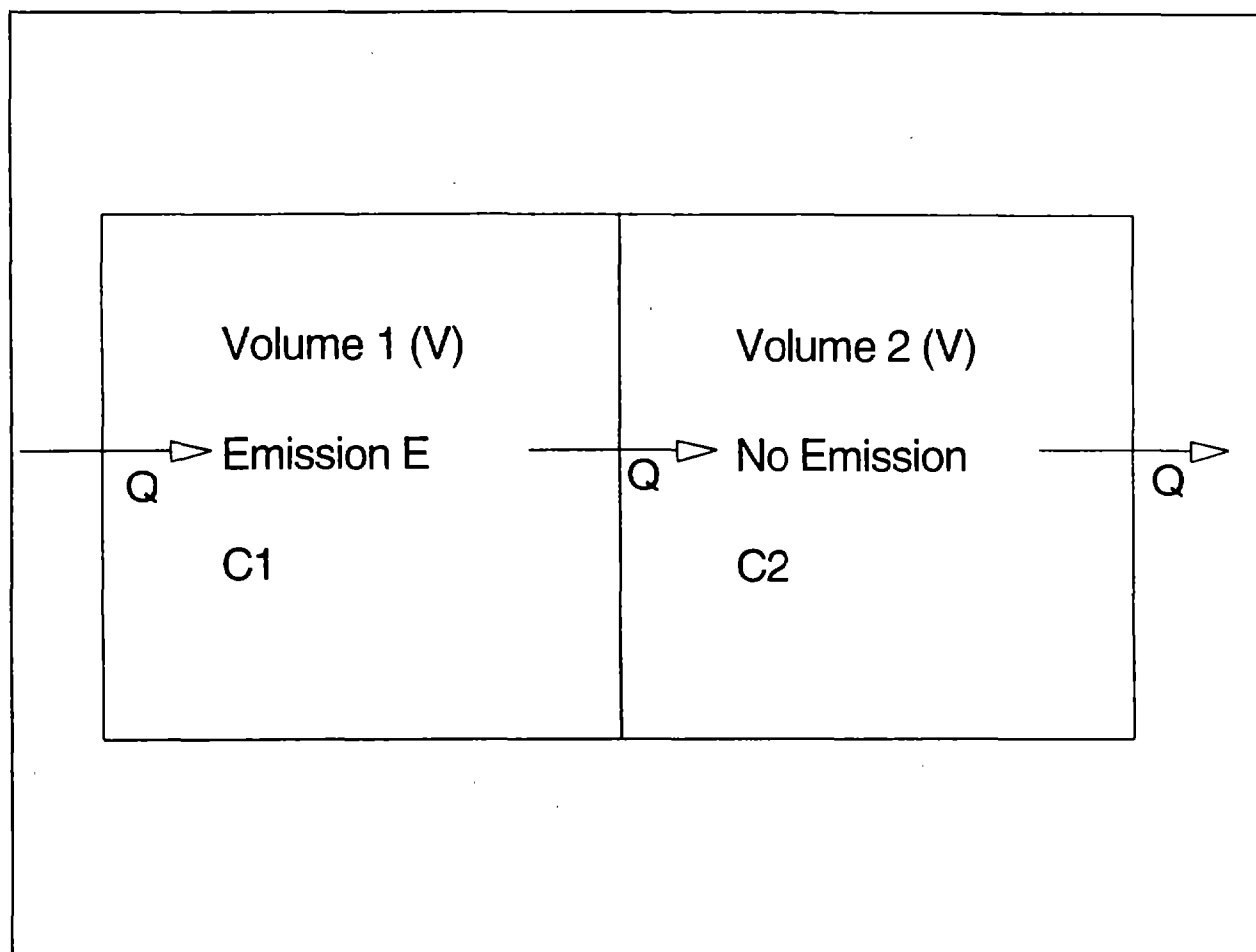


Figure 4.10 Schematic of a two-volume system with direct and constant flow-through ventilation  $Q$ , emission in Volume 1, and no emission in Volume 2



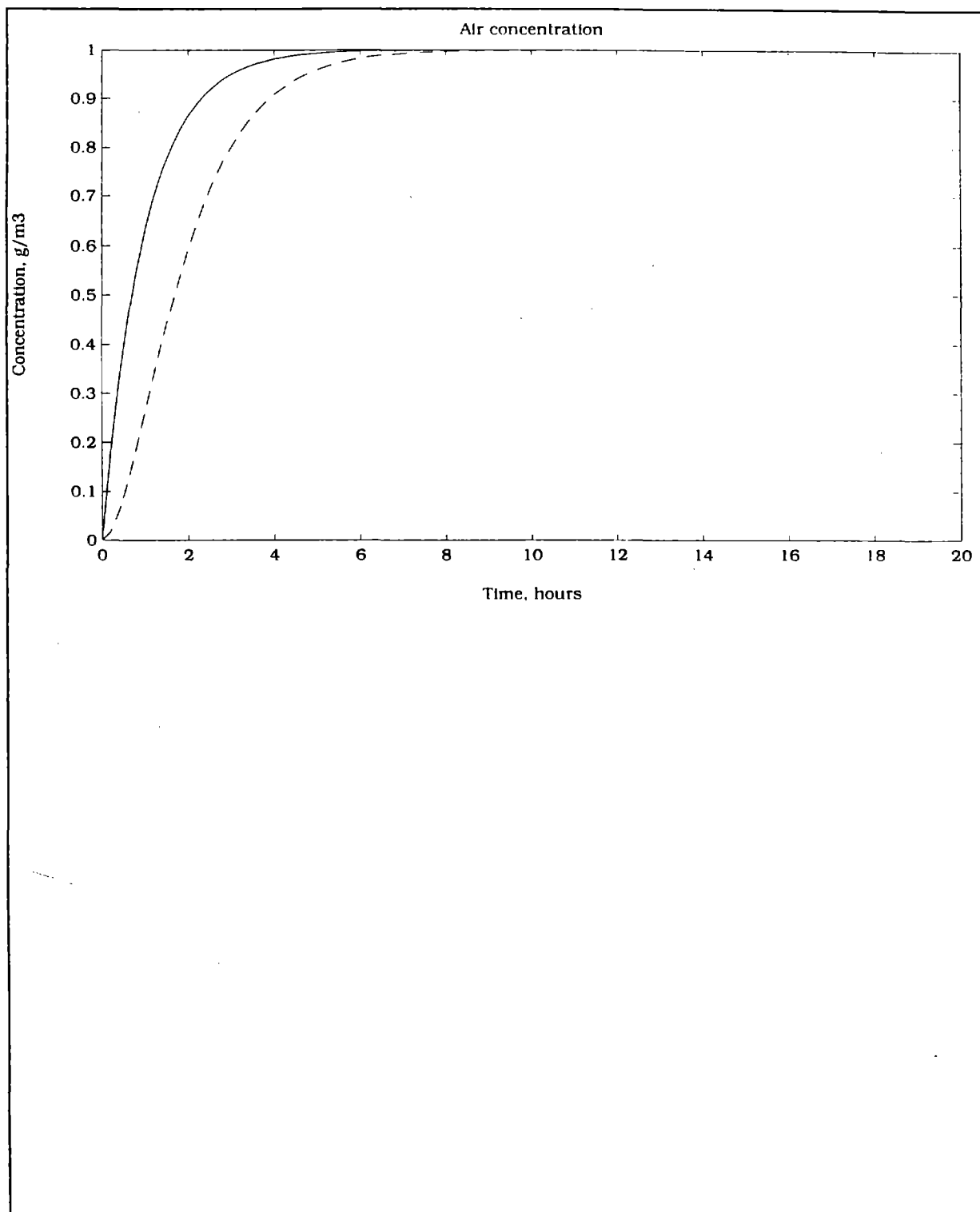


Figure 4.11 Air pollutant concentrations in Volumes 1 (solid) and 2 (dashed) predicted by Equations (4.13) and (4.14), respectively



## 5 SIMULINK™ Environment

This section describes the application software developed to model the behavior of airborne contaminants in large spaces in which the pollutants are not uniformly distributed. The software is the dynamic systems simulation package called SIMULINK™. Much of sections 5.1, 5.2, and 5.3 are derived from the SIMULINK User's Guide (MathWorks, 1992) and MATLAB for Windows User's Guide (MathWorks, 1991). We provide herein only a brief outline of SIMULINK™'s capabilities, referring the reader to the MathWorks' documentation for further details. We limit ourselves to consideration of those aspects of SIMULINK™ relevant to the modeling of contaminant dispersion in indoor air.

### 5.1 SIMULINK™: A general description

SIMULINK™ is a software package for simulating dynamic (time-dependent) systems,<sup>1</sup> and which is in turn based on MATLAB®, a numerical computation and graphics package. Both packages are designed to be user-friendly. SIMULINK™ makes use of block diagram windows, or elements, to facilitate model design and use. SIMULINK™ is a Windows™-based program that utilizes many convenient features, such as mouse-facilitated manipulation of elements, connectors, and option menus.<sup>2</sup> The elements represent various components of a dynamic system and mask underlying mathematical expressions. Hence, the SIMULINK™ environment automatically processes the mathematical details of dynamic systems and allows the user to conceptualize a physical system with block diagrams, defining connections and interrelationships in a physically intuitive fashion.

MATLAB® is a software package for numerical computation that provides a workspace in which variables can be defined or imported from data files and equations can be solved directly. This eliminates the need to write programs in traditional languages such as FORTRAN. The package integrates numerical analysis, matrix computation, signal processing, and graphics. Although designed primarily for matrix operations, scalar quantities can be accepted as well. Variables can be saved in files for later use and/or plotted with MATLAB's graphics capabilities. SIMULINK™ provides an interface between this powerful computational environment and the user, allowing use of MATLAB's capabilities without requiring extensive knowledge of its operation.

SIMULINK™ makes use of block or element icons that represent equations, systems of equations, or variables within these equations. Each icon models a physical process and introduces an underlying mathematical description. Connected to one another, a series of icons can be used to

---

<sup>1</sup> Specifically, SIMULINK™ solves systems of initial value problems.

<sup>2</sup> SIMULINK™ is also available for Macintosh, Sun, and X-Windows platforms.

represent a mathematical description of the behavior of the system of interest. The user deals exclusively with SIMULINK™ elements, and the underlying equations remain hidden.<sup>3</sup>

## 5.2 SIMULINK™ main library

The SIMULINK™ main library contains seven main element groups, each of which contains a class of elements useful in system dynamics applications. The majority of the elements used in this report are members of five of the seven main groups. Elemental members of these five groups are shown in Figure 5.1; for convenience, members of the linear and nonlinear are combined. The Sources library contains elements that generate signals, or input, to systems. For example, a source element might be used to represent the rate of chemical emission in a volume. The Sinks library contains elements that accept signals. Sink elements are used to monitor signals or define variables for further manipulation or plotting in MATLAB® workspace. The Linear and Nonlinear libraries contain elements that represent linear operations (such as addition and subtraction) and potentially nonlinear operations (such as multiplication). The Connections library contains elements that enable the user to combine signals, thereby greatly simplifying element diagrams.

In addition, the SIMULINK™ main library contains two other groups. The Discrete library contains elements used to manipulate discrete signals such as samples taken from a continuous signal. The Extra library contains examples of collections/combinations of elements from the first six libraries that are frequently used. Many examples (not shown) in the Extra library illustrate a major advantage of SIMULINK™ — the grouping of elements into a single icon. This powerful feature permits complex systems to be represented as input/output processors, and serves as the basis of the indoor air dispersion modeling elements described in the section 5.4.

## 5.3 Examples of SIMULINK™ elements

Figure 5.1 shows individual elements selected for use from the SIMULINK™ main library. All of the more complex elements described in section 5.4 are constructed from these basic elements. The first group of elements is taken from the Source element in the SIMULINK Library. The Constant element is a source term that outputs the value of the specified parameter. The time element (labeled "clock" Figure 5.1) is a counter that outputs the time at each step of the simulation. This element is not strictly necessary since SIMULINK™ maintains an internal clock, but it is useful for creating plots of time-dependent variables. The Signal Generator element produces one of four waveforms: sine wave, square wave, sawtooth wave, or random noise. The amplitude and

---

<sup>3</sup> The user does retain some control over the methods and parameters used by SIMULINK™ to integrate (solve) differential equations. Also, if desired, the user may access the underlying mathematical constructs by creating routines within the MATLAB™ framework.

frequency can be adjusted. Frequency units are radians per unit of time. This element is useful for defining emissions that vary periodically.

The second group of elements is taken from the Linear and Nonlinear Operator SIMULINK™ Library elements. The Sum element accepts any number of inputs (the element shown here has been set to accept two inputs), adds or subtracts them as specified, and produces an output. The Product element accepts any number of inputs (the element here has been set to accept two inputs), multiplies them, and outputs the product. The Fcn element, or Function element, provides the user with a means to define a functional dependence of his or her own choice as a function of an array of input parameters. The Integrator element integrates the input with respect to time from a specified initial value, producing an accumulated output. The Switch element provides a switch between outputs based upon three input values. The output is selected from the first two inputs based on a user-defined condition and the value of the third input. If the condition is met by the third input, the first input value is selected and output. If it is not met, the second value is selected for output. The Transport Delay element is used to introduce a time delay to a signal.

The third group of elements is taken from the Connections block in the SIMULINK™ Library. The Inport element provides a link to transfer data to a subsystem from the larger (parent) system. The Outport element provides a link to transfer data from a subsystem back to the parent system. The Mux (or multiplexer) element groups several scalar line inputs into a single vector line output. This element is useful for minimizing the number of connecting lines in a block diagram. Its counterpart is the Demux (or demultiplexer) element. The Demux element ungroups the single vector line input into its original scalar lines.

The fourth group of elements is taken from the Sinks element in the SIMULINK™ Library. The Scope element accepts a scalar input and displays its value during simulation. This element is useful during system development to monitor block outputs. The To Workspace element accepts a vector input and creates a matrix of values of the input for use in the MATLAB® workspace. This element is useful for saving simulation results and subsequently plotting them with the MATLAB® graphics package.

## 5.4 SIMULINK™ elements developed for indoor air modeling

Figure 5.2 shows SIMULINK™ elements developed for indoor air modeling applications. These elements comprise three major functional categories: the Volume element, the Exchange element, and Emission elements. The Volume element, which is used to represent well-mixed rectangular volumes, is described in section 5.4.1. The Exchange element, which is used to specify the fluxes of pollutants between adjacent Volume elements, is detailed in section 5.4.2. Emission elements, which are used within Volume elements to characterize the release of a pollutant, are described in section 5.4.3.

The Volume and Exchange elements are complementary building blocks that can be used to construct models of pollutant transport in large air spaces that are not well-mixed. Emission elements are used within Volume elements to describe releases of pollutants.

In addition, various auxiliary elements were developed during the course of the study. As an example of these elements, Figure 5.2 includes a block that time averages the input according to Equation (4.6). This element, which is further described in section 5.4.4, enables the user to compare model predictions with time-averaged measurements.

### 5.4.1 The Volume element

The Volume element represents a well-mixed rectangular volume of air throughout which a contaminant is assumed to be distributed uniformly. As shown in its icon in Figure 5.2, the Volume element contains a series of twelve input ports (arrowheads pointing into the element) and two output ports (arrowheads pointing out of the element). The twelve inports, which are used to receive pollutant flux data from adjacent volumes, are identical. Each of the twelve inports is itself a vector of three inputs that describe exchange parameters from an adjacent volume element: the contaminant flux into the Volume element from an adjacent volume, the back exchange rate of air from the Volume element into the adjacent volume, and the rate of air flow from the adjacent volume into the Volume element (the air exchange rates between the Volume and adjacent elements are not necessarily equal, and either air exchange rate can be zero). Output ports of the Volume are its time-dependent contaminant concentration (top port) and an air flux check (bottom port). The latter output is a sum of all air flows into and out of the Volume element and is useful as a monitoring check in constructing systems of elements, since to satisfy the continuity of air flow, this sum should be zero.

Figure 5.3 is the detailed schematic of the Volume element, which is expanded from its icon form shown in Figure 5.2. In essence, the block diagram in Figure 5.3 is a symbolic representation of the mass conservation equation for a control volume [Equations (4.9) and (4.10)]. The mass of the pollutant in the volume (the product of concentration and volume) serves as the state variable of integration. The mass balance for the pollutant is controlled by the closed loop located in the

center of the diagram. The mass of pollutant is tracked by the block labeled  $M_i$ , which is simply the integrated value of the rate change of pollutant mass with time, represented by the  $dM/dt$  block.

The  $dM/dt$  block is a summation element of four terms that increase or decrease the mass of the pollutant present in the Volume element. Ordered from top to bottom, these terms are (1) the external pollutant flux that enters from outdoors or from internal sources of ventilation, (2) the summed pollutant fluxes that enter from other Volume elements, (3) emission of the contaminant within the volume, and (4) the removal of the pollutant from the Volume due to transfer to other Volumes, chemical reaction and deposition. The nature of these contributions is reflected by the signs of the summation element; positive signs indicate that terms (1)–(3) increase the mass of the pollutant within the volume, while the negative sign assigned to term (4) reflects a decrease in the mass of pollutant.

Within Figure 5.3, user-defined input elements (that is, parameters and variables that may be set by the user) are highlighted in dark gray. A list of user-defined inputs is provided as follows; the block titles identify elements of Figure 5.3, each of which is identified by a short block description.

### User-Defined Input Blocks for the Volume Element

<u>Block Title</u>	<u>Block Description</u>
Length (x)	The length of the Volume. A conventional Cartesian (x,y,z) coordinate system is assumed.
Width (y)	The width of the Volume.
Height (z)	The height of the Volume.
Surf	The surface area in the Volume upon which pollutants deposit or react.
S React	The rate at which pollutants deposit or react at a given surface.
B React	The bulk rate at which pollutants react within the whole of the Volume.
Ventilation into volume from Outdoors	The rate at which air is supplied to the Volume from external ventilation (i.e., air that enters the Volume from sources other than adjacent Volumes).
Concentration in ventilated air	The concentration of the pollutant in air supplied to the Volume by external ventilation.
Emission	The rate of pollutant emission within the Volume.
Ventilation Rate to Outdoors	The rate of air flow out of the Volume that is transferred to locations other than adjacent Volumes.

Additional blocks are used to represent calculations and the mathematical relationships between variables. For example, the volume of the element is calculated with a product block with the user-specified values of length, width, and height.

As discussed above, the twelve inputs and two outputs of the Volume element are used to communicate with other Volume elements. These ports are shaded in light gray in Figure 5.3. The twelve inputs, which are located in the upper left-hand corner of the Volume element, feed into a block labeled Tri-Flux Connector in which the vector components described above are



separated and summed into three variables that represent (1) the total rate of air flow from the Volume element into all connecting (adjacent) elements, (2) the total flux of mass into the Volume element from all connecting elements, and (3) the total rate of air flow into the Volume element from all connecting elements. By definition, the use of twelve inports allows the Volume to communicate with a maximum of twelve other Volume elements. This number was selected to provide a practical but flexible Volume element.<sup>4</sup> Since SIMULINK™ ignores unused ports, a Volume element can be connected successfully to fewer than twelve bordering Volume elements.

The two outputs are located to the right of the block diagram (Figure 5.3) and are shaded in light gray. The first output is the time-dependent pollutant concentration in the Volume element, which is calculated as the product of the pollutant mass and the inverse of volume. The second output — Air Flow Check — is an algebraic sum of all air fluxes into and out of the Volume element. Under normal conditions, the value of this sum should be zero to satisfy the continuity requirement.<sup>5</sup> Hence, the Air Flow Check serves as a useful monitoring variable during model development.

#### 5.4.2 The Exchange element

The Exchange element is used to specify the exchange of air and pollutant between adjacent Volume Elements. The Volume and Exchange elements can be used to model pollutant transport in large, open spaces by describing a system of interconnected volumes. To do so, the space is divided into smaller regions, and each region is represented by a Volume element. Each interface between adjacent regions is then represented by an Exchange element that connects the bordering Volume elements. Examples of using Volume and Exchange elements to represent physical systems are presented in Chapter 6.

The icon representation of the Exchange element is shown in Figure 5.2. The Exchange element contains two inports that accept the pollutant concentrations of bordering Volume elements, and two outputs that direct ventilation and contaminant flux data back to the bordering Volume elements. Each output is a vector of three variables defined in a manner consistent with the Volume element inport to which it connects. The data of each output consist of the contaminant flux into the Volume element from an adjacent element, the back flow rate of air from the Volume

---

<sup>4</sup> For complex systems, it may be desirable to connect a single Volume element to more than twelve bordering elements. In such cases, provision for additional connections can be made by increasing the number of inports and expanding the size of the Tri-Flux Connector element.

<sup>5</sup> Under some conditions, it may be desirable to allow the mass of material in a Volume element to change. For example, the ignition of a fire may cause an initial generation of mass within a Volume that is not immediately ventilated.

element into an adjacent volume, and the rate of air flow from an adjacent element into the Volume element.

The inports and outports of the Exchange element are matched so that the top (or left) inport receives the concentration of one Volume element (e.g., Volume 1) and the top (or left) outport transmits this concentration to a second Volume element (e.g., Volume 2). Thus, if the concentration outport of Volume 1 is connected to the top inport of the Exchange element, then (1) the top outport of the Exchange element should be connected to one of the inports of Volume 2, (2) the concentration outport of Volume 2 should be connected to the bottom inport of the Exchange element, and (3) the bottom outport of the Exchange element should be connected to one of the inports of Volume 1. The sense of these conventions is illustrated in Figure 5.4.

The procedures that the Exchange element uses to convey transport information are illustrated in Figure 5.5, which is the full block diagram of the Exchange element (as unmasked from the icon representation in Figure 5.2). The transport parameters that must be provided are the planar area of the interface shared by the bordering Volume elements and two velocities that represent the magnitude of the air flow in each direction across the boundary plane.<sup>6</sup> These air velocities should correspond to the integrated average of the positive components of a time-averaged velocity profile over the boundary plane. That is, they should reflect the movement of air in each direction, and not simply the net flow in one direction, and should account for the potential for flow opposite the dominant flow direction.

Figure 5.6 demonstrates the calculation of flow velocities for use in Exchange elements. The upper portion of the figure presents two hypothetical velocity profiles that (in a two-dimensional sense) might represent the exchange between two Volume elements as a function of height. In these examples, Volumes 1 and 2 are assumed to be on the left and right sides of the centerline, respectively. Analytical equations for the assumed velocity distribution are presented below each profile.

In the example on the left of Figure 5.6, the velocity profile is evenly distributed about the centerline axis. Thus, the net flow across the cross-section is zero. Flow rates for use in Exchange elements, however, must be evaluated separately in each direction across the boundary plane. This separate evaluation is reflected by the limits of the two integrals, in which the average velocity  $u_{1 \rightarrow 2}$  is calculated for the top half of the profile and the average velocity  $u_{1 \leftarrow 2}$  is evaluated over the bottom half of the profile. In the example on the right, the velocity profile is skewed to create a predominant flow from Volume 1 (left) to Volume 2 (right). Again, average velocities are calculated as integrals of the analytical profile, with integration limits determined by

---

<sup>6</sup> The Exchange element could alternatively be constructed using volume flow rates (in units of volume/time) instead of the product of area and velocity.

the crossover point where the velocity changes direction. The relative values of  $u_{1 \rightarrow 2}$  and  $u_{1 \leftarrow 2}$  depend upon the value of the parameter "a", which, as indicated in Figure 5.6, corresponds to the distance from the origin of the y-axis. If  $a=0$ , the profiles on the left and right are identical, and hence so are the values of  $u_{1 \rightarrow 2}$  and  $u_{1 \leftarrow 2}$ . The general relationship for other values of "a" is given as follows:

$$\begin{array}{lll} 0 < a < 1, & u_{1 \rightarrow 2} > u_{1 \leftarrow 2} > 0, \\ 0 > a > -1, & u_{1 \leftarrow 2} > u_{1 \rightarrow 2} > 0, \\ a \geq 1, & u_{1 \rightarrow 2} > 0, & u_{1 \leftarrow 2} = 0, \\ \text{and} & a \leq -1, & u_{1 \leftarrow 2} > 0, & u_{1 \rightarrow 2} = 0. \end{array}$$

The three user-defined inputs of the Exchange element are shaded in dark gray in Figure 5.5 and are summarized as follows:

### User-Defined Input Blocks for the Exchange Element

<u>Block Title</u>	<u>Block Description</u>
Area of exchange	The area of the rectangular plane that is shared by adjacent (bordering) Volume elements.
Velocity Room 1 to 2	The average airflow velocity from Volume 1 to Volume 2, where (by convention) the concentrations of Volumes 1 and 2 enter the top and bottom inports to the Exchange element, respectively.
Velocity Room 2 to 1	The average airflow velocity from Volume 2 to Volume 1.

The inports and outports of the Exchange element, as previously discussed for the icon representation (Figure 5.2), are highlighted in light gray in Figure 5.5. Again, the inports labeled 1 and 2 (top and bottom on the Exchange element icon) are assumed to receive the contaminant concentrations from Volumes 1 and 2, respectively, and the outports labeled 1 and 2 (again top and bottom on the icon) are assumed to transfer flux data to Volumes 2 and 1, respectively.

### 5.4.3 Emission elements

Pollutants can be released by any number of mechanisms, and it is often difficult to characterize the responsible processes. In some cases, emissions can be estimated directly by measurement. In other cases, however, measurements may be impractical due to the cost and/or lack of availability of sophisticated monitoring, the infeasibility of assessing fugitive emissions, or the impracticality of being able to anticipate accidental releases.

Consequently, reliable models that estimate pollutant emissions serve as surrogates to direct measurements, especially if they are based on the physical principles that influence contaminant release from a particular process. Additionally, the predictive capability of such models can be useful in evaluating contingencies for accidental releases and changes in processes.

Models are also limited, however, since either the characteristics of many emission sources are not well-known, or if the controlling mechanisms are characterized adequately, critical data may be unavailable. For some processes, theoretical and practical knowledge are sufficient to develop credible emission models that depend upon readily available data for input.

Emission elements are designed to fit into the Volume element as a substitute for the user-defined emission input in which the emission rate of the pollutant is simply specified at a known (or assumed) value. The three examples of Emission elements described in this section are (1) solvent evaporation from an open tank, (2) volatile organic emission from coil coating operations, and (3) the accidental release of a vapor from a tank of liquid with a boiling point lower than ambient temperature.

The Emission elements presented herein should not be interpreted as an exhaustive collection. Instead, they are intended to serve as examples of a much larger set of elements that could be developed to model process-specific pollutant emissions.

#### 5.4.3.1 Solvent evaporation from a rectangular tank

Solvents are used widely in industrial processes for degreasing, cleaning, and other purposes. In many cases, an opportunity exists for solvents to evaporate. As a generic example, the evaporation of a volatile solvent from an open tank is examined.

The emission rate  $E$  from a rectangular source such as an open tank containing a volatile liquid can be estimated using the following equation (Incropera and DeWitt, 1981):

$$E = \frac{0.037 D_a R_e^{4/5} S_c^{1/3} A}{L V} [C_v - C] \quad \text{if flow is turbulent} \quad (R_e \geq 500,000)$$

$$E = \frac{0.664 D_a R_e^{1/2} S_c^{1/3} A}{L V} [C_v - C] \quad \text{if flow is laminar} \quad (R_e < 500,000)$$
(5.1)

where

- $D_a$  is the diffusion coefficient of the chemical in air,
- $R_e$  is the Reynolds number for the tank and air flow rate, defined as  $uL/v_{air}$ ,
- $S_c$  is the Schmidt number for the chemical in air, defined as  $v_{air}/D_a$ ,
- $u$  is the velocity of air above the tank,
- $L$  is the length of the tank in the direction parallel to air movement above the tank,
- $A$  is the area of the tank,
- $V$  is the volume into which chemical disperses,
- $v_{air}$  is the kinematic viscosity of air,
- $C$  is the concentration of the chemical in the air in the general vicinity of the tank,
- and  $C_v$  is the concentration of chemical in air just above the liquid surface, which can be estimated from the vapor pressure of the chemical.

The Emission element designed to emulate Equation (5.1) is displayed in Figure 5.7, which represents the unmasked icon labeled "Emission from rectangular tank g/s" in Figure 5.2. As indicated by the title, the element predicts a chemical emission rate in units of g/s. User-defined inputs, which include chemical-specific properties, tank dimensions, and other parameters, are described in the following list, which are shaded dark gray in Figure 5.7.

### User-Defined Input Blocks for the Emission Element to Estimate Solvent Evaporation from a Rectangular Tank

<u>Block Title</u>	<u>Block Description</u>
Diffusivity in air	Molecular diffusivity of the chemical (solvent) in air ( $\text{m}^2/\text{s}$ ). Values for many chemicals may be obtained from Perry and Green (1984) or U.S. EPA (1987).
Vapor Pressure	Vapor pressure of the chemical at standard pressure and the temperature of the liquid (atm).
Molecular weight	Molecular weight of the chemical (g/mole).
Temperature	Temperature of the liquid chemical (K).
Kinematic viscosity	Kinematic viscosity of air at the temperature in the volume ( $\text{m}^2/\text{s}$ ).
Crossover Re	Reynolds number at which the flow changes from laminar to turbulent (nominally 500,000 for boundary layer flow).
Length	Dimension of the opening in the tank parallel to air movement (m).
Width	Dimension of the tank opening perpendicular to air movement (m).

The units specified for each variable are necessary to maintain dimensional consistency. The element has two inports and one output that interface with the Volume element. These ports are shaded light gray in Figure 5.7. The inport labeled "Concentration in host volume  $\text{g}/\text{m}^3$ " is designed to be connected to the well-mixed pollutant concentration in the volume that hosts the tank (calculated as the mass divided by the volume within the Volume element). If necessary, the units of the concentration may have to be adjusted to  $\text{g}/\text{m}^3$ . The second inport requires the specification of the velocity above the tank. This provision is designed to allow the user to scale this velocity from other flow variables in the host Volume element if desired.

### 5.4.3.2 Volatile organic emission from coil coating operations

This Emission element exemplifies the use of empirical data to derive a generic model of the rate at which volatile organic compounds will be released as fugitive emissions during a common industrial practice. Specifically, this element characterizes the coating of metal coil surfaces, which is the linear process by which protective or decorative organic coatings are applied to a flat metal sheet or strip packaged in rolls or coils (U.S. EPA, 1985). The coating process involves the application of a thin layer of liquid-borne material. Ventilation controls are used to capture the evaporating carrier fluid, but are less than 100% effective. Fugitive emissions are typical at two points in the operation: after the application of the film, and in the vicinity of the curing oven and quenching station.

The rate of volatile emissions from a typical coil coating operation can be estimated as (U.S. EPA, 1985):

$$E = \frac{0.623 \text{ ATVD}}{S} \quad (5.2)$$

where

- E is the mass emission rate (lb/hr),
- A is the rate at which metal is coated (ft<sup>2</sup>/hr), estimated as the product of line speed (ft/hr) and strip width (ft),
- V is the volatile organic content of the coating (as a volume fraction),
- D is the density of the volatile compounds (lb/gal),
- S is the solids content of the applied coating (as a volume fraction),
- and T is the dry film thickness of the coating (in).

U.S. EPA (1985) categorizes each of the variables in Equation (5.2) based upon a survey of industrial practices. Operations are classified as small, medium, and large in scale, and are differentiated by the nature of the carrier fluid as either solventborne or waterborne. Typical parameters for each of the six possible combinations have been incorporated within the Emission element labeled "Coil coating emissions g/s" in the Figure 5.2 library. The element contains a single output that delivers the mass emission rate in units of g/s. The unmasked element is depicted in Figure 5.8, which contains an input parameter that allows the user to choose from the six possible combinations of operation size and carrier fluid. This input feeds into six masked icons that control the selection of each parameter used in Equation (5.2) to estimate the mass emission rate. Each of these parameter subelements is constructed in a similar fashion, an example of which is shown in Figure 5.9. Based upon the value of the input key, a look-up table is used to determine the appropriate parameter value as a function of operation size and carrier fluid. Alternatively, the U.S. EPA (1985) default value of any parameter can be overridden by setting the user-defined value greater than zero. This feature is executed through the switch

element that selects the user-defined value if the user-defined value is less than zero, and otherwise chooses the U.S. EPA (1985) default value. By default, the user-defined value is set to -1 to defer to use of the U.S. EPA (1985) values.

### 5.4.3.3 Vapor release from a ruptured tank

In contrast to the previous two examples, this Emission element demonstrates a time-dependent pollutant release that could result from the rupturing of a tank storing a chemical in liquid form that has a boiling point lower than ambient temperature. Assuming that the liquid in the tank is at approximately the same temperature as its surroundings, headspace in the tank will contain the chemical in vapor form at a pressure greater than atmospheric. As a consequence, the accidental rupturing of the tank will allow the vapors to exhaust from the tank, thereby allowing more liquid to evaporate. Assuming that the tank is well-insulated such that adiabatic conditions apply, the latent heat transferred during boiling will lead to a decrease in the temperature of the liquid. Since the vapor pressure of a liquid decreases with temperature, a temperature will be reached at which the vapor pressure in the tank is reduced to atmospheric pressure, and the flux of vapors from the tank will cease.

This element is applicable to chemicals that (1) have a vapor pressure higher than standard atmospheric pressure at typical storage or process temperatures and (2) will attain a vapor pressure less than atmospheric pressure with a moderate amount of evaporative cooling. Examples of such chemicals include hydrogen fluoride and ammonia.

For simplicity, we assume that a hole forms in the tank or piping above the height of the liquid surface so that vapor alone issues from the hole. Two first-order differential equations can be used to model the state of the boiling liquid and emission rate. The first relates the mass of the liquid in the tank to the rate at which vapor leaves the tank:

$$\frac{dM}{dt} = -A u \rho_v \quad (5.3)$$

where

M is the mass of liquid in the tank (kg),  
 t is time (s),  
 A is the cross-sectional area of the hole (m<sup>2</sup>),  
 u is the velocity of the effluent vapor (m/s),  
 and  $\rho_v$  is the density of the vapor exiting the tank (kg/m<sup>3</sup>).

The second differential equation is an energy balance that equates the heat of vaporization of the liquid-vapor phase change with the internal energy of the liquid:



$$H_{lg} \frac{dM}{dt} = M C_p \frac{dT}{dt} \quad (5.4)$$

where

$H_{lg}$  is the latent heat of vaporization (kcal/kg),  
 $C_p$  is the specific heat of the liquid at constant pressure (kcal/kg-K),  
 $T$  is the temperature of the liquid-vapor system (K),

and other variables are defined in Equation (5.3). Since four variables ( $M$ ,  $T$ ,  $u$ , and  $\rho_v$ ) vary with time, four equations are necessary for mathematical closure, and thus two additional independent relationships are necessary. First, we assume that the vapor phase obeys the ideal gas law:

$$P = \rho_v R T \quad (5.5)$$

where

$P$  is the pressure in the tank (Pa),  
 $R$  is the gas constant (gas specific) (Pa-m<sup>3</sup>/K-g),

and  $\rho_v$  and  $T$  are the density and temperature of the vapor, as defined previously. The addition of pressure as a variable requires the specification of still another relationship for closure (thus two additional equations are still needed). Assuming that the temperature of the system does not vary over a large range, an approximate relationship relating pressure and temperature can be written:

$$P = a e^{bT}$$

where the constants  $a$  and  $b$  are parameters obtained by curve-fitting empirical data. The final relationship is derived from compressible flow theory and relates the exit velocity to other system variables:

$$u = \sqrt{\frac{2kRT}{k-1} \left[ 1 - \left( \frac{P_a}{P} \right)^{\frac{k-1}{k}} \right]}$$

where

$P_a$  is atmospheric pressure (Pa),  
 $k$  is the ratio of the ratio of the specific heat at constant pressure ( $C_p$ ) to the specific heat at constant volume ( $C_v$ ) for the vapor phase,

and  $P$ ,  $R$ , and  $T$ , are defined above.

Equations (5.3)–(5.7) have been programmed into the Emission element shown in Figure 5.10. Consistent with the system of equations, the element contains two integration blocks — one for the mass of liquid ( $M$ ) and one for the temperature ( $T$ ) of the system. The constitutive relationships are masked in function blocks, which are represented by the symbol  $f(u)$  in the block diagram. These blocks permit the specification of a user-defined functional relationship that can depend on an arbitrary number of variables that are channeled through Mux blocks.

User-defined inputs to the Ruptured Tank Emission element are summarized in the following list and are highlighted in dark gray in Figure 5.10.

#### User-Defined Input Blocks for the Emission Element to Estimate the Vapor Emission Rate from a Ruptured Tank

<u>Block Title</u>	<u>Block Description</u>
$H_{fg} / C_p$	Ratio of the latent heat of vaporization to the specific heat of the liquid at constant pressure (K).
Spec heat ratio $k$	Ratio of the specific heat at constant pressure to the specific heat at constant volume for the vapor phase.
Gas Constant	The chemical specific gas constant for use in the ideal gas law (defined as the universal gas constant divided by the molecular weight of the chemical) ( $\text{Pa}\cdot\text{m}^3/\text{g}\cdot\text{K}$ ).
Area of hole	Cross-sectional area of the hole through which vapor is released.
Atm. Pressure	Atmospheric pressure (Pa).
Pressure	The constants $a$ and $b$ that define the chemical-specific relationship between vapor pressure and temperature are specified in this function [more complex relationships than Equation (5.6) may be established in this function if desired].

In addition, initial values must be specified for both the mass and temperature of the liquid that should reflect conditions at the beginning of the release. The single output of the Emission

element, which is highlighted in light gray in Figure 5.10, provides a time-dependent emission rate in kg/s.

#### 5.4.4 Time-averaging element

As demonstrated by the Volume, Exchange, and Emission elements, the basic SIMULINK™ elements can be used as building blocks to construct sophisticated elements capable of simulating complex mathematical models. The masking feature, whereby a complex series of elements is transformed into an icon that simply processes input and yields output, is an extremely powerful tool since the complex model is reduced to the level of another building block.

A number of building blocks for indoor air modeling applications have been developed in this study. In some cases, complex building blocks are embedded in even other elements. For example, the Emission elements described in section 5.4.3 are designed to be used as block components in Volume elements.

The time-averaging element described in this section does not fit into a specific category, but its general utility warrants documentation. As discussed in Section 4.2, the potential for adverse health effects to result from exposure to a chemical often depends upon the integrated, or total, exposure over time. Thus, time-averaged concentrations may be a more appropriate measure of exposure than instantaneous concentrations, since the latter often fluctuate with time and hence are an uncertain estimate of average exposure. The situation is even more complex for personal exposure measurements since they also average spatial fluctuations in pollutant concentrations due to the movement of individuals.

The icon of the time-averaging element in Figure 5.2 has two inports and one outport. The inports expect (1) a variable to be averaged and (2) time. The full (unmasked) element is portrayed in Figure 5.11. The time-averaging element simply maintains the integral of the variable with time and divides by the elapsed time to provide a time-averaged value of the variable at any point in time. Thus, the time-average is itself a function of time, since the time-average is calculated from the beginning of the simulation, which is a fixed point, to some later time that includes the time-dependent history of values over the elapsed (time-dependent) simulation period.

## 5.5 SIMULINK™ simulations

Complementing SIMULINK™'s user-friendly graphical interface are sophisticated mathematical algorithms for simulating dynamic, or time-dependent, systems.<sup>7</sup> Each integration element within a block diagram introduces a state variable that is (1) initially set at a user-specified value<sup>8</sup> and is (2) simulated for a period of time. Temporal changes in the state variables are governed by the mathematical equations that underlies the physical system represented by the block diagram.

As their name implies, integration elements integrate changes in the value of a state variable during the course of a simulation. Mathematically, SIMULINK™ employs numerical integration techniques for this purpose. In such methods, first-order differential equations are discretized to finite timesteps. New values of the state variables at the next point in time ( $t+\Delta t$ ) are predicted from the values at the current time ( $t$ ), with the rate of change governed by the time-dependent evaluation of the slopes of the differential equations.

SIMULINK™ affords the user control over the basic factors that affect the course of the numerical simulation. Within the SimulationParameters menu, the values of the starting time and stopping time of the simulation are specified. These parameters specify the period of integration. Additional user-defined parameters are minimum and maximum timesteps and numerical tolerance; these parameters affect the speed and accuracy of the simulation. Finally, the user is allowed to choose from seven different integration algorithms. The choice of these algorithms also influences the speed and accuracy of the simulation, and some methods are best suited to specific types of applications. The available options, along with a discussion of their relative advantages, are presented in the SIMULINK User's Guide (MathWorks, 1992).

---

<sup>7</sup> More correctly, SIMULINK™ has the capability to simulate initial value problems involving first order differential equations. Typically, initial value problems consider time as the variable of differentiation, but other variables may also be used.

<sup>8</sup> An initial value for a state variable is set by opening the integration elements within the block diagram. This action reveals a SIMULINK™ menu for the integration element that permits the user to specify a numerical constant for the initial value, which by default is set to zero.

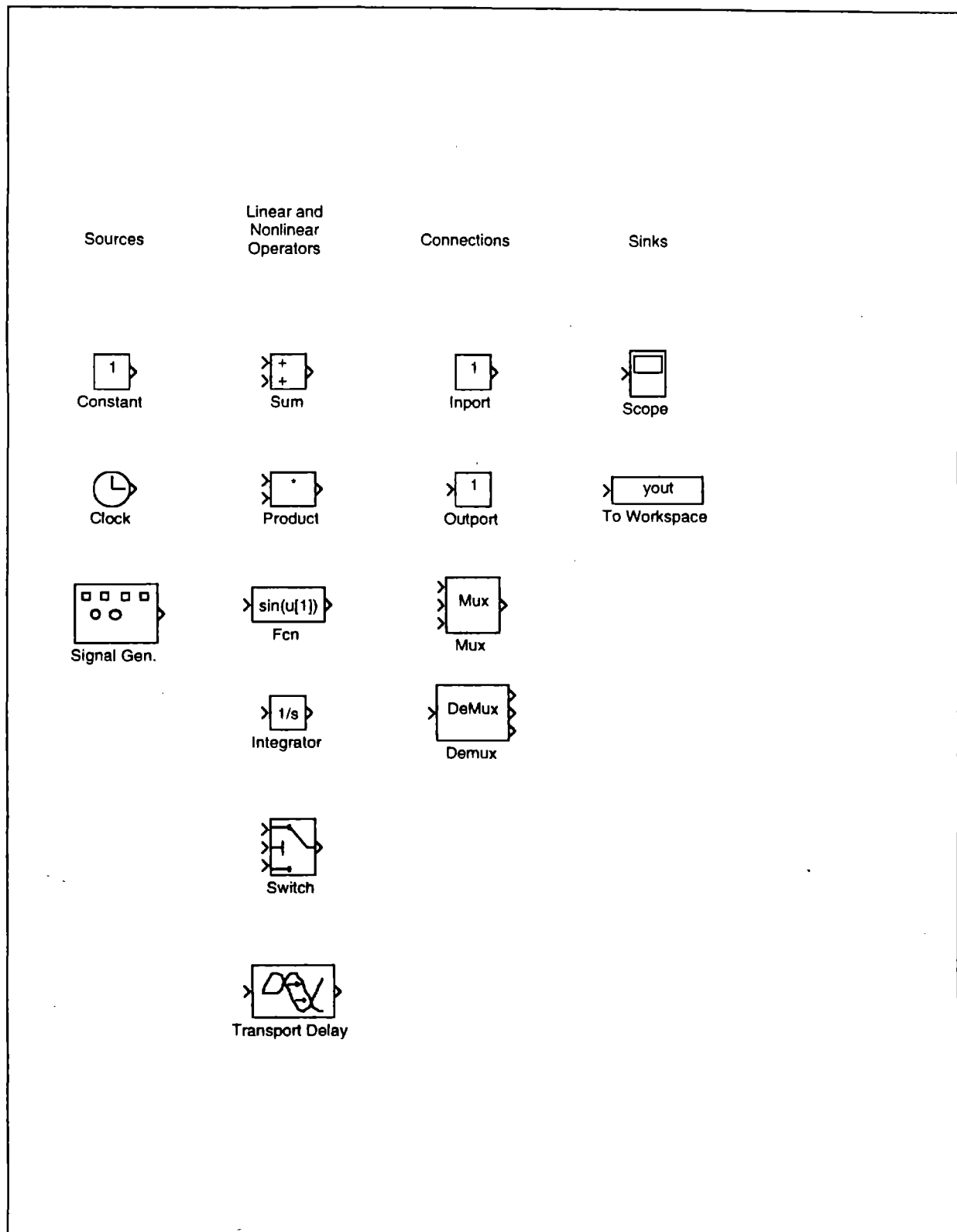


Figure 5.1 SIMULINK™ elements used in the analyses

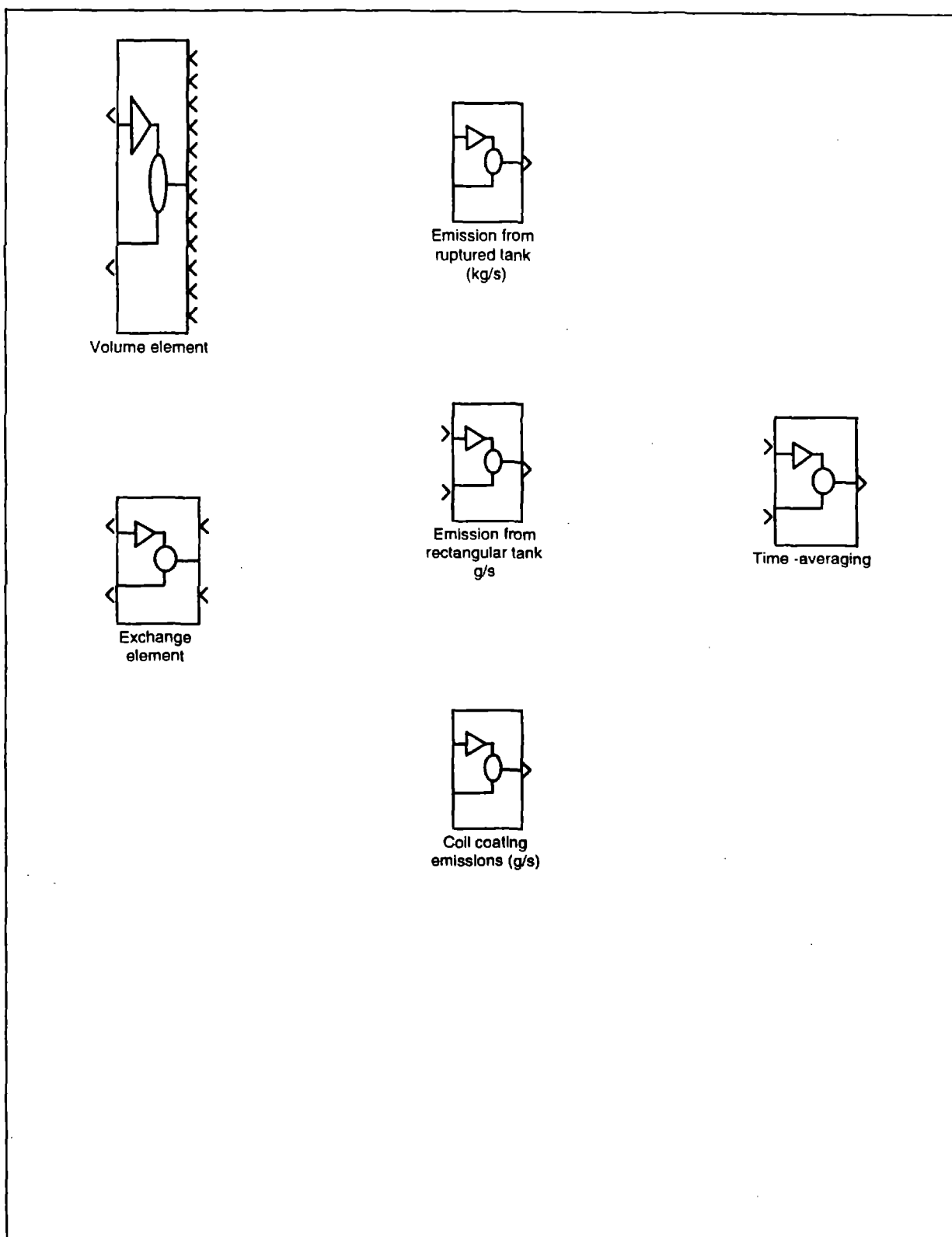


Figure 5.2 SIMULINK<sup>™</sup> elements developed for indoor air modeling applications

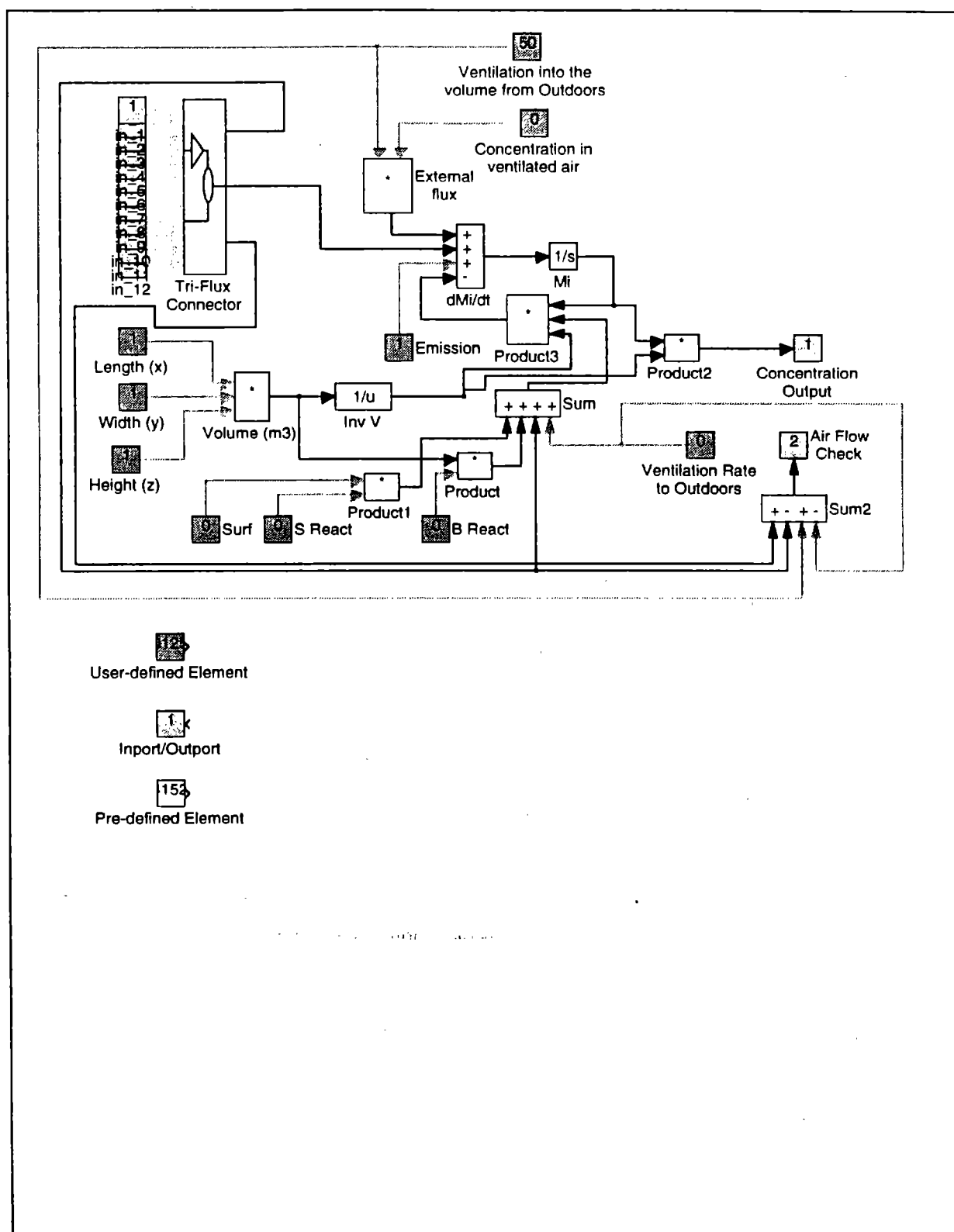


Figure 5.3 Block diagram for the Volume element

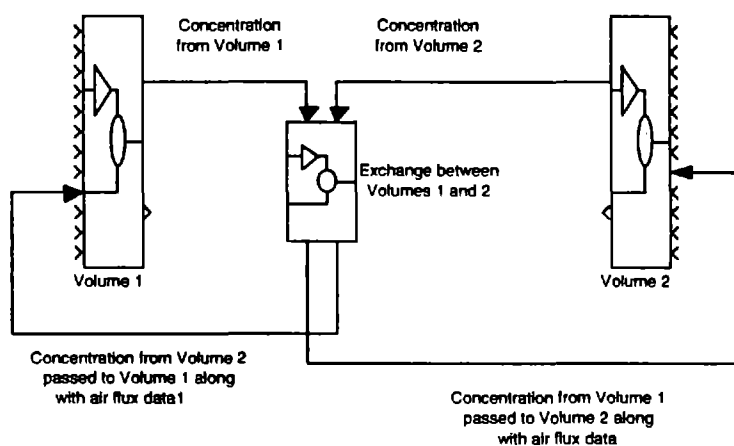
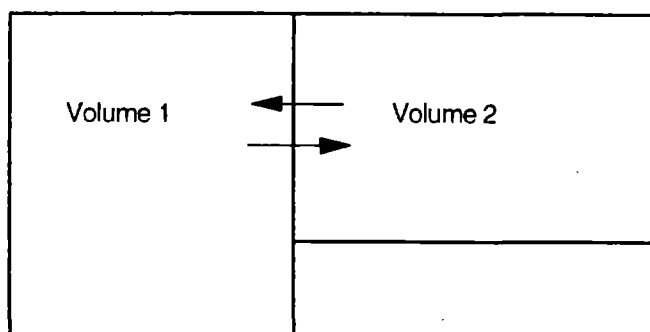


Figure 5.4 Conventions used to connect two Volume elements with an Exchange element



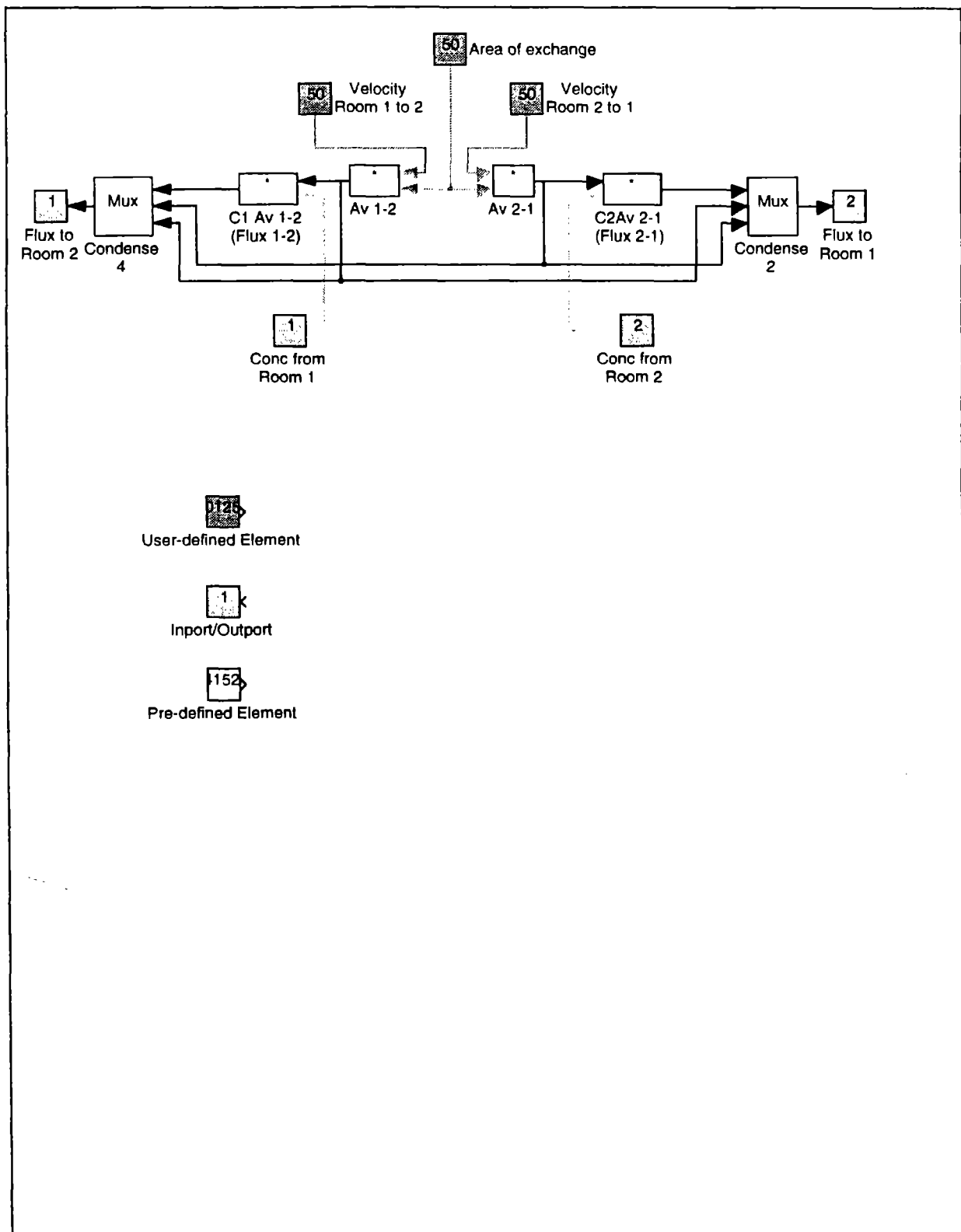
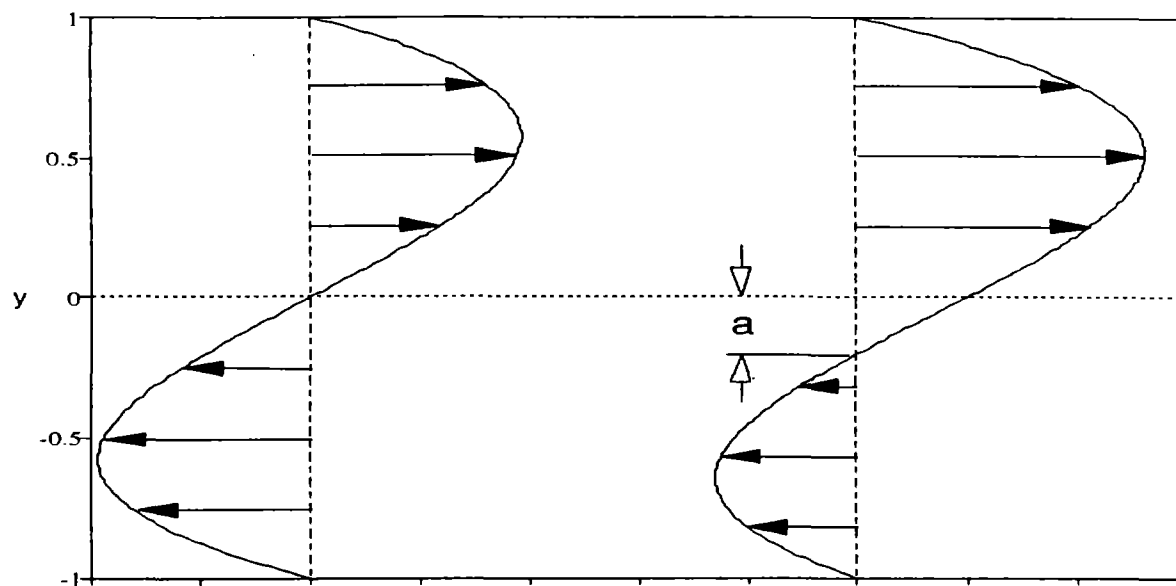


Figure 5.5 Block diagram for the Exchange element



$$u = y - y^3$$

$$u = y - y^3 + a(1 - y^2)$$

$$u_{1 \rightarrow 2} = \frac{\int_{y=0}^1 u \, dy}{\int_{y=0}^1 dy} = \frac{1}{4}$$

$$u_{1 \rightarrow 2} = \frac{\int_{y=-a}^1 u \, dy}{\int_{y=-a}^1 dy} = \frac{\frac{1}{4} + \frac{2}{3}a + \frac{a^2}{2} - \frac{a^4}{12}}{1 + a}$$

$$u_{1 \leftarrow 2} = \frac{-\int_{y=-1}^0 u \, dy}{\int_{y=-1}^0 dy} = \frac{1}{4}$$

$$u_{1 \leftarrow 2} = \frac{-\int_{y=-1}^{-a} u \, dy}{\int_{y=-1}^{-a} dy} = \frac{\frac{1}{4} - \frac{2}{3}a + \frac{a^2}{2} - \frac{a^4}{12}}{1 - a}$$

Figure 5.6 Examples of the calculation of volume flux rates for use in Exchange elements

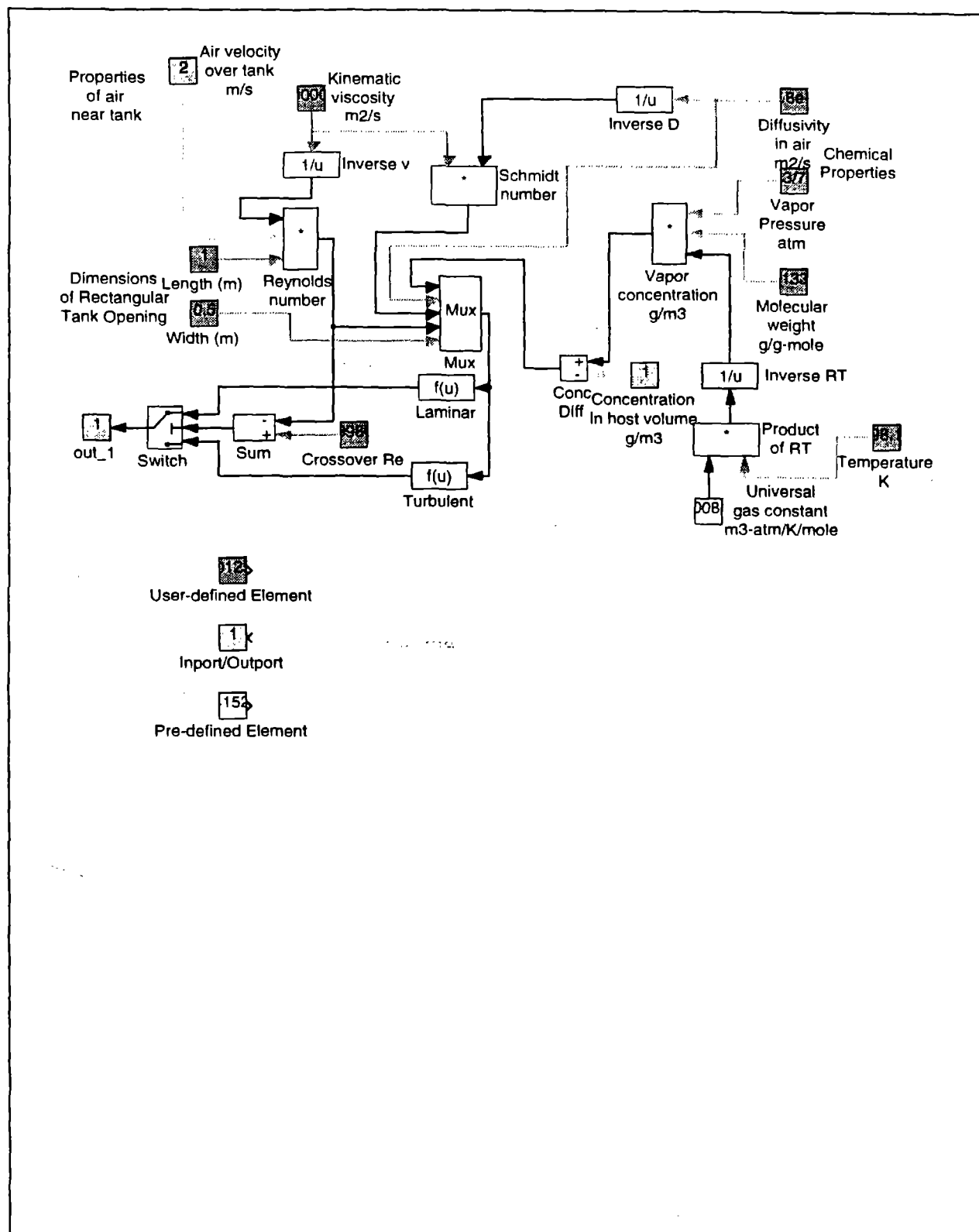


Figure 5.7 Emissions from a rectangular tank

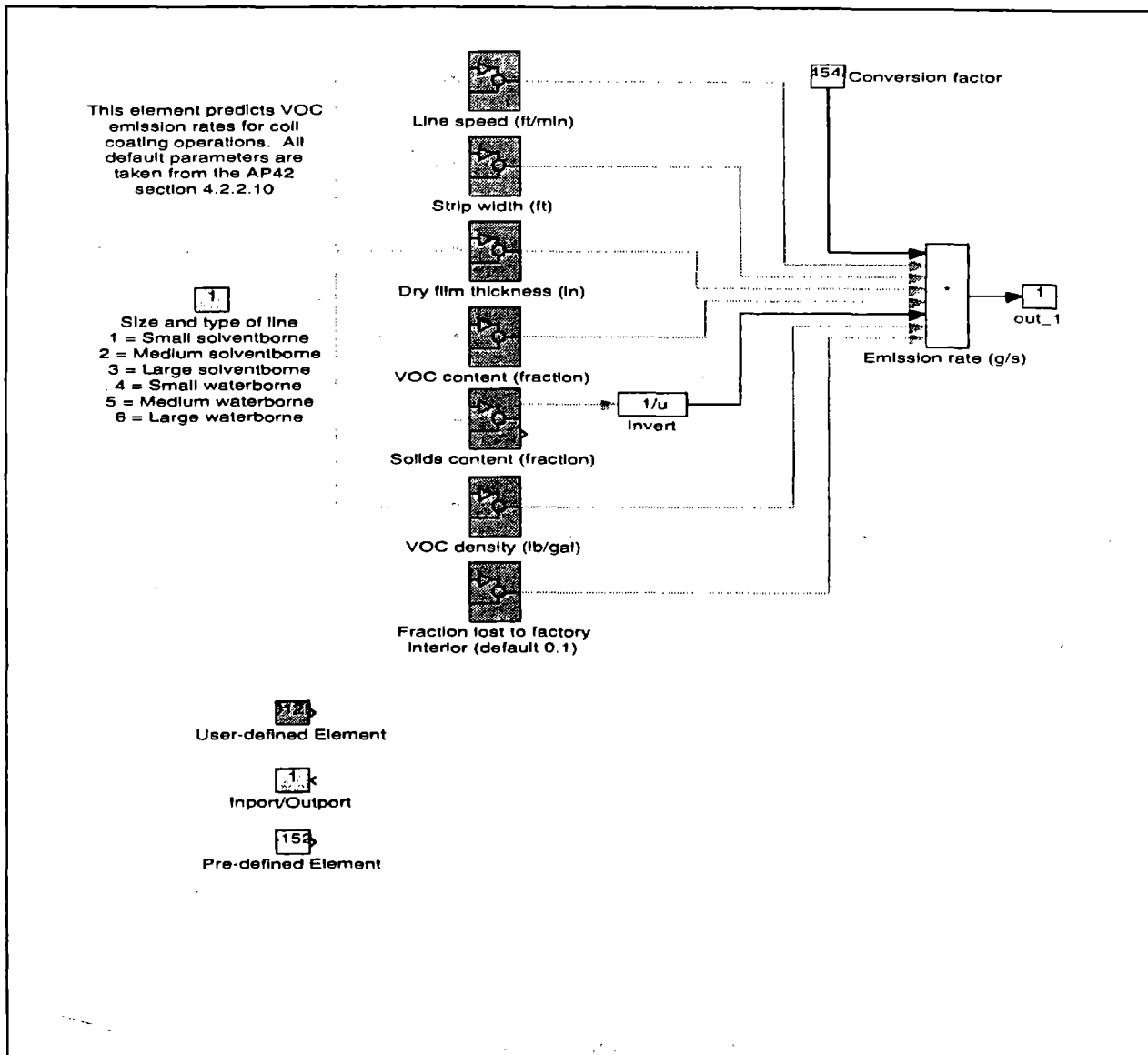


Figure 5.8 Emissions from a coil-coating operation

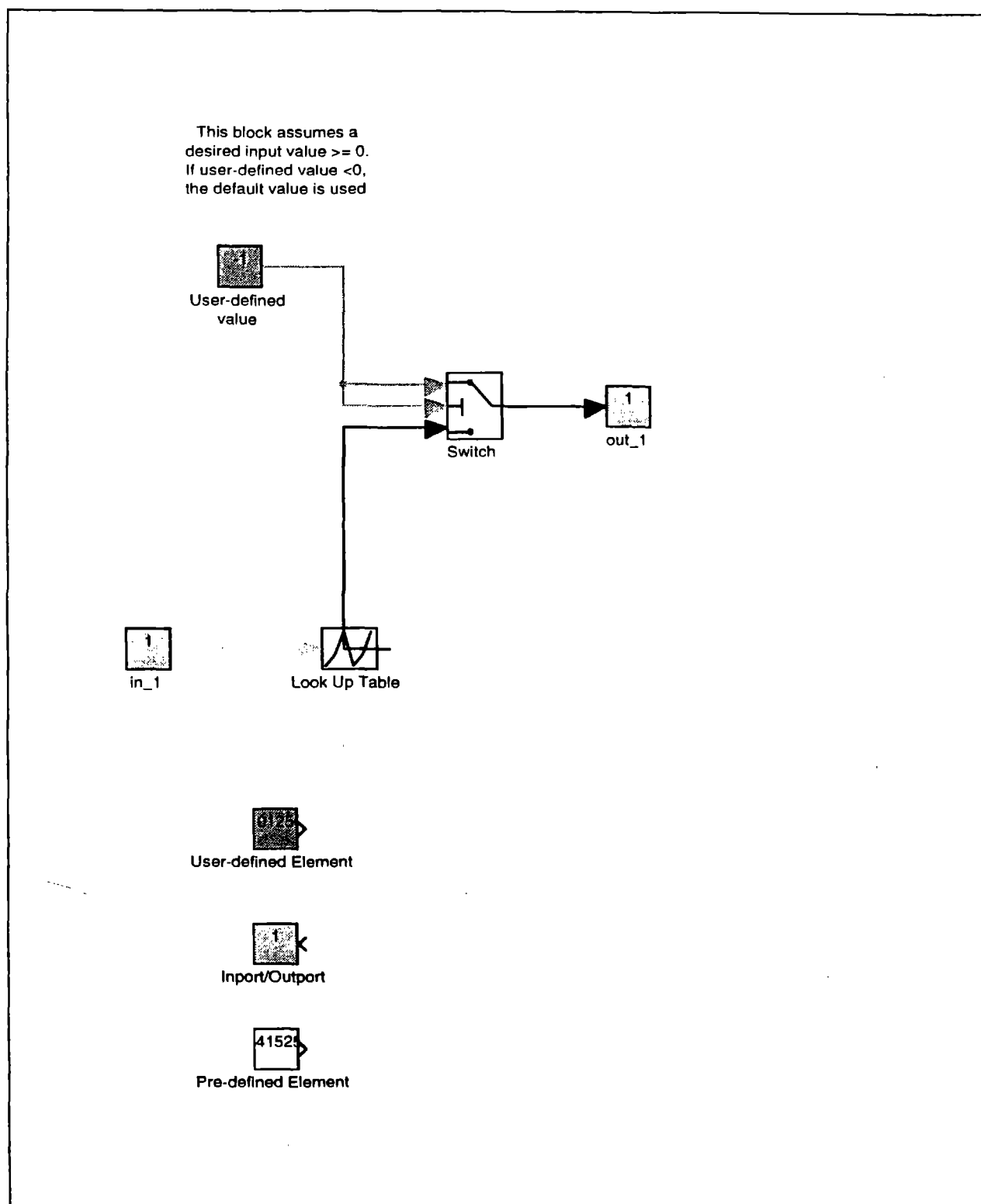


Figure 5.9 Example of the simultaneous use of a lookup table and default override option as implemented in the Coil coating Emission element

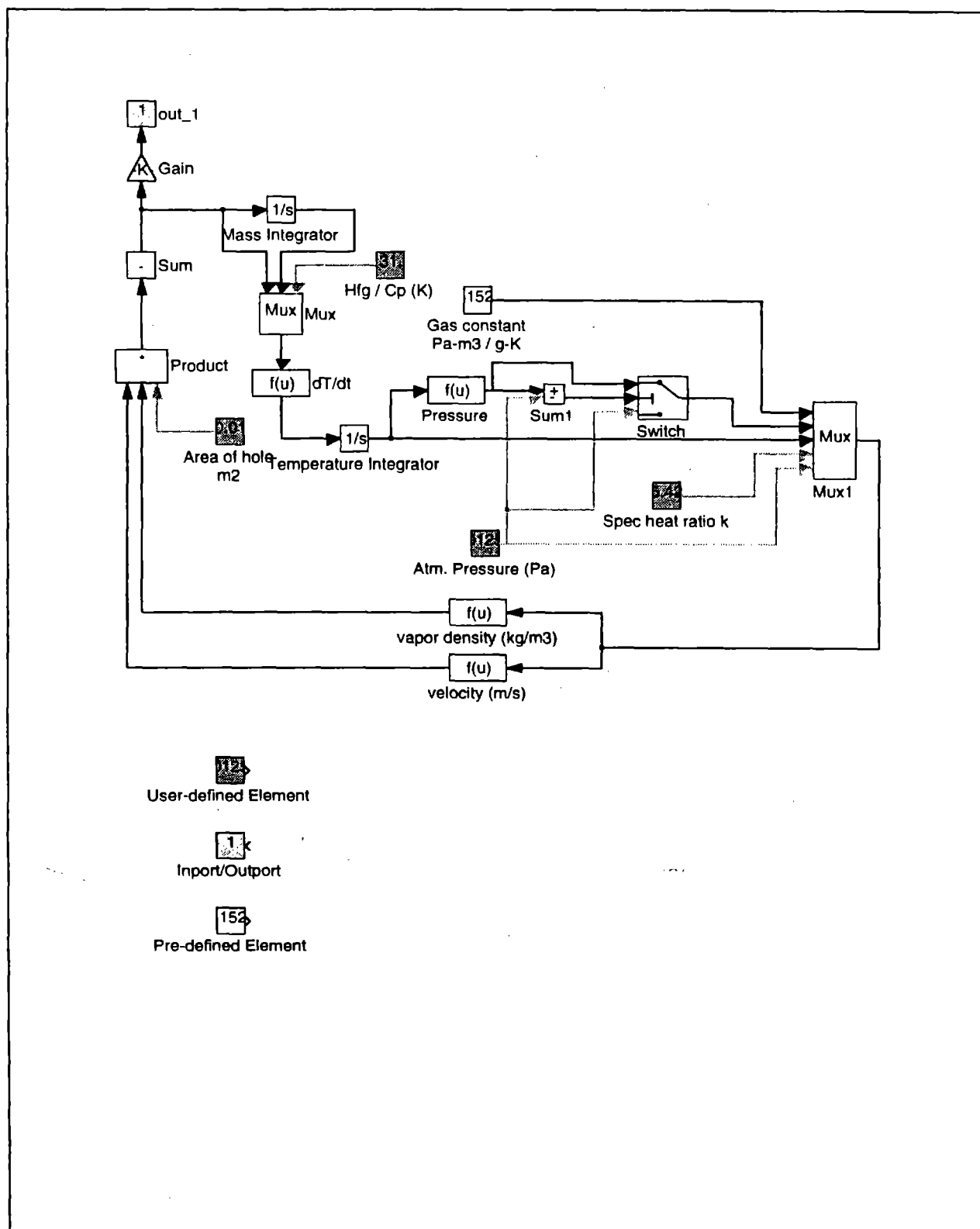


Figure 5.10 Vapor release from a ruptured tank

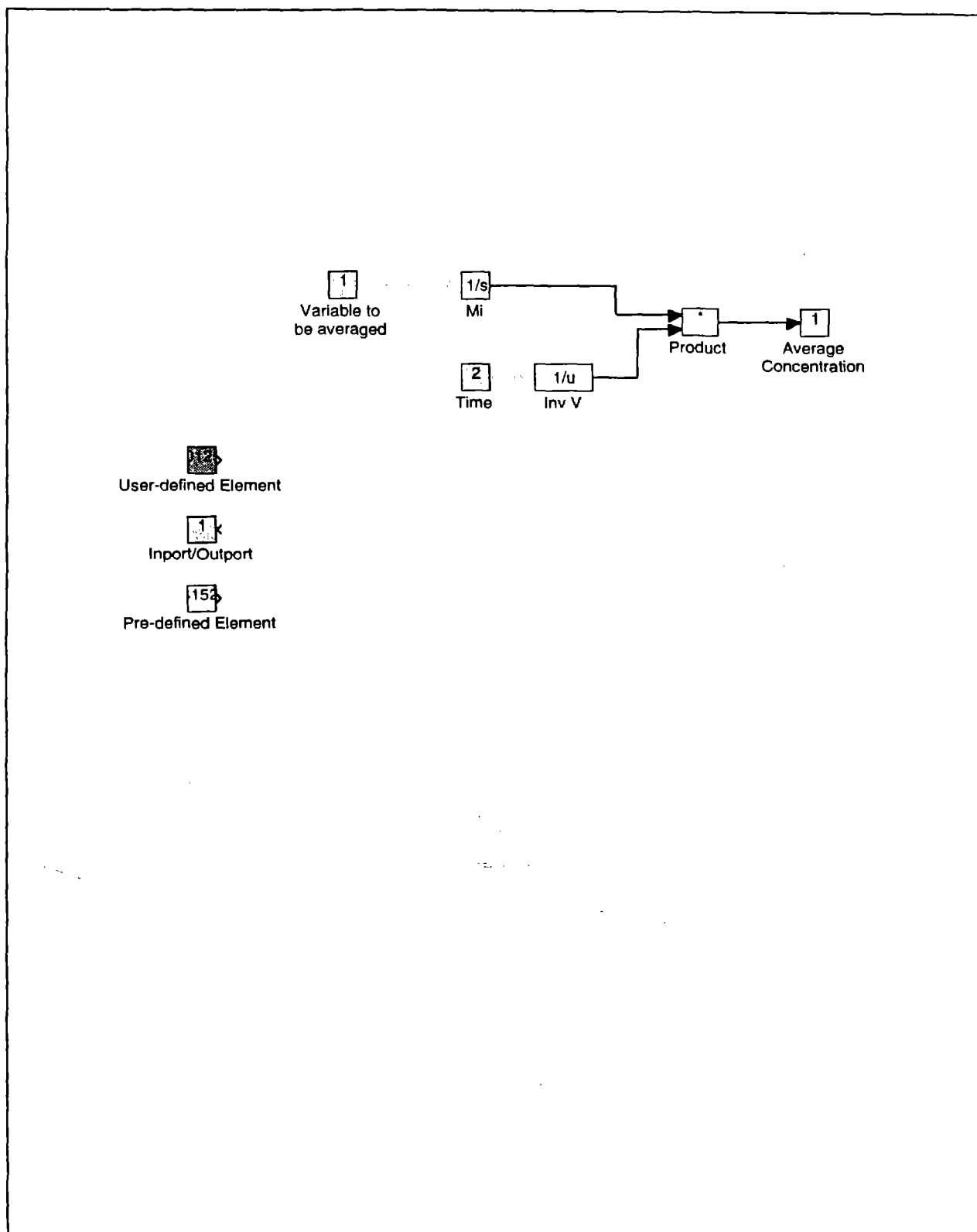


Figure 5.11 Time-averaging element





## 6 Applications

This chapter demonstrates the use of the SIMULINK™ elements developed for indoor air modeling. Four problems are considered: two contrived examples are developed to illustrate the modeling techniques, and two detailed applications are examined that address actual indoor air issues. The first application simulates the behavior of ozone in the indoor environment. The second application is based on an extensive NIOSH Industrial Hygiene Sampling Survey Report. The approach to each of the four problems is similar: the physical scenario is described, a model is developed from the SIMULINK™ elements, and the simulation results are reported and discussed.

### 6.1 Illustrative examples

The two illustrative examples described in this section are intended to introduce the user to the process of simulating heterogeneously mixed air spaces with SIMULINK™. The first example, which considers two connected volumes, is relatively simple and demonstrates the basic use of the indoor air modeling elements. The second example considers a region with eight Volume elements and serves to emphasize the ability of SIMULINK™ to deal with relatively large and complex problems.

#### 6.1.1 Two-volume example

In Section 4.3, an example based on a single emission source and two volumes was developed and solved analytically for simple initial conditions. In this section, this same problem is modeled using SIMULINK™ elements.

The SIMULINK™ block representing the first volume is shown in Figure 6.1. The dimensions are defined such that the volume is  $100 \text{ m}^3$ . The contaminant emission rate is set at  $100 \text{ g/hr}$  and there are no sinks (reactions or deposition). Clean air is vented into the volume at a rate of  $100 \text{ m}^3/\text{hr}$ . Note that the air exchange with Volume 2 is not specified in Volume 1, but instead in the Exchange element that connects the two Volume elements, as shown in Figure 6.2. Here it can be seen that the area of air exchange is  $20 \text{ m}^2$  and the air velocity from Volume 1 to Volume 2 is  $5 \text{ m/hr}$ , resulting in an air exchange rate of  $100 \text{ m}^3/\text{hr}$ . The air velocity from Volume 2 to Volume 1 is set to zero, establishing no return airflow from Volume 2 to Volume 1.

The SIMULINK™ block representing the second volume is shown in Figure 6.3. The volume of Volume 2 is set to  $100 \text{ m}^3$  — the same as Volume 1. The emission rate is set to zero so that the only source of pollutant is that arriving from Volume 1. As demanded by the conservation of air

flow, ventilation of  $100 \text{ m}^3/\text{hr}$  to the outdoors is assigned to Volume 2. The initial pollutant concentration in both Volumes 1 and 2 is set to zero.<sup>1</sup>

Figure 6.4 shows the SIMULINK™ block representation of the entire system. A time-averaging block has been included, and five variables are established in the MATLAB® workspace: air pollutant concentrations in Volumes 1 and 2, time-averaged air pollutant concentrations in Volumes 1 and 2, and the time output. The time output is included because it is required for plotting.<sup>2</sup>

The predicted air concentrations are plotted as a function of time for the first 20 hours of simulation in Figure 6.5. The instantaneous concentration profiles in Volumes 1 and 2 are essentially identical to their analytical analogues displayed in Figure 4.11. This similarity indicates that (1) the construction of the two-volume system is consistent with the theoretical development of Section 4.3 and (2) the SIMULINK™ simulation is reasonably accurate (to at least visible limits).

Obviously, the ability to reproduce analytical solutions with numerical integration is of limited interest since the solution is already available in a convenient, tractable form. Analytical treatment, however, quickly becomes impractical or impossible once the complexity of governing equations increases. In such cases, the flexibility of numerical integration is invaluable. For example, consider an extension of this simple example in which the chemical emission rate is time-dependent, switching on and off at periodic intervals. An analytical solution can be constructed by superimposing solutions to a unit-step problem, alternating positive and negative inputs at the same frequency as emission changes. Since an additional term must be added with each step change in emission, the analytical solution becomes more and more unwieldy as it progresses.

The analysis of such a problem is facilitated through implementation of the SIMULINK™ indoor air modeling algorithms. Figure 6.6 shows an alternate on/off emission block that can be substituted for the constant emission rate block contained in the Volume element shown in Figure 6.1. This element produces an intermittent emission that alternates between on and off every hour. The

---

<sup>1</sup> The specification of initial values is accomplished by opening the mass integration elements in each of the Volumes and setting the initial value to zero. As noted in Section 5.5, the user gains access to the initial value by opening a SIMULINK™ integration block. Note that the state variable of a Volume element is the mass of the pollutant within the volume, and not the pollutant concentration in the volume. Consequently, the initial value is calculated as the product of volume and the initial pollutant concentration.

<sup>2</sup> MATLAB® does not automatically save the time values generated by the clock, hence they must explicitly be saved with a "to workspace" element.

oscillation is accomplished by a Signal Generator block set to generate a Square Wave of unit amplitude and period of two hours. Since the Signal Generator begins its first cycle with a value of -1, it is necessary to multiply its output by -1 with the Reverse Sign constant block. The result is used to toggle the Switch block between 0 and 1. The output of the Switch block is multiplied by the emission strength of 100 g/hr, resulting in an output to the system that varies between 0 and 100 g/hr over alternate and equal periods of one hour.

The time-dependent air pollutant concentrations in Volume 1 and 2 that result from numerical simulation of the alternating emission element are plotted in Figure 6.7. Again, zero concentrations in Volumes 1 and 2 are assumed at the beginning of the simulation.<sup>3</sup> From the analytical solution for the case of constant emissions [Equation (4.4)], it can be shown that, for the given parameter values, three hours are required before 95% of the steady-state concentration is attained. Since the alternating on/off emission period of one hour is less than the time required to approach this equilibrium, the air concentration does not reach 1 g/m<sup>3</sup>, as in the constant emission case. After an initial transient response, the modeled concentrations converge to the sawtooth pattern shown in Figure 6.7. The air pollutant concentration varies between 0.3 and 0.7 g/m<sup>3</sup>. Concentrations in Volume 1 are identical to those shown in Figure 4.6 (a one volume case with similar periodic emissions). The concentrations in Volume 2, however, lag those of Volume 1, a consequence of the longer time that is needed to establish the movement of the pollutant from Volume 1 through Volume 2.

Variations/extensions of this problem are easily implemented in the SIMULINK™-based indoor air modeling elements. For example, the time-dependent Emission block can be modified to limit the time of emission to any desired fraction of the period, instead of one-half as in the previous example. Figure 6.8 shows a second Signal Generator block with a Transport Delay to provide a time lag. Signals from both generators have a period of five hours. The Transport Delay delays the first signal by 1 hour, resulting in emissions that occur every five hours and last for only one hour. Figure 6.9 shows the resulting air concentrations obtained in a SIMULINK™ simulation. As in Figure 6.7, the plot has a sawtooth appearance. In this case, however, the period between emission events is almost long enough for the system to reach equilibrium (a concentration of zero with no emission). The result is a lower time-averaged air concentration of 0.2 g/hr, which reflects the fraction of the periodic cycle over which emissions occur.

---

<sup>3</sup> Due to the abrupt changes in emission rates that occur as the source is switched on and off in this example, simulations require relatively small timesteps (on the order of one hour or less) to produce reasonably accurate results. As noted in Section 5.5, the choice of time step and other simulation parameters can affect the performance of a simulation.

### 6.1.2 Eight-volume example

The two-volume example of Section 6.1.1 is not of sufficient complexity to demonstrate the capabilities of the SIMULINK™ element-based approach. Therefore, a more elaborate example is developed in this section consisting of eight volumes and a two-dimensional flowfield in which return airflow occurs.

The configuration of the system is depicted in Figure 6.10, in which a two-dimensional, rectangular space is divided into eight equal-sized elements. Each of the eight volumes is defined to be 0.5 m by 0.5 m by 4 m, corresponding to a total volume of 1 m<sup>3</sup>. Air supplies and exhausts are established to simulate a ventilated space. An arbitrary airflow pattern derived from potential flow theory is shown in Figure 6.11.<sup>4</sup> (In an actual application, the airflow pattern preferably would be assigned on the basis of measurements.) Airflow velocities at the interfaces between volumes are determined by taking the derivatives of the streamfunction, which is contoured in Figure 6.11. Air flows into and out of each control volume are defined by integrating velocity components normal to the interface. The resulting volumetric flow rates, in relative units, are indicated in Figure 6.12.

---

<sup>4</sup> Standard potential flow theory was used to generate the flowfield shown in Figure 6.11. A finite difference algorithm was used to solve the Laplace's equation, which describes steady-state potential flow:

$$\nabla^2 \psi = 0$$

where  $\psi$  is the streamfunction. Fixed boundary values were assigned to nodes on the borders of the finite difference grid; the streamfunction values at the boundary nodes were designed to provide inflows in Volumes 1, 3, 5, and 8, and outflows in Volumes 6 and 7. Iterative methods were used to solve Laplace's equation at all interior nodes. Figure 6.11 plots the resulting streamfunctions.

Using a standard Cartesian coordinate system, horizontal (x-axis) and vertical (y-axis) velocities  $u$  and  $v$  were computed as:

$$u = \frac{\partial \psi}{\partial y}$$

$$v = -\frac{\partial \psi}{\partial x}$$

Finally, cross-boundary fluxes were calculated by integrating the horizontal and vertical velocity components across vertical and horizontal planes, respectively, as appropriate.

A mass balance equation must be written for each of the eight volumes. Combining and simplifying Equations (4.9) and (4.10), the appropriate form of the mass balance equation for a well-mixed volume with no chemical sink terms is:

$$V_i \frac{dc_i}{dt} = E_i - c_i \sum_{\substack{j=0 \\ j \neq i}}^n Q_{i \rightarrow j} + \sum_{\substack{j=0 \\ j \neq i}}^n Q_{i \leftarrow j} c_j \quad (6.1)$$

where  $i$  is a subscript that identifies the volume for which the mass balance is performed,  
 $j$  refers to an adjacent volume that may exchange air and pollutant fluxes with volume  $i$ , which (in general) can be (1) any of other volume in the model except the volume  $i$  itself or (2) an external reservoir (referenced by the subscript 0),  
 $n$  is the number of volumes in the system (eight in this example),  
 $c$  is the concentration of the pollutant in the volume of interest (subscript  $i$ ) or an adjacent volume or reservoir (subscript  $j$ ) (in units of mass/volume),  
 $E_i$  is the rate at which the pollutant is released within volume  $i$  (mass/time),  
 $Q_{i \rightarrow j}$  is a volume flow rate of air out of volume  $i$  into an adjacent volume or external reservoir  $j$ ,  
 and  $Q_{i \leftarrow j}$  is a volume flow rate of air into volume  $i$  that is provided by an adjacent volume or external reservoir  $j$ .<sup>5</sup>

Application of Equation (6.1) to each of the volumes in Figure 6.12 produces a set of eight linked equations. Many of the coefficients of these equations are zero, since non-zero values are only possible for adjacent volumes. Table 6.2 is a list of the coefficients assumed for this example. The air flow rates listed in Table 6.2 must be carefully interpreted in the context of Equation (6.1). Specifically, the following conventions are assumed:

Variable in Equation (6.1)	Location in Table 6.2
$Q_{i \rightarrow j}$	Underlined values, located in the lower-left triangle below the main diagonal
$Q_{i \leftarrow j}$	Values not underlined, located in the upper-right triangle above the main diagonal

The coefficients listed in Table 6.2 are embedded in the interconnected series of Volume and Exchange elements depicted in Figure 6.13, which serves as the SIMULINK™ block diagram for the

<sup>5</sup> As written, Equation (6.1) assumes a single external reservoir (such as the outdoors). The equation is easily extended for cases in which multiple external reservoirs exist.

eight-volume example.<sup>6</sup> In addition, an arbitrary distribution of pollutant sources is assumed. Specifically, an emission rate of  $1.0 \mu\text{g}/\text{m}^3$  is assumed in Volume 1, and an emission rate of  $0.5 \mu\text{g}/\text{m}^3$  is assumed in each of Volumes 3, 5, and 8 (for reference, these emission rates are also listed in Table 6.2).

The construction of the eight-volume system provides communication among all combinations of the eight volumes — careful examination of Figure 6.12 reveals that a contaminant released in Volumes 1 and 5 will eventually reach all eight volumes, and that a pollutant released in any of Volumes 2, 3, 4, 6, 7, and 8 will eventually distribute throughout all six volumes.<sup>7</sup> As a result, in the presence of invariant emission rates, equal steady-state pollutant concentrations will be reached in communicative volumes (Volumes 1 and 5, and Volumes 2, 3, 4, 6, 7, and 8). In fact, the particular specification of parameters yields the same steady-state concentration in all eight volumes. Under the assumption of complete mixing, the steady-state concentration within flux-connected volumes is equal to the total pollutant emission rate divided by the overall ventilation rate. For Volumes 1 and 5, combined contaminant emissions and ventilation are  $1.5 \mu\text{g}/\text{hr}$  and  $1.5 \text{ m}^3/\text{hr}$ , respectively. The remaining six Volumes contribute an additional  $1.0 \mu\text{g}/\text{hr}$  of emissions and  $1.0 \text{ m}^3/\text{hr}$  of ventilation, thus processing total emission and ventilation rates of  $2.5 \mu\text{g}/\text{hr}$  and  $2.5 \text{ m}^3/\text{hr}$ , respectively. Both of these combinations result in a steady-state

---

<sup>6</sup> Note that Table 6.2 lists volume flow rates, whereas the Exchange element described in Section 5.4.2 requires area and velocity inputs. Since the volume flow rate is simply the product of the flow velocity and the area of exchange, the coefficients in Table 6.2 are implemented within Exchange elements as flow velocities with the concurrent assumption of a unit area of exchange.

<sup>7</sup> The notion that pollutants eventually distribute throughout the eight-Volume system appears inconsistent with the streamline pattern in Figure 6.11, which suggests that a dividing streamline meandering through Volumes 2, 3, and 7 isolates the airflows of the left and right sides of the system. Strictly, this dividing streamline would prevent communication between various Volumes and prohibit, for example, any fraction of pollutant emissions in Volume 8 from ever reaching Volume 6. This mathematical constraint is violated by the application of well-mixed volumes in which all fluxes are uniformly mixed and made available to adjacent volumes. Under this algorithm, a fraction of the pollutant released in Volume 8 enters Volume 4, wherein it mixes uniformly throughout, and similar transfers proceed through Volumes 3, 2, and 6, as indicated in Figure 6.12. There is, however, some physical justification for this inconsistency. The potential flow solution that produces the streamline pattern does not consider turbulent dispersion processes or other time-dependent fluctuations in flow that produce pollutant mixing under typical real-world conditions. These dispersive processes are implicitly incorporated by the assumption of uniform mixing within the Volume element. These considerations suggest that the optimal size of Volume elements may be related to the dispersion characteristics of the setting such as turbulent eddy length scales and physical dimensions of the system.

concentration equal to  $1 \mu\text{g}/\text{m}^3$  ( $1.5 \mu\text{g}/\text{hr} \div 1.5 \text{ m}^3/\text{hr}$  in combined Volumes 1 and 5, or  $2.5 \mu\text{g}/\text{hr} \div 2.5 \text{ m}^3/\text{hr}$  in combined Volumes 2, 3, 4, 6, 7, and 8).

The time-dependent pollutant concentration profiles of the one-hour simulation are presented in Figure 6.14 (Volumes 1–4) and Figure 6.15 (Volumes 5–8). One distinguishing characteristic of the concentration profiles is the initial response of each Volume. Air pollutant concentrations in those volumes in which emissions occur (1, 3, 5, and 8) rapidly increase in an exponential fashion, while the concentrations in volumes 2, 6, and 7 exhibit an initial lag. This parabolic lag results because of the time needed to transfer pollutants into these volumes, as previously discussed in Section 4.3.

A second feature of significance to the concentration profiles of Figure 6.14 and Figure 6.15 is the relative rapidity at which steady-state is approached in the different Volumes. Volumes 1 and 5 are quickest to approach the steady-state concentration of  $1 \mu\text{g}/\text{m}^3$ , a consequence of a relatively rapid turnover of air and a one-way isolation (in terms of horizontal transport) from the remainder of the system. The other six volumes approach steady-state more slowly, with characteristic response times dependent upon the web of flux rates that connect the system. Of particular note is Volume 4, which is located in a relatively stagnant corner as indicated by Figure 6.11. This Volume experiences the slowest rate of increase in air pollutant concentration because of its relatively slow rates of mixing with other Volumes.

Many other theoretical elaborations of this example are possible that could further demonstrate the utility, convenience, and power of the SIMULINK™ indoor air modeling elements. Instead, subsequent sections of this chapter apply the modeling algorithms to realistic indoor air pollution problems in order to demonstrate practical aspects of the SIMULINK™ approach.

## 6.2 Indoor Ozone Modeling

Ozone is one of the criteria pollutants regulated by the Clean Air Act for which a National Ambient Air Quality Standard has been established to protect human health. The primary standard for ozone states that a one-hour average concentration of 120 ppb ( $240 \mu\text{g}/\text{m}^3$ ) shall not be exceeded more than once per year. Many areas of the United States are not in compliance with this standard, and stricter regulation of the precursor chemicals that lead to ozone formation has been mandated by the 1990 Clean Air Act Amendments.

Concerns over the adverse impact to human health from long-term exposure to ozone concentrations lower than the ambient standard have focussed some attention on indoor ozone levels since people spend the majority of their time indoors. Fortunately, ozone levels typically are lower indoors than they are outdoors because (1) ozone is a strong oxidizing agent that reacts on surfaces (such as carpets) and with other chemicals in the air (such as water vapor),

and (2) there are relatively few indoor sources of ozone, which is predominantly created from photochemical reactions in the atmosphere. There are, however, some potentially significant sources that can add to the ozone assimilated from outdoors. For example, operation of photocopiers and printers can produce and release ozone, especially if they not serviced adequately.

This example demonstrates the application of the indoor element modeling approach to ozone. Similar to the previous examples, the parameters of the system are assumed. This problem more closely resembles an application, however, because we (1) examine a specific pollutant in a realistic setting and (2) exercise professional judgement in modeling that is consistent with recent findings in the literature.

Three aspects of indoor air modeling are illustrated by this application. First, the ability of the indoor element approach to model first-order chemical reactions is demonstrated. Second, implications of the well-mixed assumption that serves as the foundation of many indoor air models are discussed in the context of an illustrative example. Third, the relative importance of indoor/outdoor source contributions of ozone is explored.

### 6.2.1 Physical setting

We model the distribution of ozone in a single, but not well-mixed, room. The room is divided into four elements of equal size, as shown in Figure 6.16. The overall dimensions of the room (width  $\times$  length  $\times$  height) are  $10\text{ m} \times 7.5\text{ m} \times 4\text{ m}$ , for a total volume of  $300\text{ m}^3$ , and each element is  $5\text{ m} \times 3.75\text{ m} \times 4\text{ m}$ , or  $75\text{ m}^3$  in volume. For reference, the subdivisions (regions) of the room are labeled from 1 to 4. A photocopier, fresh air supply (from the outdoors), and air vent (to the outdoors) are located in regions 1, 3, and 4, respectively.

A rate of 0.5 air exchanges per hour is assumed to be delivered by the ventilation system. This exchange rate is similar to values measured by U.S. EPA (1988) in a modern office building. With this assumption, volumetric air flow of  $150\text{ m}^3/\text{hr}$  ( $0.5/\text{hr} \times 300\text{ m}^3$ ) is assumed to enter volume 3 from the outdoors and exit volume 4 to the outdoors. The circulation between volumes is designed to move air throughout the room and provide some mixing via counter flow. The sense and magnitude of the assumed ventilation pattern are depicted in Figure 6.16.



## 6.2.2 Ozone sources and reaction

Two sources of ozone are assumed. First, the outdoor air that enters the room in region 3 is assumed to contain ozone at a concentration of  $200 \mu\text{g}/\text{m}^3$  (no loss within the ventilation ducts is considered). Second, the photocopier is assumed to release ozone while it is operating.

Consistent with the literature on ozone behavior indoors, ozone is assumed to react, and hence decrease in concentration, within the room. The rate at which ozone is consumed depends upon the configuration of the room, the nature and composition of surfaces, other chemicals present in the air, and other factors. For simplicity, we assume that ozone undergoes a reaction with other chemicals present in carpeting on the floor, and the deposition to the floor is modeled as a first-order removal process. The deposition velocity is estimated by (1) assuming ozone is uniformly mixed throughout the entire room and (2) requiring a steady-state mass balance between the deposition of ozone to the floor and the overall removal of ozone in the room:

$$A v_d C_i = (C_o - c_i) Q \quad (6.2)$$

where

$v_d$  is the deposition velocity of ozone,  
 $C_i$  is the concentration of ozone in indoor air,  
 $C_o$  is the concentration of ozone in outdoor air,  
 $A$  is the area of floor to which ozone deposits,  
 and  $Q$  is the overall rate of ventilation into the room.

Equation (6.2) can be written explicitly for the deposition velocity:

$$v_d = \frac{Q}{A} \left( \frac{C_o}{C_i} - 1 \right) \quad (6.3)$$

Using a typical value of 3 for the ratio of  $C_o$  to  $C_i$  (Weschler, Hodgson, and Wooley, 1992), and the previously defined values of  $150 \text{ m}^3/\text{hr}$  and  $75 \text{ m}^2$  ( $10 \text{ m} \times 7.5 \text{ m}$ ) for  $Q$  and  $A$ , respectively, a deposition velocity of  $4 \text{ m/hr}$  is estimated for this application.<sup>8</sup>

<sup>8</sup> The deposition velocity estimate of  $4 \text{ m/hr}$ , or  $0.1 \text{ cm/s}$ , is within the range of empirical observations of ozone deposition velocity in outdoor settings (Seinfeld, 1986).

### 6.2.3 SIMULINK™ model of indoor ozone dispersion

Figure 6.17 is a diagram of the indoor ozone application that is constructed with the SIMULINK™ indoor air modeling elements described in Section 5.4. Four volume elements represent the four subdivisions of the room. Each of these elements is configured in a similar manner; as an example, the unmasked block diagram of Volume 1 is illustrated in Figure 6.18. The Volume 1 element is distinguished by the photocopier emission element, which is absent from the other three volume elements. Values of other parameters that differ between elements are summarized as follows:

Volume	Ventilation Rate out of Volume	Ventilation Rate into Volume	Ozone Concentration in Air Entering Volume
1	0	0	—
2	0	0	—
3	0	150 m <sup>3</sup> /hr	200 µg/m <sup>3</sup>
4	150 m <sup>3</sup> /hr	0	—

The four exchange elements shown in Figure 6.17 define the air circulation between volume elements. The air exchange rates, as depicted in Figure 6.16, are:

Air flowrate from Volume:	Air flowrate (m <sup>3</sup> /hr) into Volume:			
	1	2	3	4
1	—	100	25	—
2	25	—	—	100
3	100	—	—	100
4	—	25	25	—

### 6.2.4 Ozone modeling simulations

Two simulations are presented that illustrate two issues relevant to ozone concentrations in indoor air: (1) the heterogeneity of ozone concentrations in indoor air that can result from finite mixing rates and (2) the relative importance of multiple sources — both indoor and outdoor — that can lead to exposure to ozone. The two simulations differ with respect to pollutant sources. Both simulations import ozone-containing air from the outdoors. In the first simulation, this ventilation influx is the only source. In the second simulation, ozone is also assumed to be generated by an internal source (in this case, a photocopier) for varying durations of time.

### 6.2.4.1 Simulation with only an outdoor source

In this simulation, ozone concentrations in the four-volume system (see Figure 6.16) originate solely from polluted outdoor air vented into the room. The initial concentration of ozone in all four volumes of the room is assumed to be zero. Outdoor ozone begins to enter the room from an air supply in Volume 3. The ozone mixes between and deposits within all four volumes, and air is exhausted to the outdoors from Volume 4.

Figure 6.19 presents the results of a time-dependent simulation of ozone concentrations in the four-volume room. The time-dependent profiles are characteristic of the exponential solutions described in other sections of this report. The concentration in each Volume starts at zero and begins to approach a steady-state value by the end of the two-hour simulation. The characteristic time of the transient response is governed by the rates of air movement and deposition to the floor. Differences in the transient responses of each volume are influenced by the general circulation pattern. For example, steady-state is approached more quickly in Volume 3 than in Volume 2, since the buildup of ozone in Volume 2 relies on transport from Volumes 1 and 4, which in turn are dominated by the ventilation source in Volume 3.

Of greater consequence, however, is the variability among the steady-state concentrations of the four Volumes. These steady-state concentrations<sup>9</sup> vary by about a factor of six from the highest concentration (about 120  $\mu\text{g}/\text{m}^3$ , in Volume 3) to the lowest concentration (about 40  $\mu\text{g}/\text{m}^3$ , in Volume 2). The average steady-state value of 70.8  $\mu\text{g}/\text{m}^3$  is only slightly larger than the design concentration of 66.7  $\mu\text{g}/\text{m}^3$  that would be obtained if the entire system was modeled as a single

---

<sup>9</sup> The steady-state concentrations can be determined analytically through a mass balance of the fluxes of ozone for Volume. Each mass balance must include both transport and deposition. The system of equations for the specific parameters of this problem are:

$$\begin{aligned}\text{Volume 1:} \quad & 100c_3 + 25c_2 - 125c_1 - \underline{75c_1} = 0 \\ \text{Volume 2:} \quad & 100c_1 + 25c_4 - 125c_2 - \underline{75c_2} = 0 \\ \text{Volume 3:} \quad & 150c_0 + 25c_1 + 25c_4 - 200c_3 - \underline{75c_3} = 0 \\ \text{Volume 4:} \quad & 100c_3 + 100c_2 - 200c_4 - \underline{75c_4} = 0\end{aligned}$$

where  $c_0$  is the ozone concentration of the outdoor air vented into Volume 3, and  $c_1$ ,  $c_2$ ,  $c_3$ , and  $c_4$  are the respective concentrations of ozone in Volumes 1, 2, 3, and 4. The coefficients of the equations correspond to the air flows between Volumes (normalized, for convenience), except for the underlined terms that account for ozone deposition to the surface. For a  $c_0$  value of 200  $\mu\text{g}/\text{m}^3$ , simultaneous solution of the mass balance equations yields steady-state ozone concentrations of 65.1, 39.8, 120.3, and 58.2  $\mu\text{g}/\text{m}^3$ , respectively, in Volumes 1, 2, 3, and 4.

volume.<sup>10</sup> Thus, on average, the four volume system behaves in a similar manner to a single, well-mixed volume. The variability in concentrations in this example, however, is significant, and is caused by the combination of a modest internal mixing rate and a strong internal sink. The assumptions of this example, however, do not apply to all indoor air pollution scenarios. For example, the range of concentration values can be reduced by increasing the mixing rates between Volumes. In addition, the persistence of different concentrations requires the presence of an internal sink; at steady-state, a passive (non-reactive) pollutant would distribute uniformly throughout the four volumes.

Figure 6.20 presents time-averaged concentration profiles for the four-volume system. By design, time-averaged concentration profiles maintain a running average of the pollutant concentration from the beginning of the integration period. As such, the time-averaged concentration profiles of Figure 6.20 envelop the time-history of the buildup of ozone concentrations and hence evolve more slowly than the instantaneous profiles of Figure 6.19. As a consequence, the time-averaged concentrations of Figure 6.20 approach the same steady-state values of Figure 6.19, but require a longer time to develop since they remember the lower concentrations of the transient response.

#### 6.2.4.2 Simulation with both an indoor and outdoor source

In this section, an internal source of ozone emission is added that augments the flux of ozone received from the air supply system. Examples of potential sources include photocopiers and printers that may generate and release ozone during operation. As shown in Figure 6.16, the ozone generation element is situated in Volume 1, while the ozone-containing air enters the room in a ventilation duct in Volume 3.

Figure 6.21 displays the unmasked block diagram of the copier emission element embedded in Volume 1 (Figure 6.18). Three switch elements that process step function signals are used to construct emission intervals. The beginning and ending times of the emission interval are specified by the user with on and off times. For a given value of time  $t$ , the switch transmits a value of 1 if time  $t$  is between the on and off points, otherwise the switch returns a value of 0. The three switches shown in Figure 6.21 allow for the specification of three different emission periods (although the element can be easily modified to provide for an arbitrary number of emission intervals). All of the switches feed into a summation element that is multiplied by a common gain under the assumption that the copier emits ozone at a more or less constant rate during periods of active operation.

---

<sup>10</sup> For a single volume system, the concentration of  $66.7 \mu\text{g}/\text{m}^3$ , which is one-third of the outdoor concentration of  $200 \mu\text{g}/\text{m}^3$ , is a consequence of the method used to estimate the average deposition velocity [Equation (6.3)].

In this example, the copier emission element is configured to generate ozone for the three following intervals (referenced to time zero) within the modeling period:

Emission Period	On Time (hr)	Off Time (hr)
1	0.05	0.06
2	0.10	0.15
3	0.50	0.75

Hansen and Andersen (1986) measured ozone emissions from sixty-nine different photocopiers. They found an average ozone emission rate of 259  $\mu\text{g}/\text{min}$ , with a standard deviation of 302  $\mu\text{g}/\text{min}$  and a maximum of 1350  $\mu\text{g}/\text{min}$ . For purpose of illustration, we consider two different levels of photocopier emissions that correspond to the average and maximum values of Hansen and Andersen's observations. The emission profiles that are used in the modeling simulations are depicted in Figure 6.22.

Figure 6.23 displays the time-dependent ozone concentrations that result from the combination of average photocopier emissions (Figure 6.22) and ozone supplied by the ventilation system; time-averages of these profiles are presented in Figure 6.24. Within these figures, the dynamic interaction of the two sources of ozone is both striking and agrees with intuition. Photocopier emissions increase the ozone concentrations in all four volumes, but increases are most notable in Volumes 1 and 2, as evidenced by the response of the concentration profiles in Figure 6.23. The most dramatic increase in concentration occurs in Volume 1 in which the copier is located. The copier-induced increments in concentration decrease in magnitude in Volumes 2, 4, and 3, a pattern governed by the general clockwise pattern of the air flow in the four-volume system (Figure 6.16).

The transient response also illustrates the importance of the duration of emissions. The first two periods of emission from the copier force a more rapid increase in the ozone concentration of Volume 1, which is indicated by a steeper slope in the concentration profile. Upon termination of the first two periods of emission, the ozone concentration in Volume 1 continues to rise, but at a slower rate (Figure 6.23). The third emission event, however, is of sufficient duration to develop a transient concentration that exceeds the steady-state concentration obtained in the absence of photocopier emissions (Figure 6.19). Consequently, upon termination of the third emission period, the concentration in Volume 1 decreases.

The influence of photocopier emissions are even more striking under the maximum emission scenario, the results of which are presented in Figure 6.26. In the third period of photocopier emissions, the ozone concentration in Volume 1 soars to more than 250  $\mu\text{g}/\text{m}^3$ . Upon termination of photocopier emissions, the Volume 1 concentration profile quickly declines, and the concentration in Volume 1 is lower than that in Volume 3 by the end of the simulation, which is consistent with the simulation without photocopier emissions (Figure 6.19).

The presence of two sources also effects the calculation of time-averaged concentration profiles, which are depicted in Figure 6.24 and Figure 6.26. Of particular prominence are the relative impacts of ozone emissions from the photocopier, which are most significant for Volumes 1 and 2 and of lesser importance for Volumes 3 and 4. In the maximum photocopier emission example (Figure 6.26), the interaction of the two sources produces considerable differences in time-averaged concentrations. During the course of the two-hour simulation, the highest time-averaged concentration shifts between Volumes 3 and 1; at the end of the simulation period, the time-averages in these two elements are approximately equal. Also, the sensitivity to photocopier emission is directly a function of proximity to the source, as the time-averaged profiles most influenced by copier emissions are Volume 1, in which the copier is situated, and Volume 2, which receives the greatest amount of airflow from Volume 1.

A comparison of the steady-state concentrations in the presence and absence of photocopier emissions is provided in Table 6.1. Estimates for the scenarios with photocopier emissions reflect the concentrations that would be attained after sufficiently long times under periods of continuous operation. (These scenarios are not reflected in the transient profiles since the simulations (1) did not include continuous emissions and (2) were not of sufficient duration to approach steady-state conditions.) For the case of average photocopier emissions, the photocopier source is of sufficient strength to shift the maximum steady-state concentration from Volume 3 (where ozone is introduced *via* ventilation) to Volume 1 (where the photocopier is located). Under the maximum emission scenario, the photocopier becomes the dominant source (0.081 g/hr compared to 0.03 g/hr provided by ventilation), and significantly affects the ozone concentration in all four volumes.

Table 6.1 Steady-state concentrations for the indoor ozone demonstration problem

Volume	Steady-State Ozone Concentration ( $\mu\text{g}/\text{m}^3$ )		
	Without emission from copier	With emission from copier	
		Average rate	Maximum rate
1	65	154	527
2	40	87	284
3	120	130	172
4	58	79	166

The specific assumptions of this example strongly affect the pollutant distribution within the room. The implication of the results, however, should not be discounted. For pollutants such as ozone that are believed to dissipate significantly in the indoor environment, these calculations demonstrate that a large degree of internal mixing is necessary to justify the assumption of well-mixed conditions. Thus, proximity to sources and ventilation design may be important factors in determining the potential for exposure to indoor air pollutants.

### 6.3 Hoover Universal case study

The following application is based on a NIOSH industrial hygiene survey of the Hoover Universal Plant in Greenfield, Ohio (Boeniger, 1986) conducted as part of a larger epidemiological/industrial hygiene study of workers in the flexible polyurethane industry. Boeniger (1986) details the results of a study conducted to characterize worker exposures to toluene diisocyanate (TDI). The report describes a walk-through inspection of the facility. In this section, we highlight only those aspects of the report that are pertinent to our application.

### 6.3.1 Description of Hoover Universal facility

In 1966, the Hoover Universal facility began production of car seats, head rests, and arm rests consisting of flexible foam formed over rigid steel frames. A floorplan of the facility is shown in Figure 6.27.<sup>11</sup> The production facility is a one-floor structure with a twenty-foot ceiling. A warehouse and a storage room are adjacent to the production floor. Offices and a lunchroom are located within the main production area, although they are separated by walls.

At the time of the study, there were five process lines in operation. TDI was used at each of the lines. Four of the lines made use of a cold foam process, while one line (Line 2 in Figure 6.27) used a hot foam process. The hot and cold foam processes are similar. In both processes, foam containing an 80/20 blend of 2,4- and 2,6-TDI isomers is sprayed into molds as they move along a conveyor belt. In the hot foam process, the molds then pass through a curing oven heated to 450°F. In the cold foam process, hot water jackets or infra-red lamps are used to provide additional heat. Foam items from these lines (1, 3, 4, and 5) also pass through a crusher unit while on the conveyor belt. The crusher unit breaks the bubbles of the foam, thereby softening the item.

Exhaust and makeup ventilation are provided along the production lines. In particular, the oven on Line 2 is exhaust ventilated and booth exhaust is provided upon exit from the oven. In addition, local exhaust ventilation and make-up air are provided along the Line 2 conveyor. Lines 1 and 4 are also supplied with local exhaust and make-up air. Line 3 is exhaust ventilated at the TDI spray nozzles. Local exhaust vents are present on Line 5, but are obstructed during normal production. General air movement in the vicinity of Line 5 was observed to be negligible.

In addition to these line-specific measures, a general ventilation system also distributes fresh air to the seat assembly area, the center of Line 2, and throughout the remainder of the plant. The system provides 307,000 cubic feet per minute (cfm) of fresh air and exhausts an equal amount. In general, air appeared to move from the open doors in the west and east walls toward Line 2. Air flow velocities in the facility were measured and are indicated in Figure 6.27.

---

<sup>11</sup> Bruce Jackson, Process Engineer at the time of the NIOSH study, provided the dimensions of the production floor.



### 6.3.2 Model formulation

The floorplan of the Hoover Universal facility, as reproduced from Boeniger (1986), is presented in Figure 6.27. The system of control volumes designed to represent the floorplan is shown in Figure 6.28. Twelve control volume are defined to include all areas shown within the production area of the plant except the offices. These twelve control volumes are identified by number in Figure 6.28.

The control volumes depicted in Figure 6.28 have been delineated with respect to the density and relevance of ventilation and monitoring data. Air velocity data (Figure 6.27) are relatively sparse and limit the level of detail to which air movement may be inferred. Monitoring data reflect personal exposure to workers who were free to move about and thus are more properly interpreted as observations averaged over space. Based upon the nature of the available data, the size of control volumes for modeling purposes should be consistent with length scales associated with production activities on the factory floor. These considerations serve as the basis of the definition of the control volumes shown in Figure 6.28.<sup>12</sup> Five of the control volumes correspond to the production lines, and three more encompass the seat assembly, packaging, and finishing areas. Measurements of TDI concentrations in air are available for each of these areas to compare with model predictions. The remaining four control volumes in Figure 6.28 are defined to provide for air and contaminant movement throughout the plant. The length and width of the control volumes are estimated by scaling Figure 1 of Boeniger (1986). The ceiling height of each volume is assumed be 20 feet. Table 6.3 provides a summary of control volume dimensions.

Figure 6.28 also shows the approximate locations of vents that are part of the general air circulation system. These locations are based on Figure 1 of Boeniger (1986) and are used to estimate general ventilation rates within control volumes. As such, only their approximate locations are required. We assume the 307,000 cfm of fresh air provided and exhausted by the general circulation system is distributed equally among the 27 vents, resulting in the allocation of 11,370 cfm to each vent. The location of the vents in relation to the control volumes was used to

---

<sup>12</sup> Since the specification of the modeling domain is arbitrary, other definitions of control volumes are possible. For example, it might be desirable to define smaller control volumes to predict pollutant concentrations in the air space occupied by a single worker. Such detailed definitions, however, are inappropriate in this application for three reasons. First, only gross data on ventilation rates are unavailable. Second, knowledge of the locations and movements of monitored workers is also unavailable. Last, the precise mechanisms responsible for the release of TDI to the air are unknown. If model estimates are to be compared with observed data, these considerations emphasize the needs to (1) make comparisons over appropriate averaging scales and (2) collect data of detail sufficient for the degree of modeling precision that is desired.

allocate airflows to the control volumes in a simple manner: the airflow due to each vent located in the middle of a control volume is attributed to that control volume, and the airflow due to vents located at the borders of control volumes is split equally between the volumes. The resulting airflows were further refined during model calibration. The initial estimates and calibrated values are reported in Table 6.4.

Air fluxes between control volumes were initially based on the measurements of air velocity reported in the NIOSH report (Boeniger, 1986). The location, magnitude, and sense of these measurements are shown in Figure 6.27. The measured velocities were vectorized into north-south and east-west components, and air fluxes into and out of control volumes were calculated by estimating cross-sectional areas through which airflow occurs and multiplying these by the vectorized velocities. The estimated air fluxes are shown in Table 6.5, wherein a dual subscript notation indicates the control volume from which airflow originates and that in which it enters.<sup>13</sup> Airflows across boundaries other than those reported in Table 6.5 were assumed to be zero.

### 6.3.3 Estimation of TDI emission rates

As discussed in detail in Section 6.3.4, the measured concentrations of TDI isomers in factory air do not scale directly with source composition. Instead, it appears that 2,6-TDI is relatively more prevalent in air than in the source material. Two plausible explanations are that either 2,6-TDI is released from the source material at a greater rate than 2,4-TDI, or that 2,4-TDI undergoes more rapid reaction in the air.

TDI emission rates are difficult to estimate because the precise mechanisms that lead to its release are not known. Since workers monitored near production lines are associated with the highest observed TDI concentrations in air, it is reasonable to suspect that emissions are related to production. Several factors, however, may be responsible for releasing TDI. The source material consists of TDI monomer chemically attached to a blocking agent. Since the blocking agent is intended to prevent TDI from reacting, the virgin source material is not likely to be a major source of TDI emission to the air. Once poured into the molds, however, the blocking

---

<sup>13</sup> The cross-sectional areas listed in Table 6.5 were assigned using professional judgement to reflect the area over which a measured flow velocity applied. These cross-sectional areas do not necessarily reflect the areas common to adjacent volume that are indicated in Figure 6.28. For example, the area of 200 ft<sup>2</sup> is estimated for the exchange between Volumes 2a and 1, while an area of 100 ft<sup>2</sup> is estimated for the air flow from Volume 1 to Volume 2, despite the much larger interfacial area implied for the latter connection in Figure 6.28. Two different entries are listed in Table 6.5 for the air from Volume 10 to Volume 8 and from Volume 10 to Volume 9 in order to estimate air flows due to different velocity measurements.

agent is easily shed by the application of heat. Within the mold, the TDI monomer rapidly polymerizes into the desired foam product. In the Hoover Universal Plant, the heat-curing process is performed in one of two manners: direct heating in an oven on production Line 2, and indirect heating by hot-water jackets and infra-red lamps on the other four lines. During polymerization, some TDI monomer may escape from the mold through cracks and weepholes, either on the conveyor line or in the Line 2 furnace (which is exhaust vented). In addition, some of the monomer that fails to polymerize may remain harbored within a thin layer of gas that separates the foam product from the mold, and then subsequently be released when the mold is opened. Unreacted monomer trapped in bubbles may be liberated by the crusher units that are subsequently applied to a portion of the foam products. Finally, it is possible that TDI may further volatilize from the products while they remain on the production floor, although the failure to detect TDI in the warehouse adjacent to the production floor suggests this mechanism is unlikely to be a major source of emissions.

Unfortunately, the personal monitoring data, which reflect worker exposure and are not specific to processes, cannot be used to identify the emission factors of principal importance. Detailed differentiation of emission factors is unnecessary, however, since the modeling application is only concerned with the overall release rate within volume elements that encompass entire production lines. Thus, simple parameterization of the emission characteristics of the process is sufficient.

Even simple parameterizations of TDI emission rates, however, are impossible because the relative importance of the factors that influence emissions is unknown. Consequently, no attempt was made to model TDI emission rates. Instead, the magnitude of TDI emissions was estimated by trial-and-error comparison between model predictions and observations. Emission sources were assigned to the production processes likely to release TDI. Obviously, model predictions and observations could be calibrated to exact precision. Calibration was constrained, however, to consider processes on a relative basis and to reflect qualitative observations of suspected emission sources (Boeniger, 1986). The emission rates derived for modeling are as follows (subscripts refer to control volumes as indicated in Figure 6.28):

**Emission rates of TDI used for modeling (mg/min)**

$E_1$	20	$E_2$	20	$E_{2a}$	0
$E_3$	0	$E_4$	30	$E_5$	5
$E_6$	5	$E_7$	5	$E_8$	5
$E_9$	30	$E_{10}$	30	$E_{11}$	80

The highest emission rates (per unit volume) are associated with the production lines. Volumes 1, 2, 4, and 9, which are associated with Lines 1, 5, 4, and 3, respectively, are assigned emission rates of 20 or 30 mg/min, with the lesser rate assigned to the westernmost lines based upon the relative sizes of the Volumes. Volume 11, which encompasses Line 2, is assigned the largest emission rate of 80 mg/min, suggesting the hot foam line, whether because of production rate or process factors, emits a larger amount of TDI than the cold foam lines. A lower emission rate of 5 mg/min is assigned to the crusher, packaging, repair, and finishing areas (Volumes 5, 6, 7, and 8, respectively) under the assumption that these processes release a significant, but smaller, amount of TDI compared to the direct production lines. Finally, an emission rate of 30 mg/min is specified for the seat assembly area (Volume 10), which, because of the larger area, is consistent with the emission rate of 5 mg/min designated for the other off-line processes.

#### 6.3.4 Analysis of measured concentrations of TDI in air

Extensive measurements of 2,4- and 2,6-TDI are reported in the NIOSH report (Boeniger, 1986). Almost all of these data are based on personal breathing space samples. To obtain the data, employees were randomly selected and categorized according to job type. Since the indoor air modeling estimates air pollutant concentrations at various locations (and not for individuals who may move about the plant), only categories that were judged to be associated with a well-defined area within the plant were considered. Data from eight of the NIOSH-defined job categories are used to derive estimates of average exposure concentrations. The categories used are: workers on Line 1, 2, 3, 4, 5; seat assemblers; finishers; and packagers. In addition, Line 2 trimmers, located in the center of Line 2, were included with Line 2 workers under the assumption that their exposures are likely to be similar. Excepting janitors, the job categories selected for use here correspond to those reported in Figure 2 of the NIOSH report (Boeniger, 1986). The janitor category, as well as the clean and repair, warehouse, packer, compounder, plant inspector, and cold foam repair categories are excluded because they are not associated with a well-defined area in the plant. The warehouse and shipping warehouse categories were also excluded because they are outside the main production area and thus outside of the area of study.

To estimate average exposure concentrations in the areas of interest, all of the personal monitoring data collected by NIOSH (Boeniger, 1986) are considered. These data are compiled in Appendix A. The eight job categories considered herein include 55 of the 67 valid measurements that were collected over two different production shifts; these shifts were not differentiated since Boeniger (1986) found no significant difference between the concentrations of 2,4- and 2,6-TDI measured during morning and afternoon shifts. The screened data used to estimate average exposure concentrations are listed in Table 6.6, where they are sorted according to the area in the plant with which they are associated. Statistical summaries of these data by plant location are reported in Table 6.7.

The NIOSH report (Boeniger, 1986) indicates 2,4- and 2,6-TDI are used in a mixture at a ratio of 4 to 1. The statistical summaries reported in Table 6.7 do not reflect this ratio. Instead, the concentrations of the two congeners are roughly equal, and in some cases, the concentration of 2,6-TDI exceeds that of 2,4-TDI. The behavior of TDI isomers in air is not well understood, although reaction and adsorption mechanisms have been postulated (Dyson and Hermann, 1971; Holdren *et al.*, 1984). Boeniger (1986) speculates that the TDI isomers may react at different rates. It is also possible that the rates of volatilization and/or polymerization differ for the two isomers. In addition, these factors may vary with time and location within the plant as well, and there may be uncertainty associated with the analytical differentiation of the TDI isomers.

Since the cause of this discrepancy between isomer ratios in the source material and in the air is unknown, total TDI concentrations are used to derive average exposure concentrations. These concentrations are included in the statistical summaries in Table 6.7. Implications of using total TDI concentrations (as opposed to considering each isomer separately) are discussed in Section 6.3.6.

The statistical summaries (Table 6.7) contain averages of all observations within job categories; these averages are interpreted to represent average exposure concentrations within various production areas and are compared with model predictions in Section 6.3.5.

### 6.3.5 Modeling simulation for the Hoover Universal case study

Figure 6.29 displays the SIMULINK™ block diagram representation of the Hoover Universal Plant. The Volume elements of Figure 6.29 correspond directly to the control volumes shown in Figure 6.28 and embody the dimensions and emission rates described in Sections 6.3.2 and 6.3.3, respectively. Exchange elements specify the air flow parameters listed in Table 6.5.

The SIMULINK™ simulation was conducted for a period of twenty minutes, with initial concentrations in all Volumes set to zero. The time-dependent concentration profiles plotted in Figure 6.30 through Figure 7.1 show that steady-state air concentrations are achieved within a few minutes after emissions commence. This rapid response reflects the high rates of ventilation typical of industrial facilities such as the Hoover Universal Plant. Moreover, the rapid response minimizes differences between instantaneous and time-averaged concentrations, as indicated by Figure 7.2. In the case of the Volume 5, the control volume having the slowest time-response, the predicted time-average is essentially indistinguishable from the instantaneous concentration after about two hours. As a consequence, the time-averaged concentrations do not depend greatly on changes in emissions prior to the averaging period. Even if the plant is assumed to be completely aired out overnight, one would not expect the morning and afternoon measurements to differ significantly if emissions during operational periods are similar. This observation is consistent with the finding that morning and afternoon observations of TDI concentrations in air were statistically indistinguishable (Boeniger, 1986).

The modeled steady-state concentrations are compared with the exposure concentrations derived from measurements (Section 6.3.4) in Table 6.8. Also presented are the standard deviations and the differences between measured and predicted air concentrations. With the exception of Volume 10, all of the predictions fall within one standard deviation of the means of the measurements. In Volume 10, the predicted air is just over a standard deviation from the measured mean. In general, predictions in the western section of the plant are less than the means and those in the eastern section are higher than the measured means. This trend suggests that it may be more accurate to assume the same emission rate for each of the cold cure lines rather than to differentiate on the basis of control volume size, which (as described in Section 6.3.3) assigns lower emission rates to the lines in the western section of the plant.

### 6.3.6 Implications of the Hoover Universal modeling application

Given the fact that the TDI emissions were determined in part from a comparison of model predictions and observations, the general success of the modeling is not surprising. From a superficial perspective, the modeling may appear to be of limited value, since the application is not strictly predictive. The utility of this modeling application, however, stems from an alternate viewpoint. To this point, very little was known about the magnitude of TDI emissions from polyurethane operations. The emission rates required to produce general model agreement with observations are in essence order-of-magnitude estimates of the effective TDI emission rates from production processes. Such estimates could be useful in evaluating similar processes in other factories.

The TDI emission estimates should be treated carefully, however. As derived, the emission rates represent releases of TDI that effectively lead to exposure. No attempt was made to simulate removal mechanisms such as chemical reactions, adsorption, and deposition; should any of these processes be significant, actual emission rates could be higher than those estimated herein. Also, the issue of the relative ratios of the 2,4- and 2,6-TDI isomers discussed in Section 6.3.4 remains unresolved, both in terms of cause and importance. A more detailed approach might have to consider each isomer separately if the fate and transport parameters or toxicologic concern differ greatly for the two isomers.

Finally, the ultimate value of this modeling application is simply its successful demonstration of the indoor air modeling algorithms. The ability of the model to predict the pattern of observed TDI concentrations in air, which vary by roughly a factor of ten, suggests that the Volume element approach can be applied successfully to predict the general distribution of a pollutant in a complex indoor setting in which adequate knowledge of contaminant emission rates and air flow patterns is available.

Table 6.2 Air flow and emission rate coefficients assumed for the eight-volume example

Air flow rate (m <sup>3</sup> /hr) between Volume element or reservoir <i>i</i> (row) and Volume element or reservoir <i>j</i> (column). Dashes indicate that the two Volumes do not share an interface. A value of zero indicates that the two Volumes share an interface, but there is no flow across it in the direction indicated. Underlined values indicate a flow from the row Volume/reservoir to the column Volume/reservoir ( <i>i</i> → <i>j</i> ), while values not underlined indicate a flow into the row Volume/reservoir from the column Volume/reservoir ( <i>i</i> ← <i>j</i> ).										Assumed emission rate within volume <i>i</i> (μg/hr)
<i>i</i> =0	<i>i</i> =1	<i>i</i> =2	<i>i</i> =3	<i>i</i> =4	<i>i</i> =5	<i>i</i> =6	<i>i</i> =7	<i>i</i> =8		
<i>i</i> =0	—	1.0000	0	0.5000	0	0.5000	0	0	0.5000	—
<i>i</i> =1	<u>0</u>	—	0.6024	—	—	0.3976	—	—	—	1.0
<i>i</i> =2	<u>0</u>	<u>0</u>	—	0.0265	—	—	0.5338	—	—	0
<i>i</i> =3	<u>0</u>	—	<u>0.0951</u>	—	0.0853	—	—	0.5102	—	0.5
<i>i</i> =4	<u>0</u>	—	—	<u>0.0269</u>	—	—	—	—	0.0612	0
<i>i</i> =5	<u>0</u>	<u>0</u>	—	—	—	—	0.8976	—	—	0.5
<i>i</i> =6	<u>1.2500</u>	—	<u>0</u>	—	—	<u>0</u>	—	0.1814	—	0
<i>i</i> =7	<u>1.2500</u>	—	—	<u>0</u>	—	—	<u>0</u>	—	0	0
<i>i</i> =8	<u>0</u>	—	—	—	<u>0.0028</u>	—	—	<u>0.5584</u>	—	0.5

Table 6.3 Dimensions of SIMULINK™ control volumes

Volume Number	Width (ft) (north-south)	Length (ft) (east-west)	Height (ft)	Volume (ft <sup>3</sup> )
1	50	60	20	60000
2	50	60	20	60000
2a	50	10	20	10000
3	40	70	20	56000
4	50	60	20	60000
5	50	50	20	50000
6	40	50	20	40000
7	50	40	20	40000
8	50	40	20	40000
9	80	80	20	128000
10	100	120	20	240000
11	180	80	20	288000



Table 6.4 Allocation of ventilation airflows of general ventilation system to SIMULINK™ elements

Volume Number	Number of vents	Associated airflows into volume (cfm)	Calibrated airflow into volume (cfm)	Calibrated airflow out of volume (cfm)
1	0	0	17770	16370
2	2	22700	15130	15130
2a	0	0	0	0
3	2	22700	52700	22700
4	0.5	5700	10700	15700
5	1.5	17055	17055	44692
6	2.5	28425	28425	28425
7	2	22700	22700	28700
8	1	11370	11370	17132.5
9	2	22700	22700	38200
10	6.5	85300	73900	90400
11	7	68200	164600	119600

Table 6.5 Velocities, cross-sectional areas, and air fluxes across control volume boundaries for the Hoover Universal case study

Velocity (fpm)		Relevant Cross-sectional Area (ft <sup>2</sup> )		Air fluxes (cfm)	
$V_{2a \rightarrow 1}$	100	$A_{2a1}$	200	$Q_{2a \rightarrow 1}$	20000
$V_{1 \rightarrow 2}$	64	$A_{1 \rightarrow 2}$	100	$Q_{1 \rightarrow 2}$	6400
$V_{4 \rightarrow 2}$	100	$A_{4 \rightarrow 2}$	50	$Q_{4 \rightarrow 2}$	5000
$V_{1 \rightarrow 4}$	100	$A_{1 \rightarrow 4}$	187.5	$Q_{1 \rightarrow 4}$	15000
$V_{2 \rightarrow 5}$	100	$A_{2 \rightarrow 5}$	114	$Q_{2 \rightarrow 5}$	11400
$V_{3 \rightarrow 6}$	100	$A_{3 \rightarrow 6}$	100	$Q_{3 \rightarrow 6}$	10000
$V_{6 \rightarrow 5}$	50	$A_{6 \rightarrow 5}$	200	$Q_{6 \rightarrow 5}$	10000
$V_{4 \rightarrow 5}$	10	$A_{4 \rightarrow 5}$	500	$Q_{4 \rightarrow 5}$	5000
$V_{8 \rightarrow 5}$	25	$A_{8 \rightarrow 5}$	50	$Q_{8 \rightarrow 5}$	1250
$V_{8 \rightarrow 7}$	95	$A_{8 \rightarrow 7}$	63	$Q_{8 \rightarrow 7}$	6000
$V_{8 \rightarrow 9}$	55	$A_{8 \rightarrow 9}$	100	$Q_{8 \rightarrow 9}$	5500
$V_{10 \rightarrow 8}$	25	$A_{10 \rightarrow 8}$	100	$Q_{10 \rightarrow 8}$	2500
$V_{10 \rightarrow 8}$	80	$A_{10 \rightarrow 8}$	200	$Q_{10 \rightarrow 8}$	16000
$V_{10 \rightarrow 9}$	60	$A_{10 \rightarrow 9}$	100	$Q_{10 \rightarrow 9}$	6000

Table 6.6 Summary of NIOSH air sampling data used

Sample	Description	TDI concentration in air (µg/m³)		
		2,4-	2,6-	total
<u>Line 1</u>				
IS11	operator	11	12	23
IS31	operator	17	13	30
IS55	operator, faulted at 74 minutes	14	9	23
<u>Line 2</u>				
IS8	operator	5	11	16
IS10	operator	4	11	15
IS7	operator	3	7	10
IS5	trimmer	9	11	20
IS28	operator	5	7	12
IS27	operator	5	10	15
IS33	operator	9	15	24
IS30	trimmer	8	11	19
IS26	inspector	8	13	21
IS41	trimmer	4	5	9
IS40	trimmer	6	9	15
IS51	operator, removes seats	5	9	14
IS48	operator, burlapper	5	7	12
IS77	operator, burlapper	8	8	16
IS57	operator, seat removal	5	7	12
IS65	trimming	3	3	6
IS46	operator, burlapper	6	7	13
IS99	area in operators' area of Line 2	8	10	18
<u>Line 3</u>				
IS35	operator	9	23	32
IS63	trimmer	12	24	36
IS53	operator	10	26	36
IS94	operator	8	20	28
IS92	operator, sets up frames	5	9	14

Table 6.6 (continued) Summary of NIOSH air sampling data used

Sample	Description	TDI concentration in air (µg/m³)		
		2,4-	2,6-	total
<u>Line 4</u>				
IS21	operator	38	31	69
IS42	operator	27	21	48
IS43	operator	12	17	29
IS62	operator	18	14	32
IS91	operator	14	13	27
IS96	area by #4 line control panel	71	54	125
<u>Line 5</u>				
IS50	operator, nozzle	27	17	44
IS74	operator	18	20	38
<u>Finishing</u>				
IS4	finishing, trimmed	5	7	12
IS9	finishing, trimmed	6	8	14
IS32	finishing	9	15	24
IS25	finishing	6	10	16
IS54	finishing operator	13	12	25
IS23	finishing operator	8	4	12
IS67	finishing	3	6	9
IS78	finishing	7	7	14
IS95	finishing	6	5	11
<u>Seat Assembly</u>				
IS44	seat assembly	3	8	11
IS22	seat assembly	9	19	28
IS24	seat assembly	8	15	23
IS23	seat assembly	8	15	23
IS76	seat assembly	4	6	10
IS86	seat assembly	4	6	10
<u>Packager</u>				
IS3	packager	<2	2	2
IS81	packager	4	5	9
IS71	packager	4	6	10
IS64	packager	2	2	4

Table 6.7 Statistical summary of NIOSH data used in the study

	Line 1			Line 2			Line 3			Line 4		
	2,4	2,6	total	2,4	2,6	total	2,4	2,6	total	2,4	2,6	total
Number of samples	3	3	3	18	18	18	5	5	5	6	6	6
Maximum	17.0	13.0	30.0	9.0	15.0	24.0	12.0	26.0	36.0	71.0	54.0	125.0
Minimum	11.0	9.0	23.0	3.0	3.0	6.0	5.0	9.0	14.0	12.0	13.0	27.0
Arithmetic Mean	14.0	11.3	25.3	5.9	8.9	14.8	8.8	20.4	29.2	30.0	25.0	55.0
Std. Dev.	3.0	2.1	4.0	2.0	2.9	4.5	2.6	6.7	9.1	22.3	15.6	37.8
Geometric Mean	13.8	11.2	25.1	5.6	8.4	14.1	8.5	19.2	27.7	24.6	21.8	46.7
Geometric Std. Dev.	1.2	1.2	1.2	1.4	1.5	1.4	1.4	1.5	1.5	2.0	1.7	1.8

	Line 5			Finishing			Seat Assembly			Packager		
	2,4	2,6	total	2,4	2,6	total	2,4	2,6	total	2,4	2,6	total
Number of samples	2	2	2	9	9	9	6	6	6	4	4	4
Maximum	27.0	20.0	44.0	13.0	15.0	25.0	9.0	19.0	28.0	4.0	6.0	10.0
Minimum	18.0	17.0	38.0	3.0	4.0	9.0	3.0	6.0	10.0	0.0	2.0	2.0
Arithmetic Mean	22.5	18.5	41.0	7.0	8.2	15.2	6.0	11.5	17.5	2.5	3.8	6.3
Std. Dev.	6.4	2.1	4.2	2.8	3.5	5.6	2.6	5.5	8.1	1.9	2.1	3.9
Geometric Mean	22.0	18.4	40.9	6.5	7.6	14.4	5.5	10.4	15.9	3.2	3.3	5.2
Geometric Std. Dev.	1.3	1.1	1.1	1.5	1.5	1.4	1.6	1.7	1.6	1.5	1.8	2.1

6-29

Table 6.8 Measured and predicted air concentrations for Hoover Universal case study

Volume	Measured concentration (estimated from one or more observations) ( $\mu\text{g}/\text{m}^3$ )		Predicted concentration ( $\mu\text{g}/\text{m}^3$ )	Difference [predicted - measured] ( $\mu\text{g}/\text{m}^3$ )	Percent difference [100% $\times$ (predicted - measured) $\div$ measured]
	Mean	Standard Deviation			
1	25.3	4.0	18.7	6.6	26
2	41.0	4.2	41.0	0	0
2a	NR	NR	0	-	-
3	NR	NR	0	-	-
4	55.0	37.8	52.1	2.9	5.2
5	NR	NR	21.7	-	-
6	6.3	3.9	4.60	1.7	27
7	NR	NR	9.38	-	-
8	15.2	5.6	15.5	-0.3	2.0
9	29.2	9.1	34.0	-4.8	16
10	17.5	1.9	15.4	2.1	12
11	14.8	4.5	17.2	-2.4	16

NR - None Reported

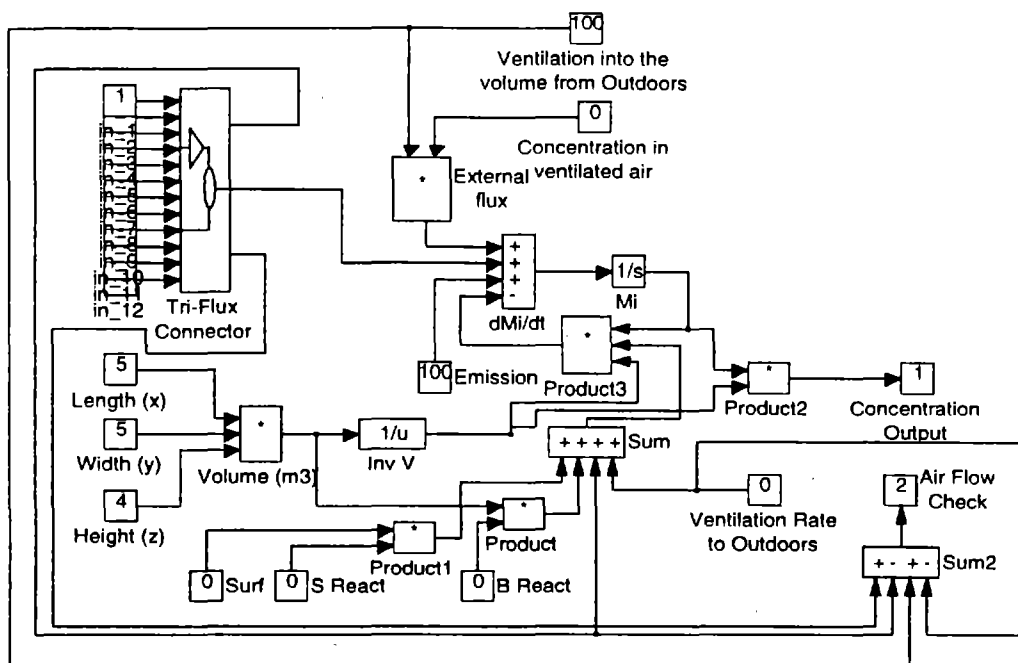


Figure 6.1 Volume element for Volume 1 of the two-volume example (see Figure 4.10 for a schematic of the two-volume system)

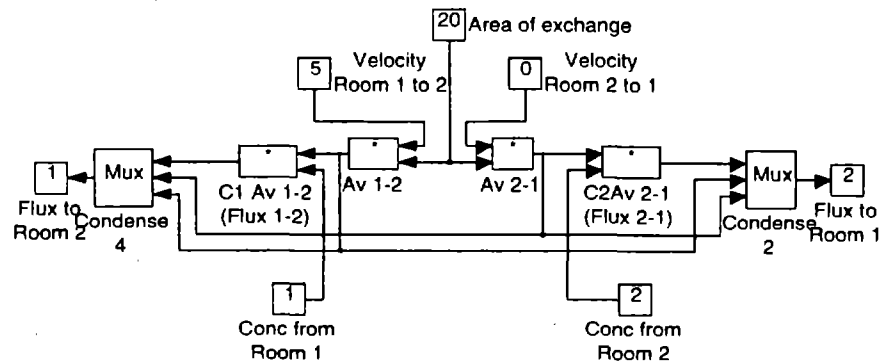


Figure 6.2 Exchange element connecting Volumes 1 and 2 of the two-volume example (see Figure 4.10 for a schematic of the two-volume system)



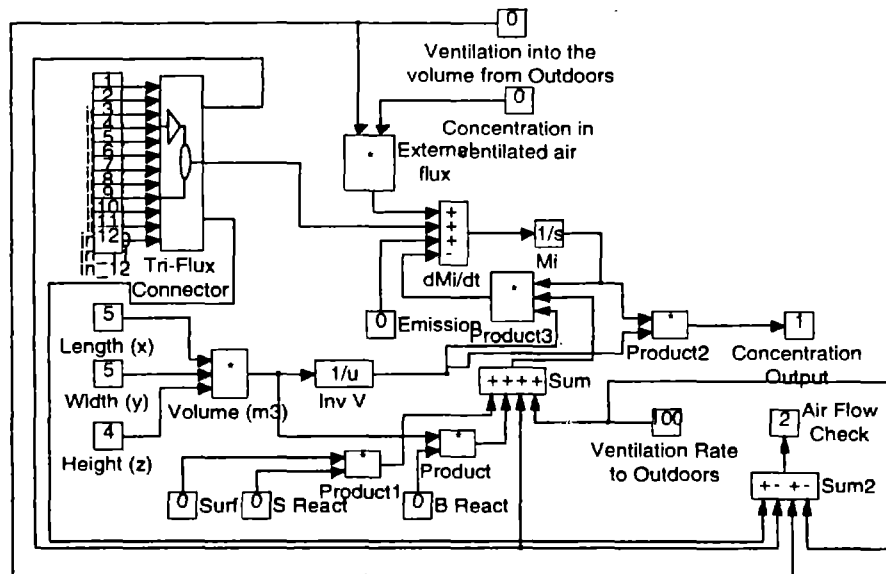


Figure 6.3 Volume element for Volume 2 of the two-volume example (see Figure 4.10 for a schematic of the two-volume system)

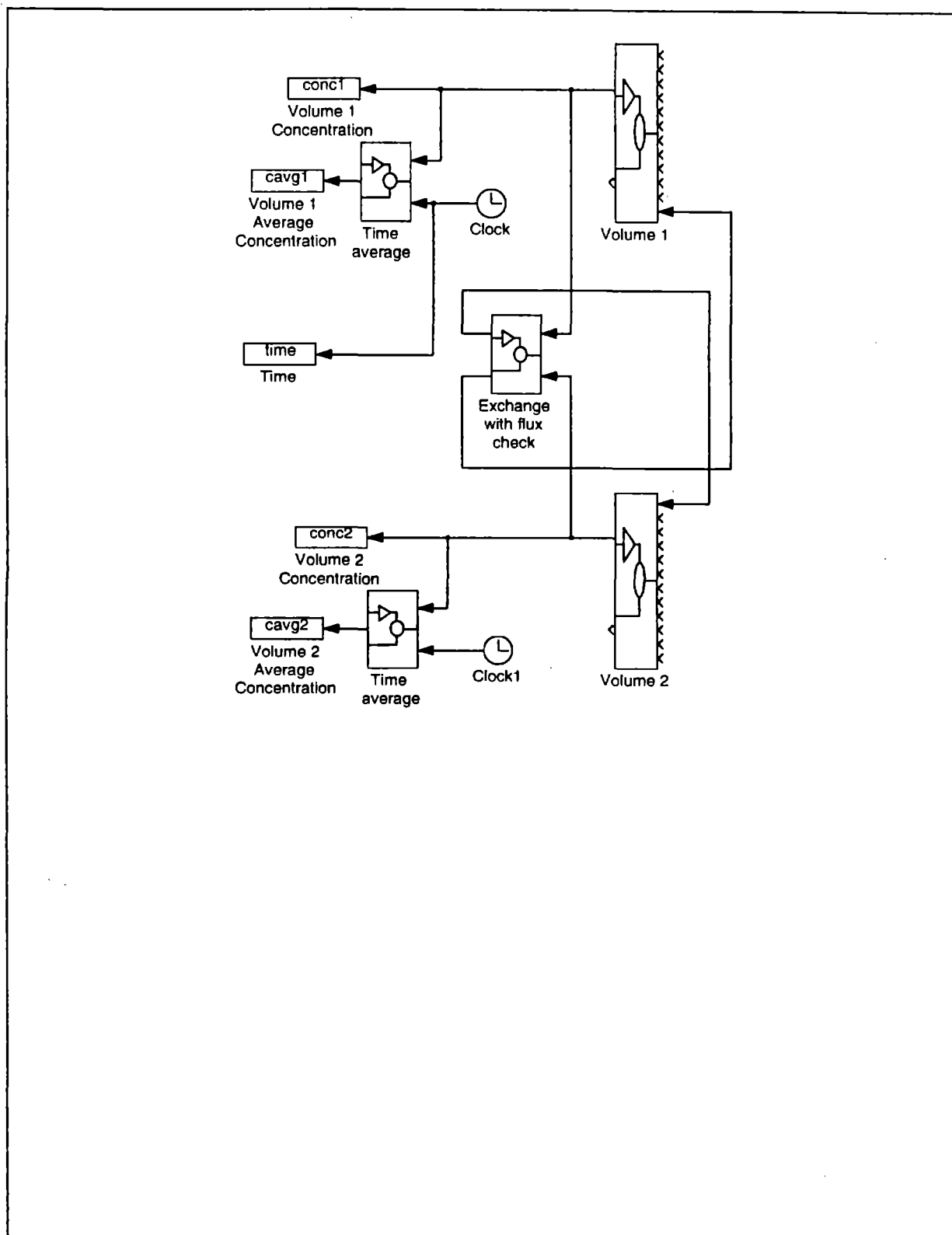


Figure 6.4 SIMULINK™ block diagram of the two-volume example

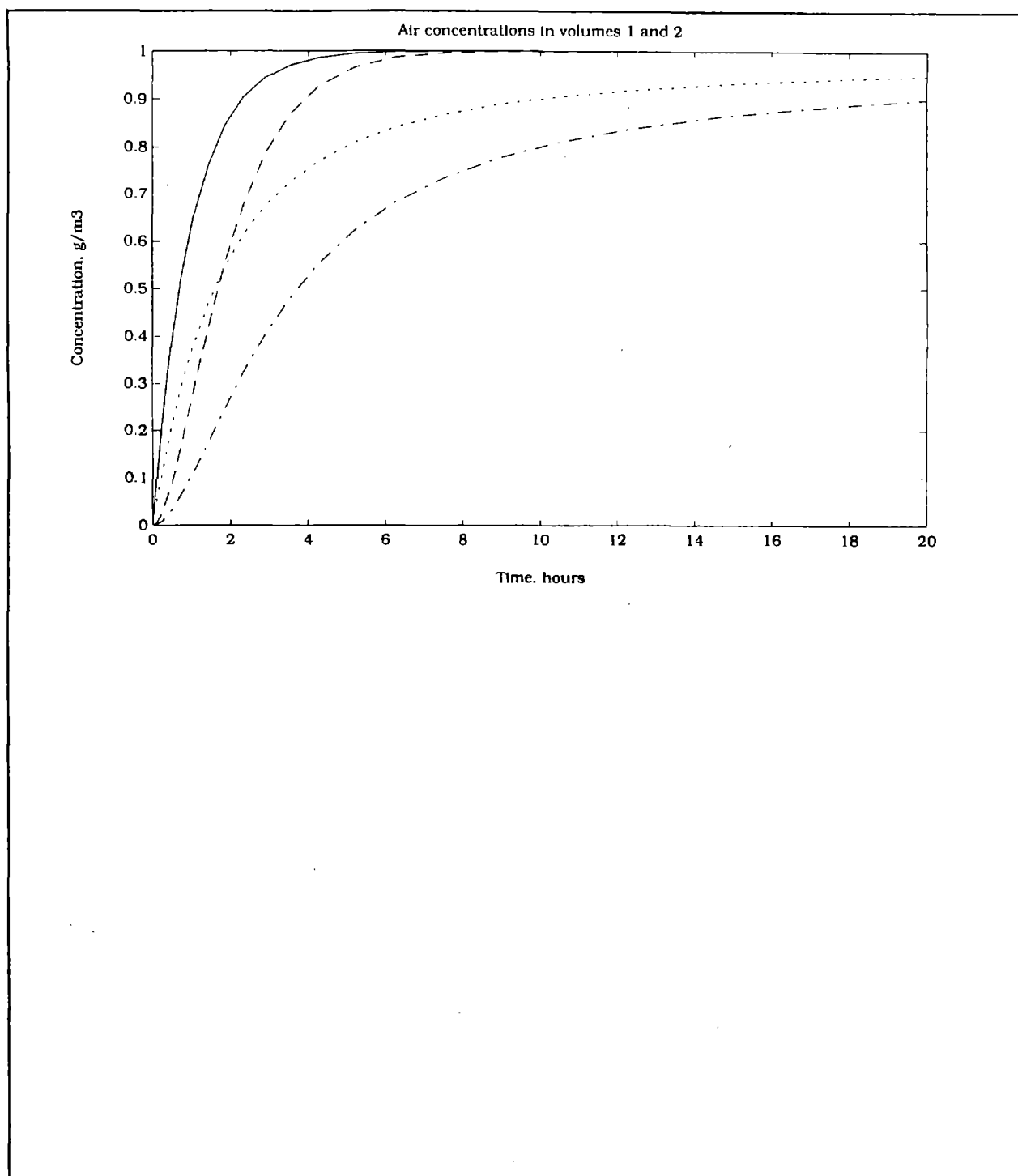


Figure 6.5 Pollutant concentrations in Volumes 1 and 2. Solid, dotted, dashed, and dash-dotted lines indicate concentrations in Volume 1 (instantaneous), Volume 1 (time-averaged), Volume 2 (instantaneous), and Volume 2 (time-averaged), respectively.

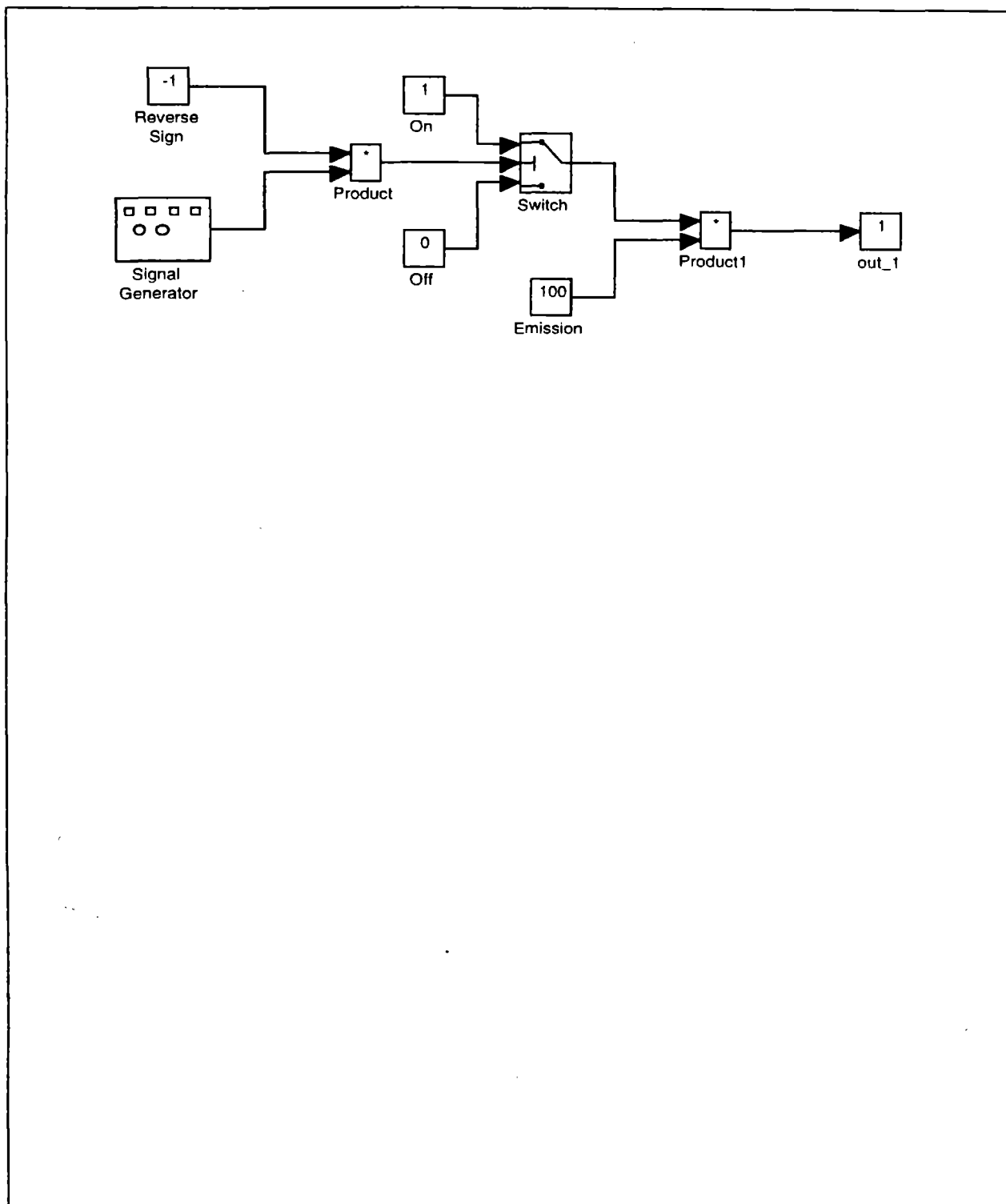


Figure 6.6 Periodic emission element with constant emission for one-hour in a two-hour cycle. This element, when reduced to icon form, is substituted into the Volume 1 element (shown in Figure 6.1).

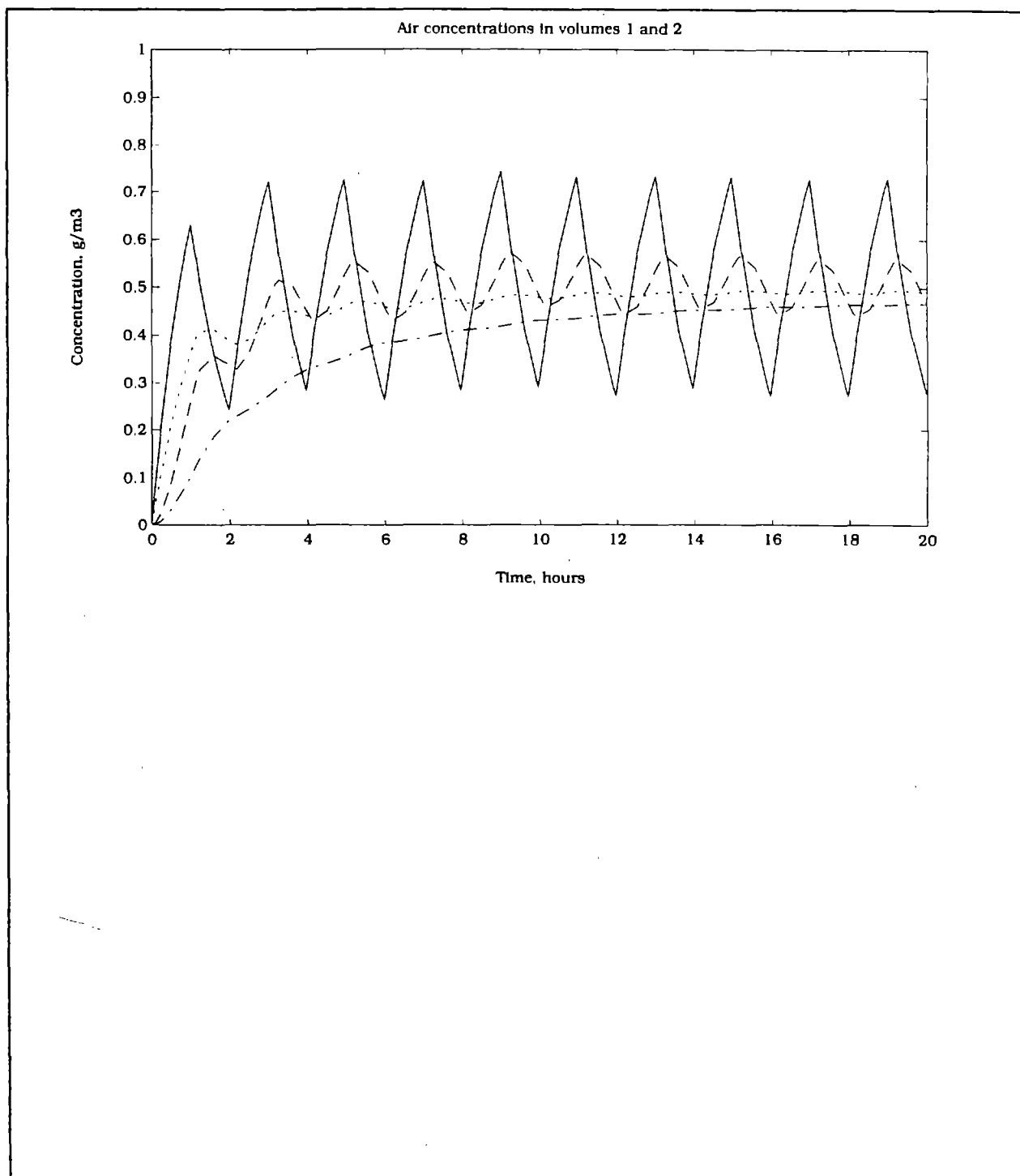


Figure 6.7 Concentrations under periodic emissions (Time On:Time Off = 1:1). Solid, dotted, dashed, and dash-dotted lines indicate the concentrations in Volume 1 (instantaneous), Volume 1 (time-averaged), Volume 2 (instantaneous), and Volume 2 (time-averaged).

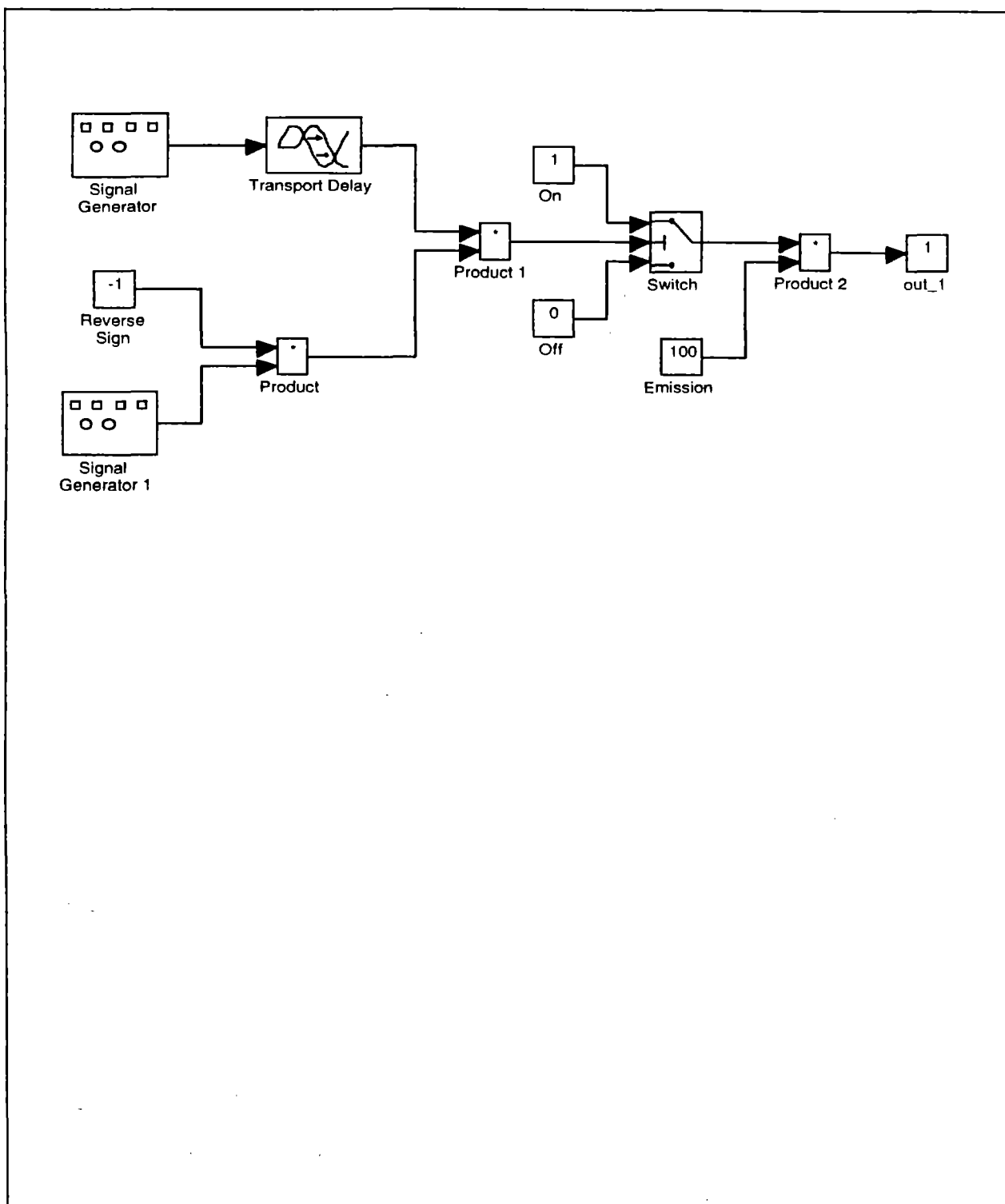


Figure 6.8 Periodic emission element with constant emission of one-hour in a six-hour period. This element, when reduced to icon form, is substituted into the Volume 1 element (shown in Figure 6.1).

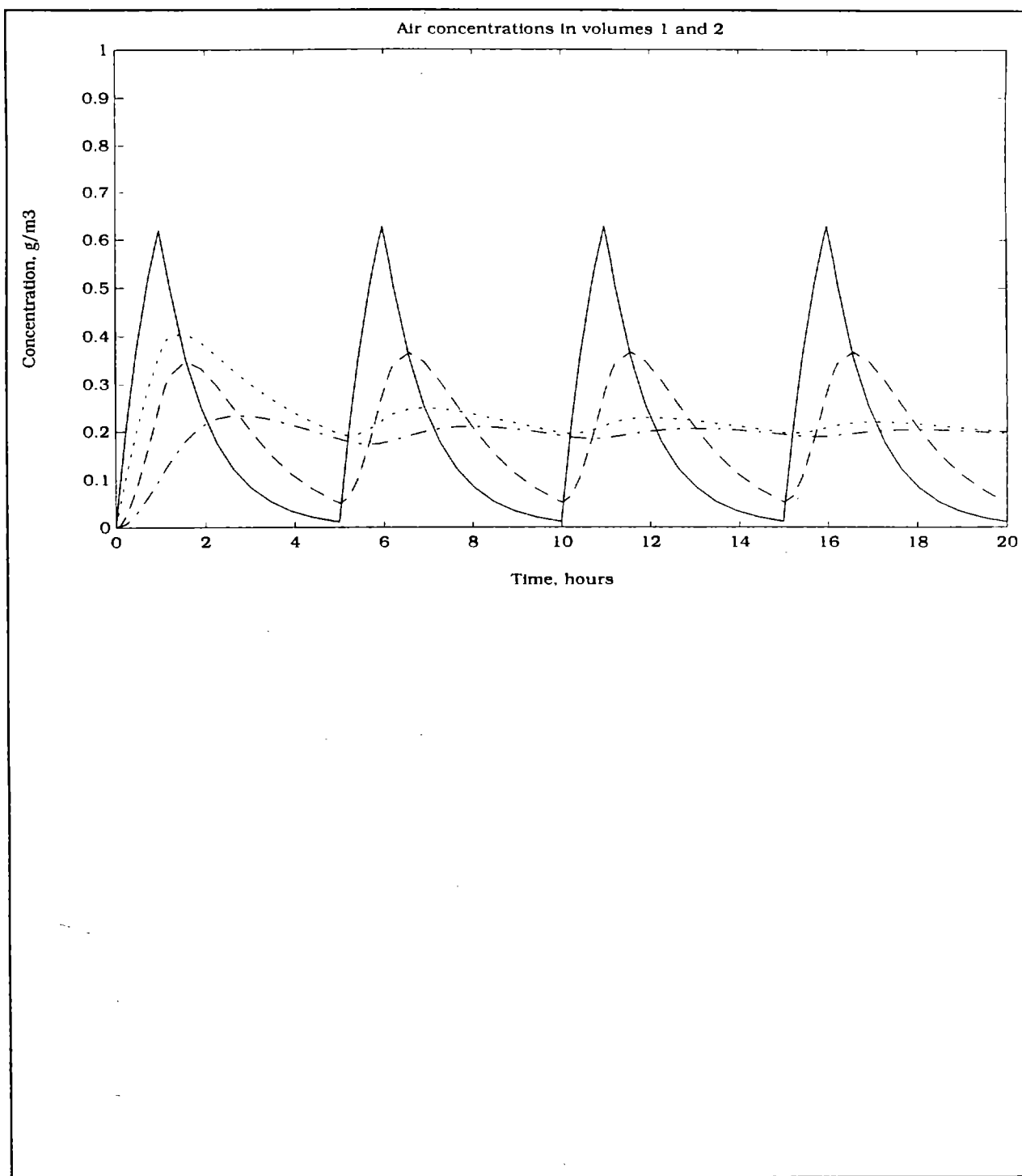


Figure 6.9 Concentrations under periodic emissions (Time On:Time Off = 1:4). Solid, dotted, dashed, and dash-dotted lines indicate the concentrations in Volume 1 (instantaneous), Volume 1 (time-averaged), Volume 2 (instantaneous), and Volume 2 (time-averaged).

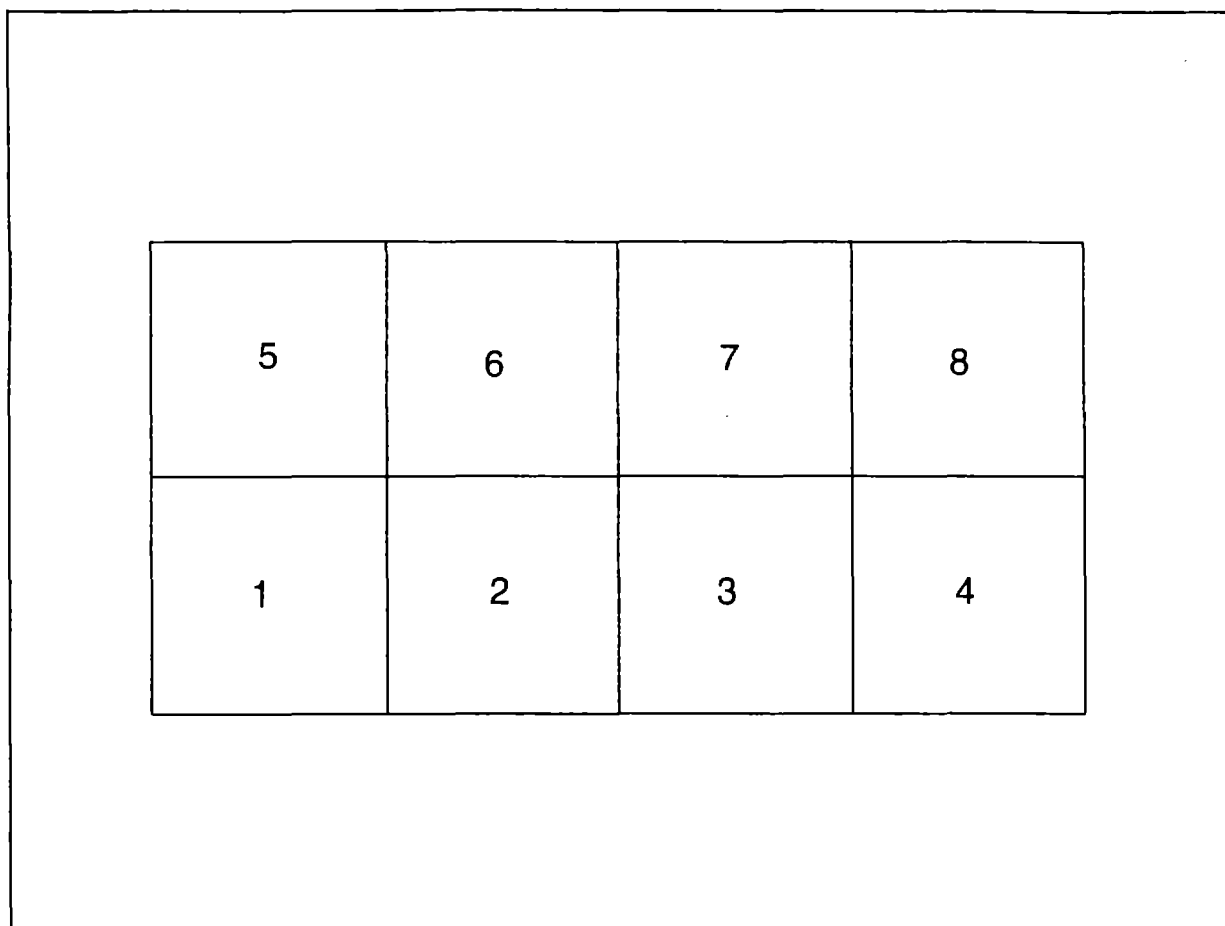


Figure 6.10 Topological diagram of a two-dimensional eight-volume system.



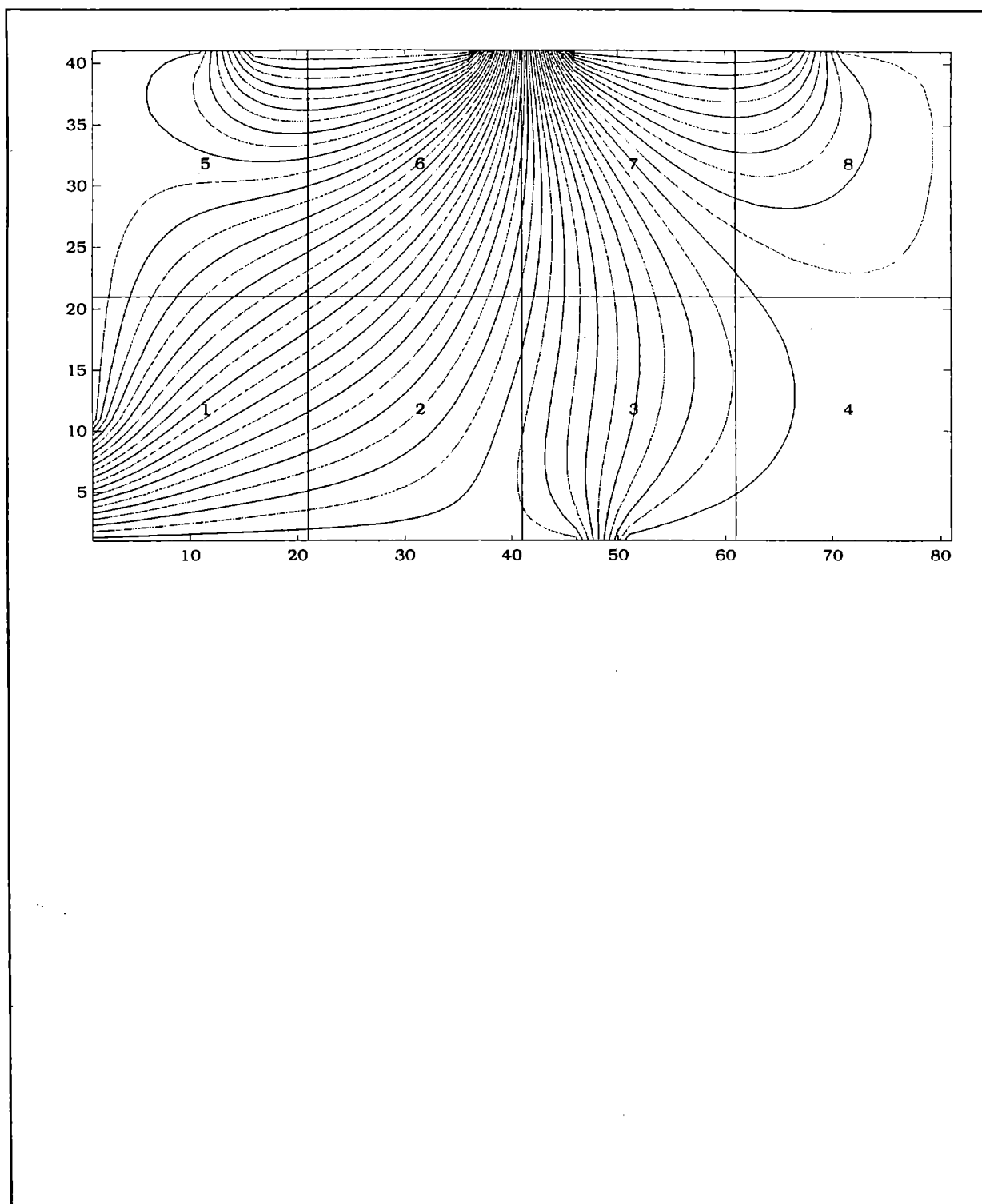


Figure 6.11 Two-dimensional air flow streamlines obtained from potential flow theory. Air is assumed to enter the room in Volumes 1, 3, 5, and 8, and exit the room from Volumes 6 and 7.

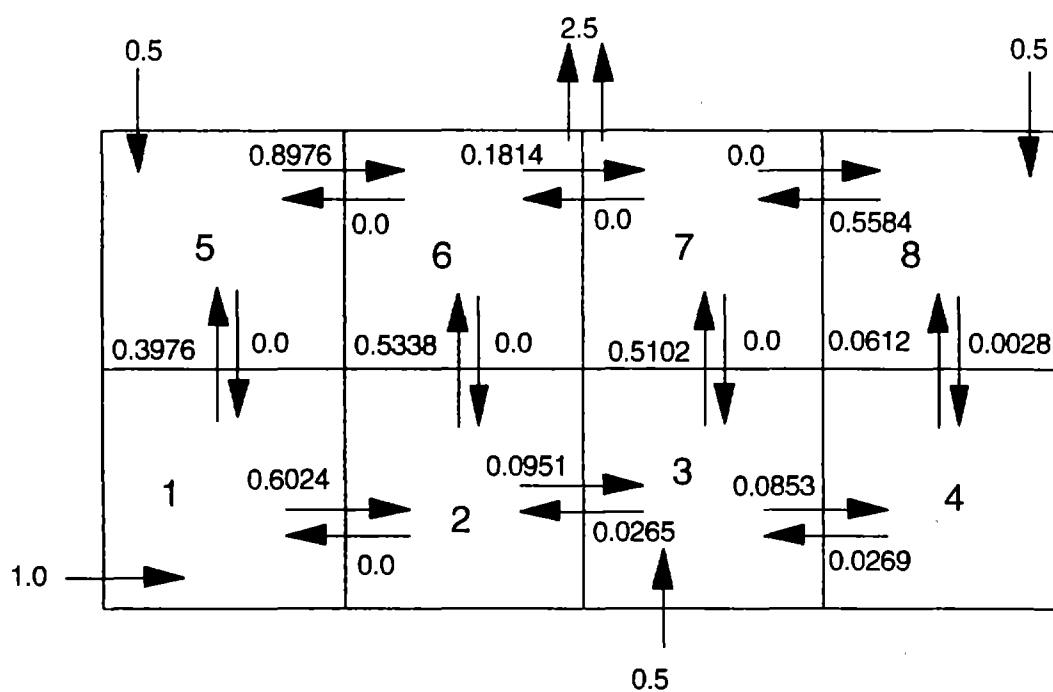


Figure 6.12 Cross-boundary air fluxes derived from integration of the streamlines shown in Figure 6.11.

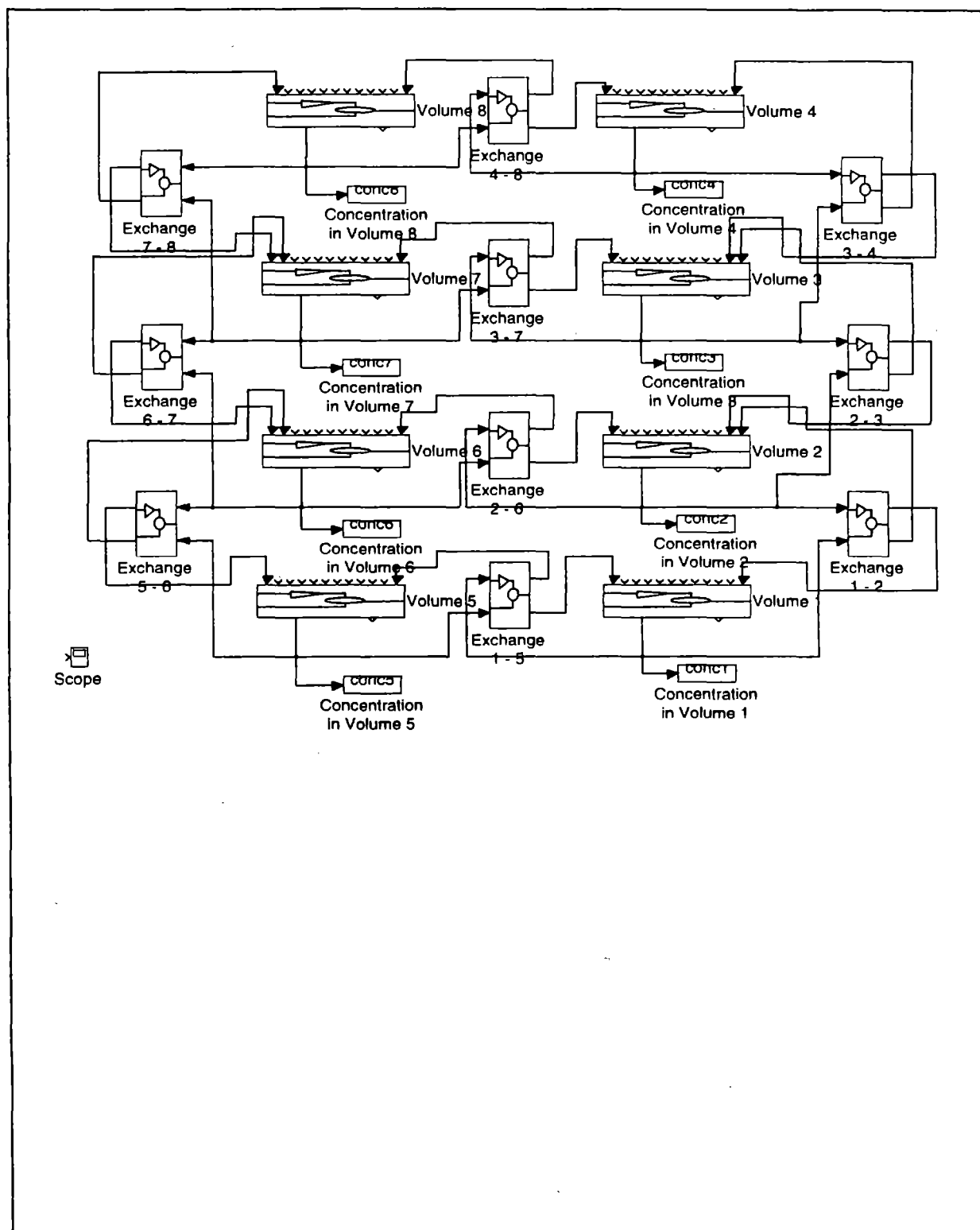


Figure 6.13 SIMULINK™ block diagram representation of the eight-volume system. The numbering and connection of Volume elements is consistent with Figure 6.10.

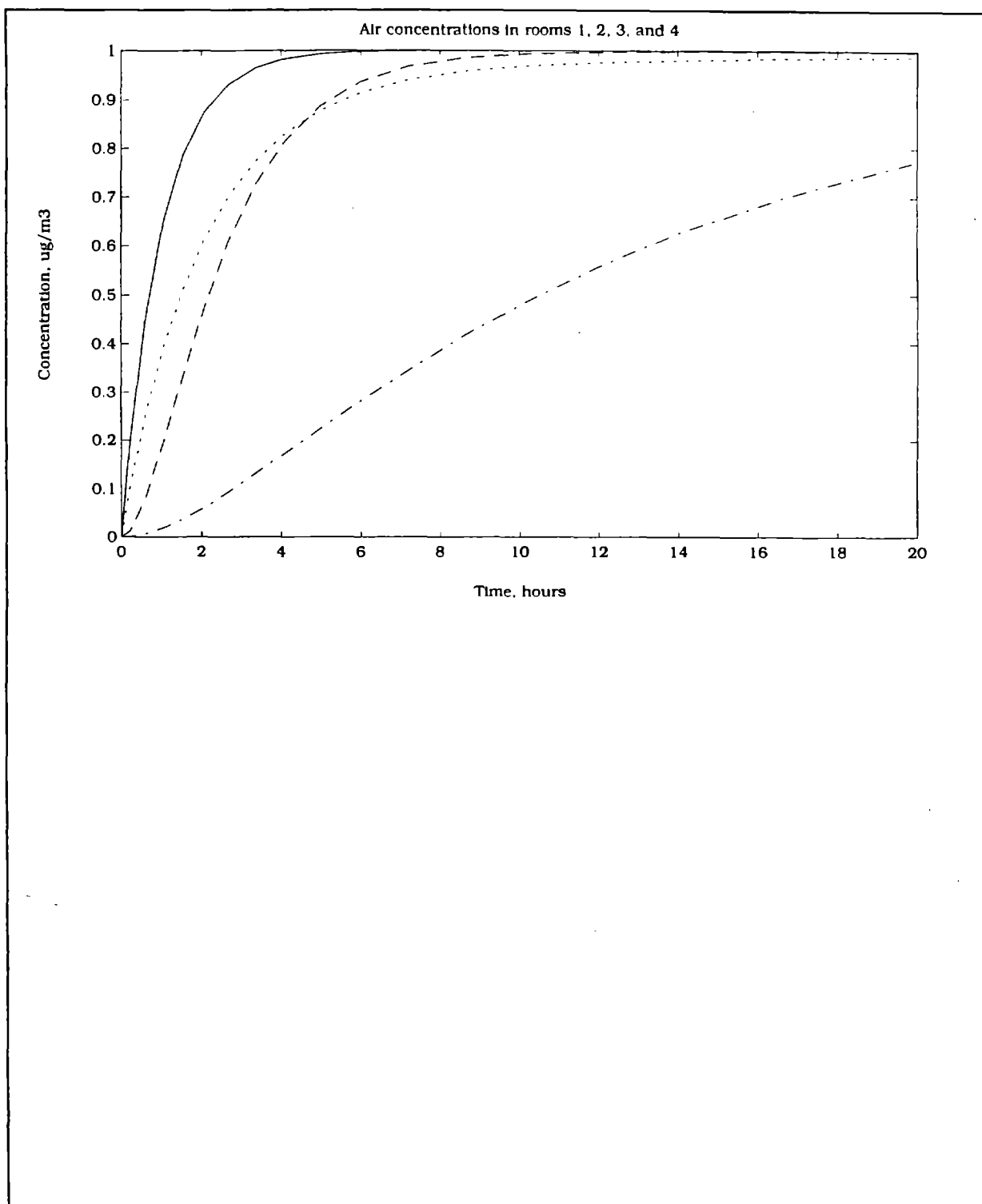


Figure 6.14 Modeled air pollutant concentrations in Volumes 1, 2, 3, 4 of the eight-volume example; Volume 1 line is solid, Volume 2 is dashed, Volume 3 is dotted, Volume 4 is dash-dot.

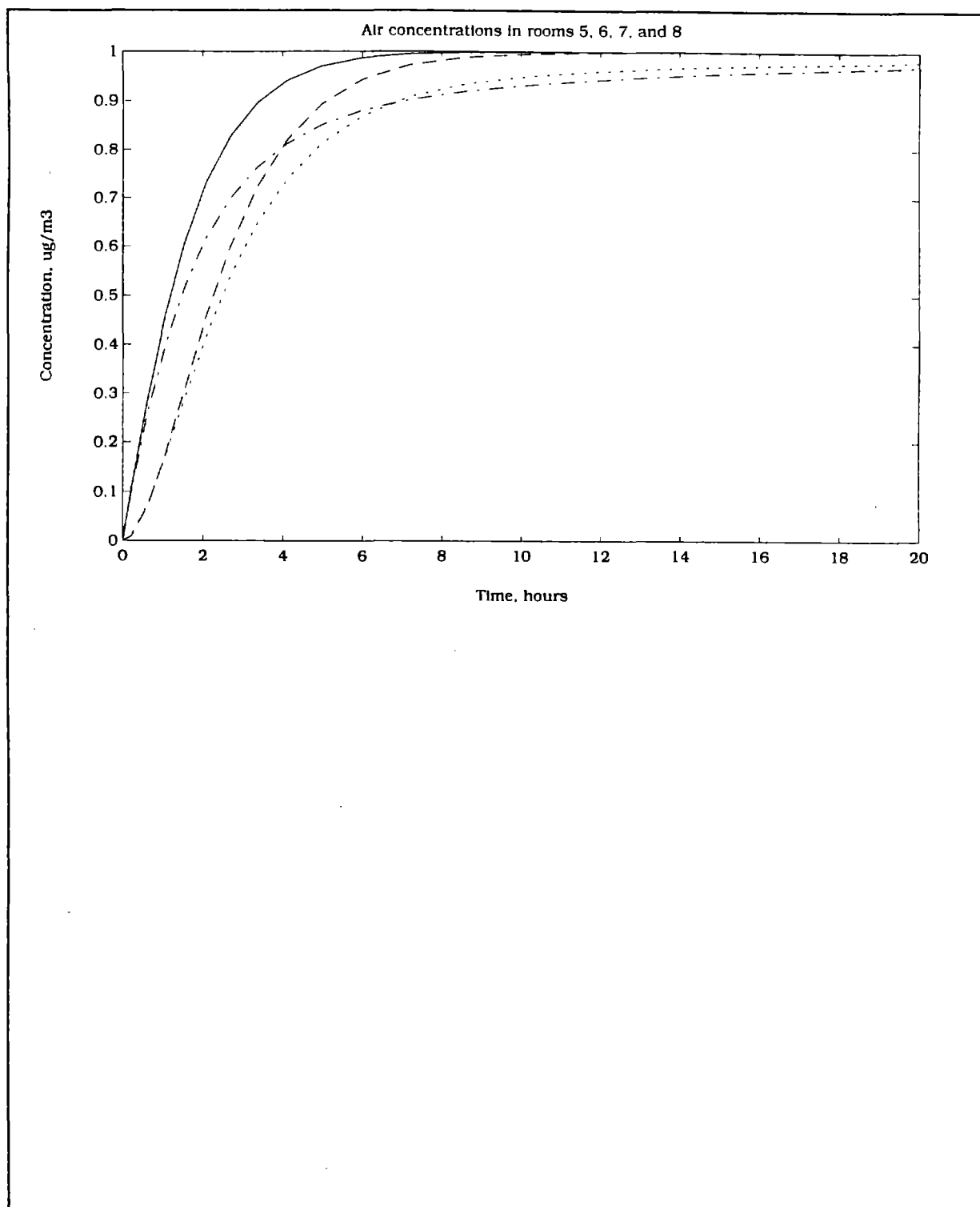


Figure 6.15 Modeled air pollutant concentrations in Volumes 5, 6, 7, 8 of the eight-volume example; Volume 5 line is solid, Volume 6 is dashed, Volume 7 is dotted, Volume 8 is dash-dot.

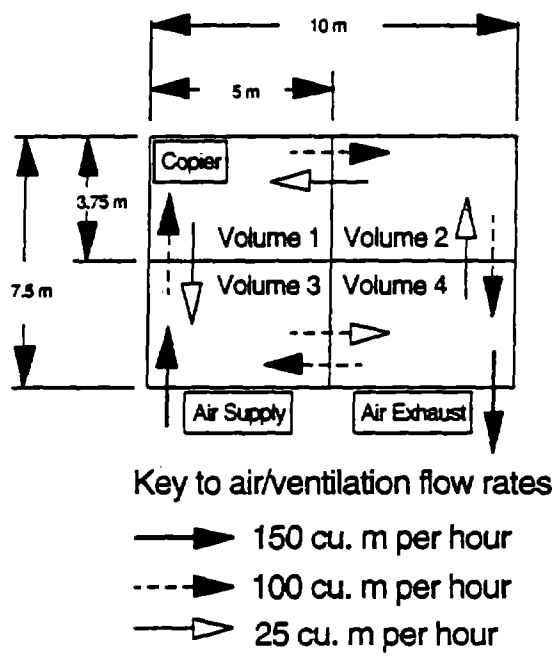


Figure 6.16 Schematic of room (overhead view) showing the locations of a photocopier (ozone source), an air supply, air exhaust to the outdoors, and the subdivisions used for modeling

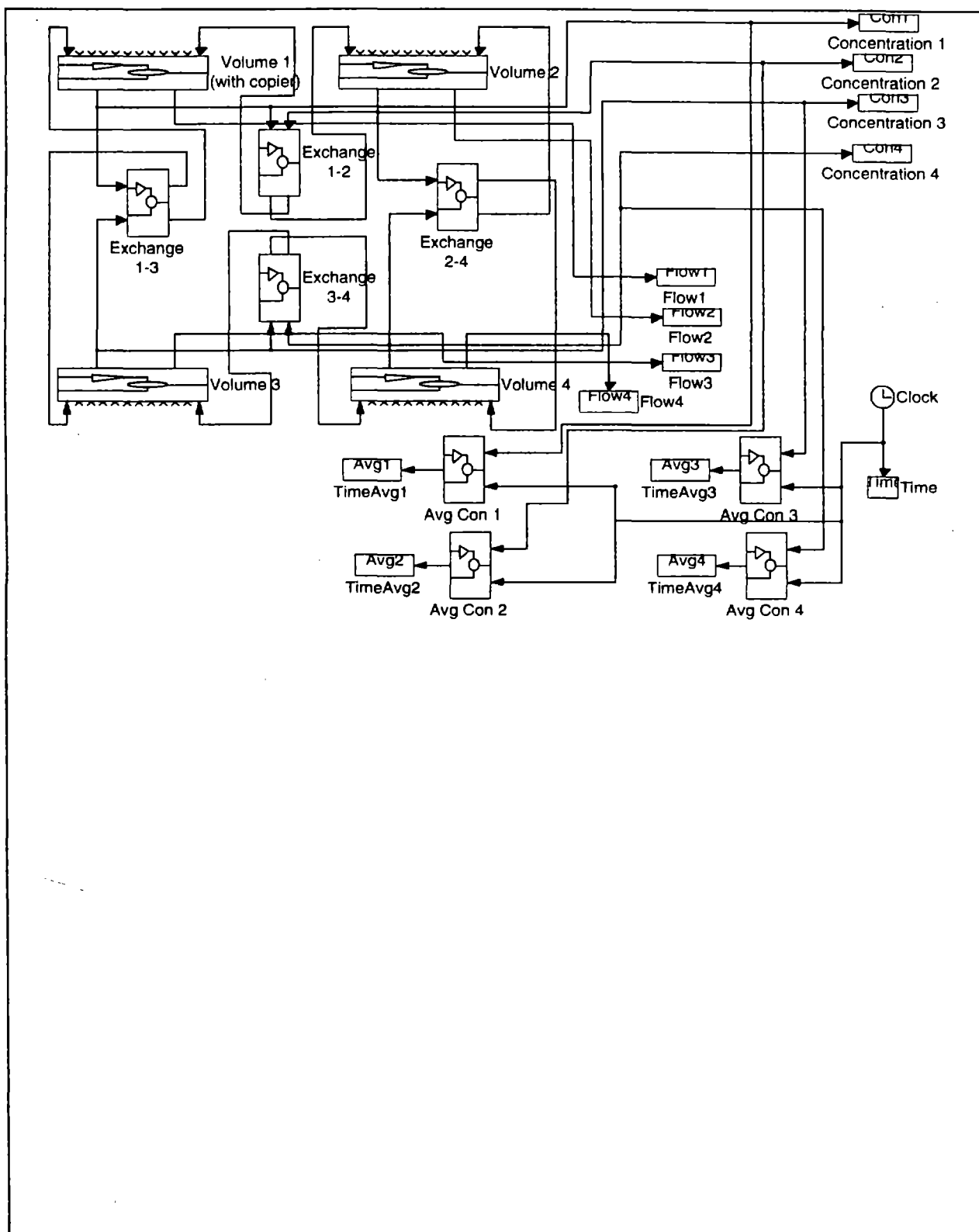


Figure 6.17 SIMULINK™ diagram of the ozone model application

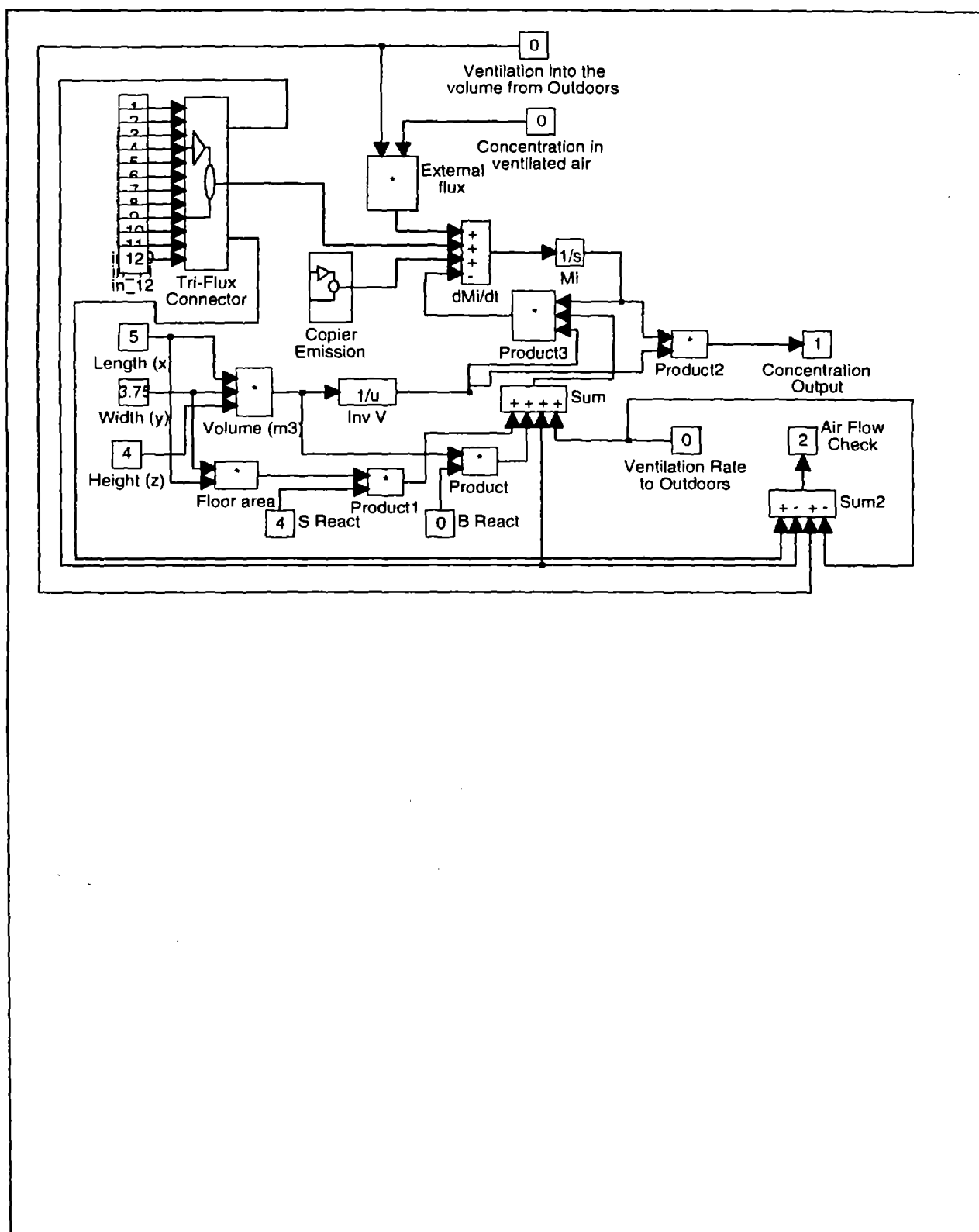


Figure 6.18 Block diagram of Volume 1 that houses the photocopy emission element



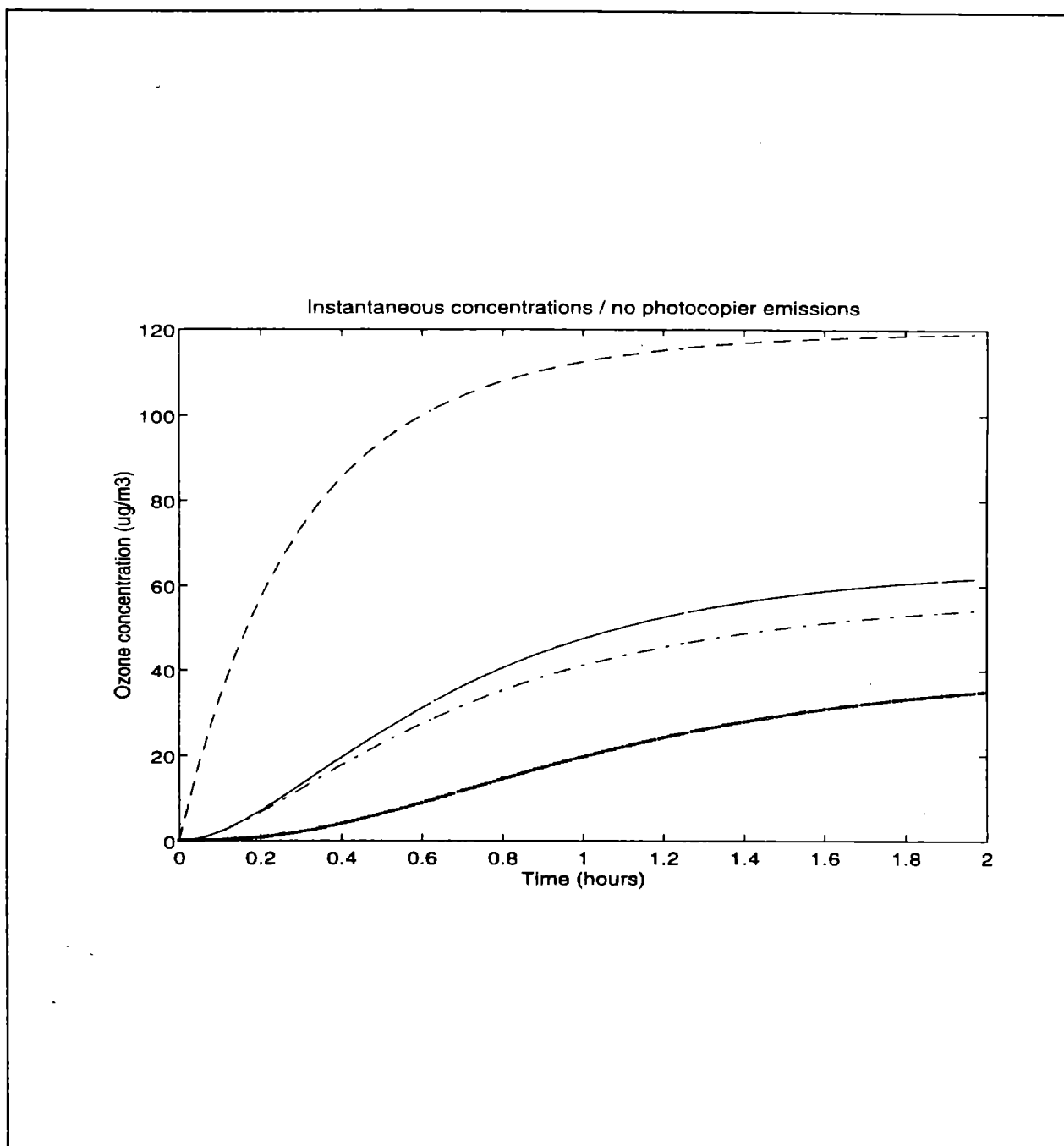


Figure 6.19 Simulation of ozone concentrations ( $\mu\text{g}/\text{m}^3$ ) as a function of time with no indoor source of ozone generation. Outdoor air containing  $200 \mu\text{g}/\text{m}^3$  of ozone enters the room, which is free of ozone initially, in Volume 3. Time-dependent ozone concentrations in Volumes 1, 2, 3, and 4 are represented by the solid, dotted, dashed, and dash-dotted curves, respectively.

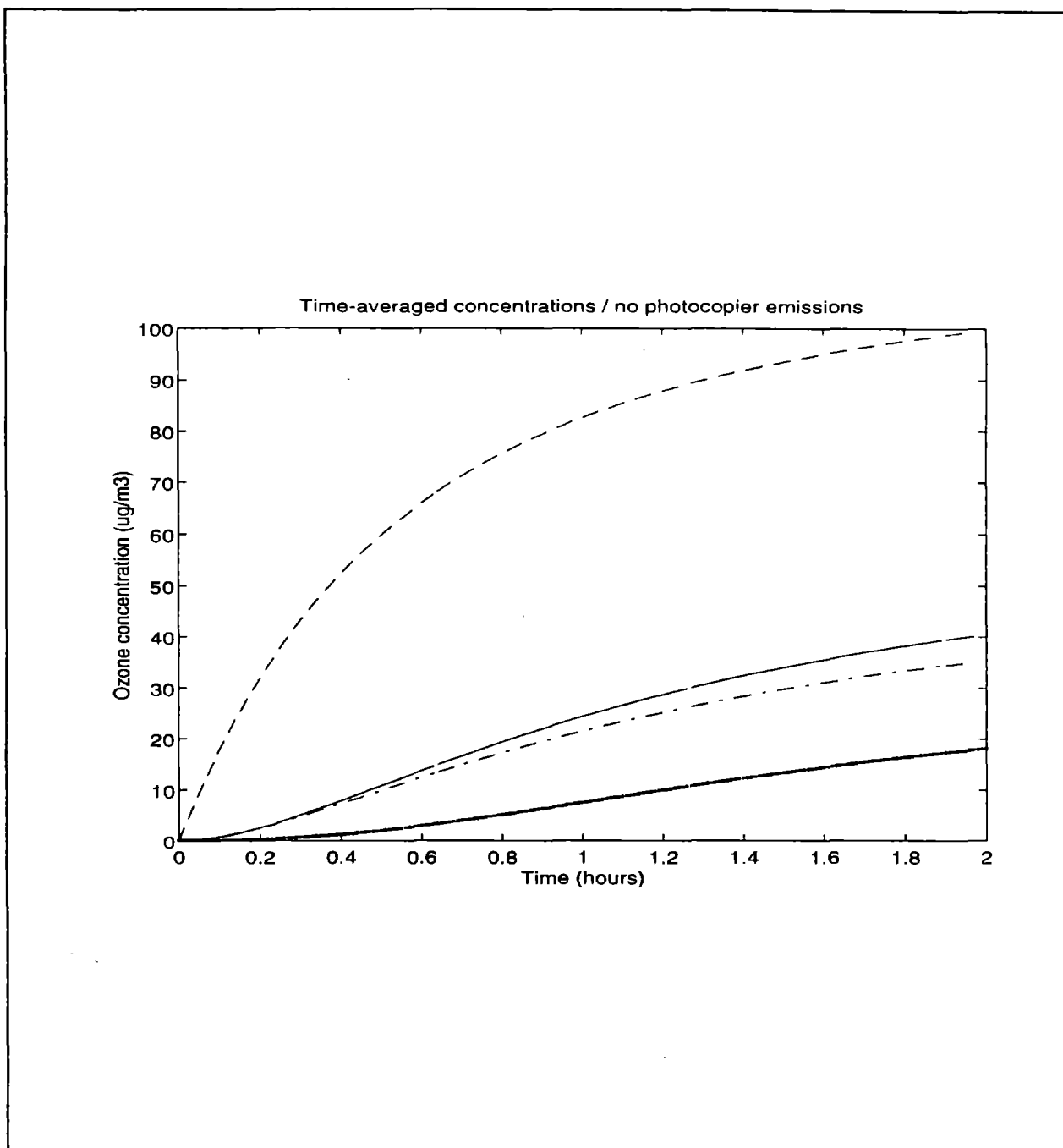


Figure 6.20 Simulation of time-averaged ozone concentrations ( $\mu\text{g}/\text{m}^3$ ) as a function of time with no internal source of ozone generation. Curves depict time-averages of the concentration profiles of Figure 6.19. Time-averaged ozone concentrations in Volumes 1, 2, 3, and 4 are represented by the solid, dotted, dashed, and dash-dotted curves, respectively.

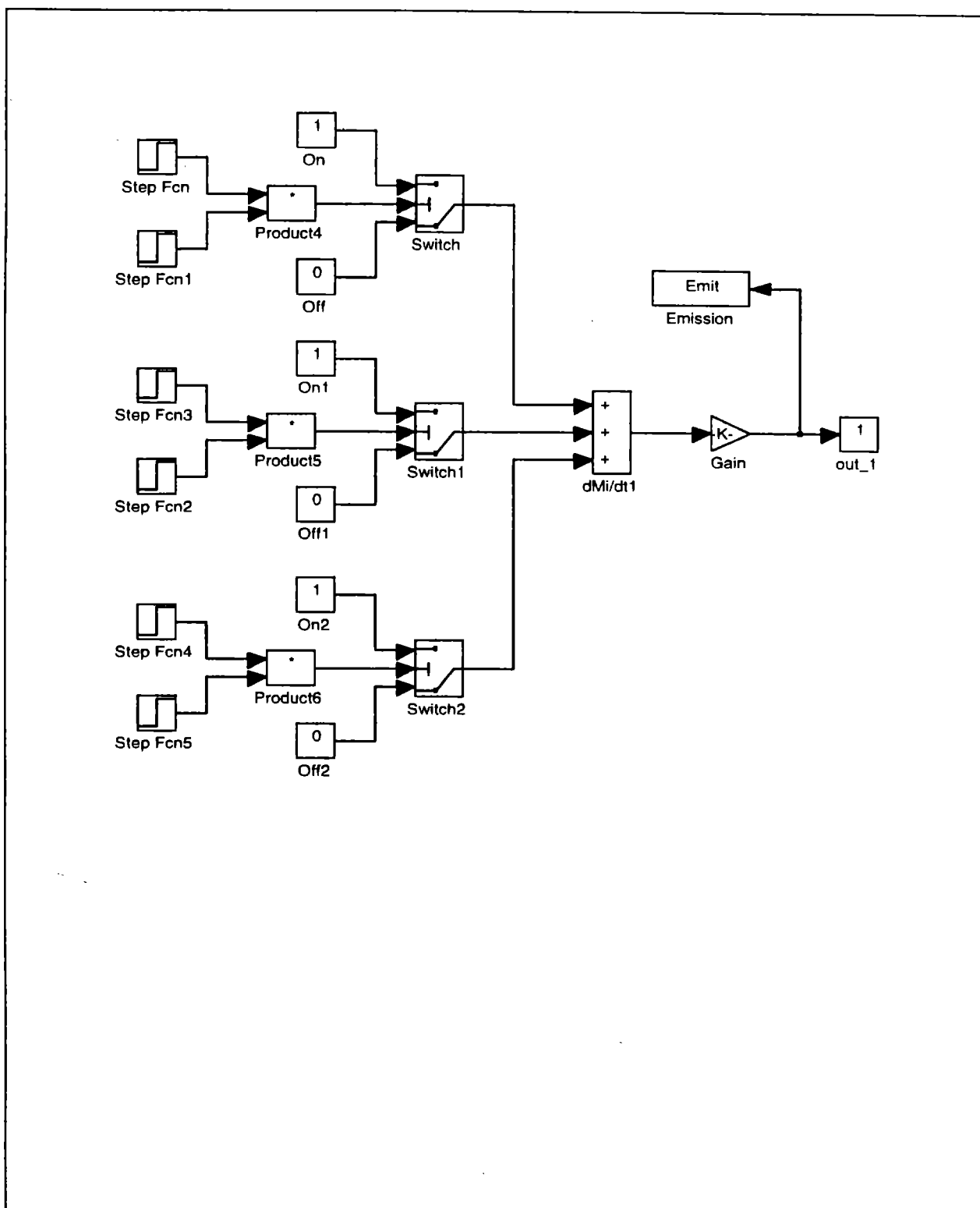


Figure 6.21 Photocopier emission element that produces step function output as a function of time

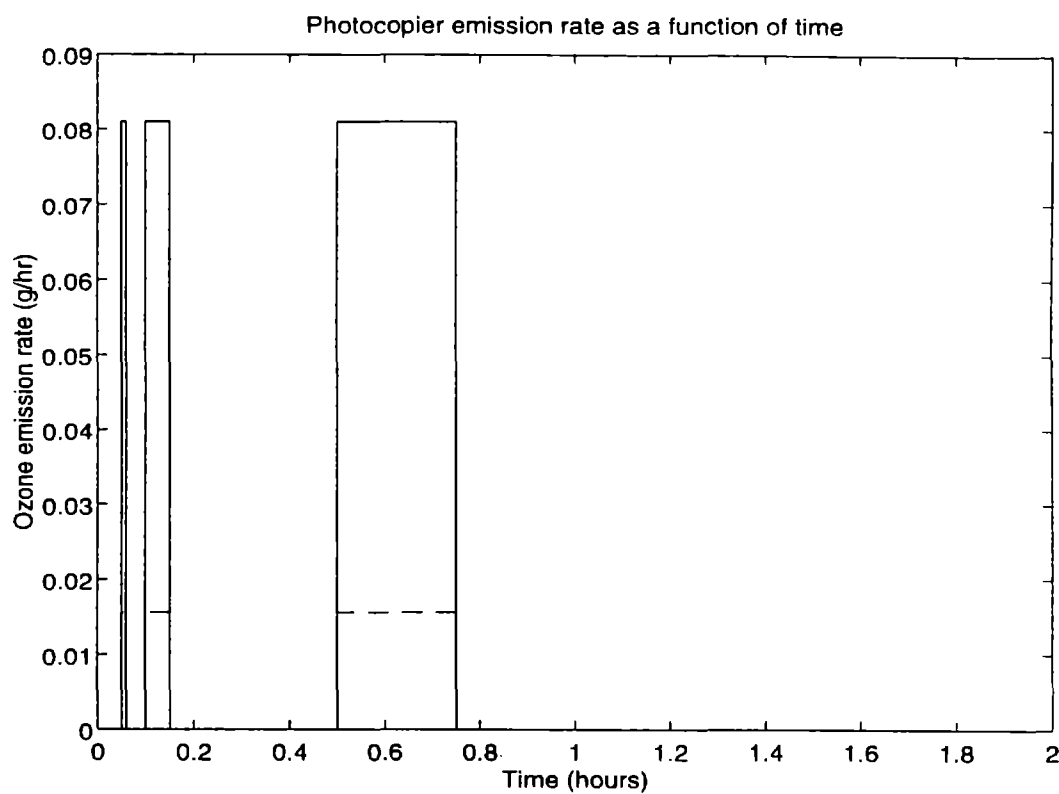


Figure 6.22 Emission rate of ozone (g/hr) from copier operation over the two-hour simulation period. The lower (dashed) and upper (solid) profiles model average (259  $\mu\text{g}/\text{min}$ ) and maximum (1350  $\mu\text{g}/\text{min}$ ) rates, respectively.

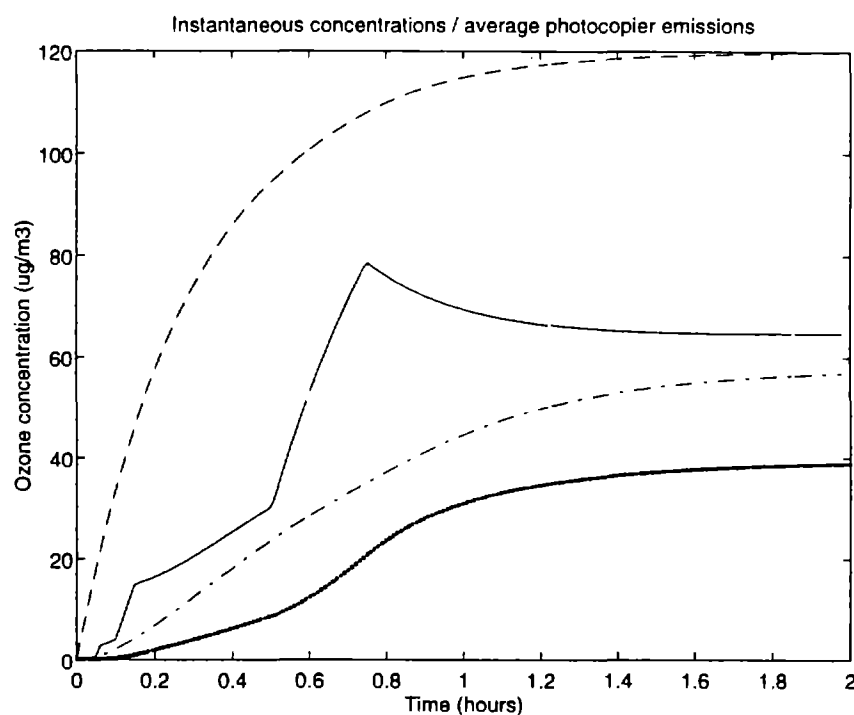


Figure 6.23 Simulation of ozone concentrations ( $\mu\text{g}/\text{m}^3$ ) as a function of time with both internal and external sources. Outdoor air containing  $200 \mu\text{g}/\text{m}^3$  of ozone enters the room, which is free of ozone initially, in Volume 3, and ozone is also emitted in Volume 1 by a copier at the assumed average rate of  $259 \mu\text{g}/\text{min}$ . Time-dependent ozone concentrations in Volumes 1, 2, 3, and 4 are represented by the solid, dotted, dashed, and dash-dotted curves, respectively.

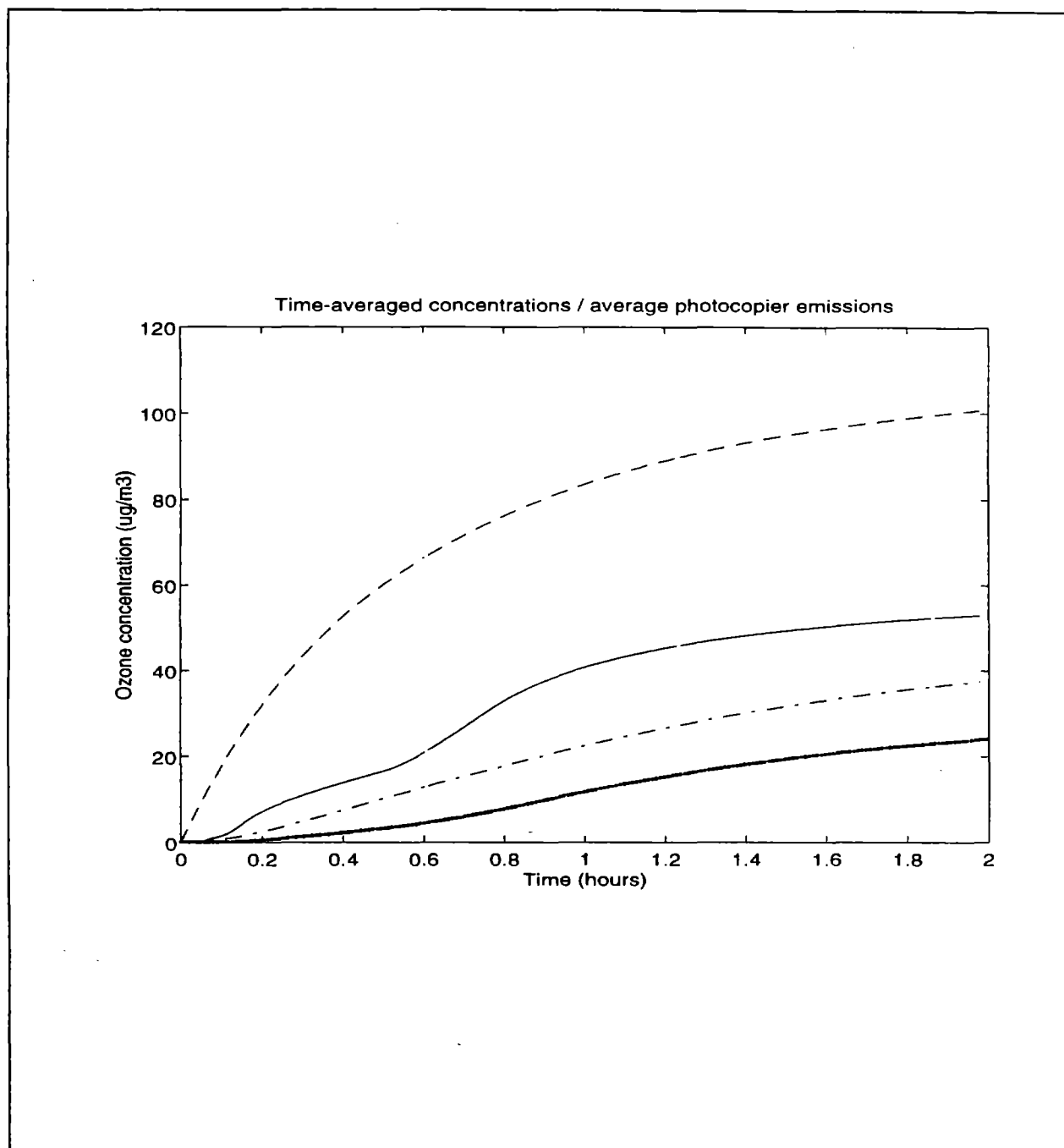


Figure 6.24 Time-averaged ozone concentrations ( $\mu\text{g}/\text{m}^3$ ) as a function of time with both internal and external sources. Time-averages are constructed from the time-dependent profiles depicted in Figure 6.23. Time-dependent ozone concentrations in Volumes 1, 2, 3, and 4 are represented by the solid, dotted, dashed, and dash-dotted curves, respectively.

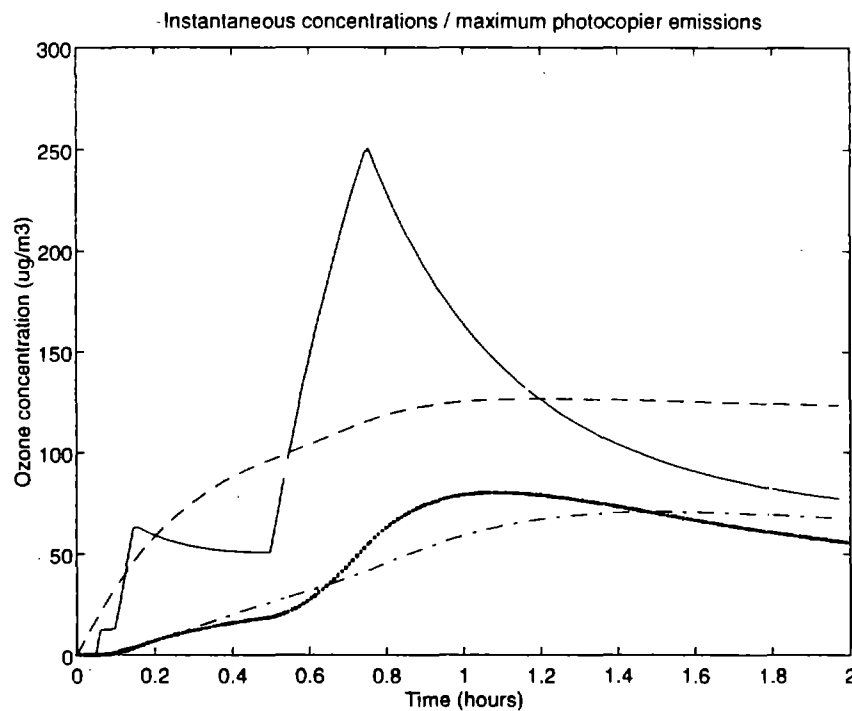


Figure 6.25 Simulation of ozone concentrations ( $\mu\text{g}/\text{m}^3$ ) as a function of time with both internal and external sources. Outdoor air containing  $200 \mu\text{g}/\text{m}^3$  of ozone enters the room, which is free of ozone initially, in Volume 3, and ozone is also emitted in Volume 1 by a copier at the assumed maximum rate of  $1350 \mu\text{g}/\text{min}$ . Time-dependent ozone concentrations in Volumes 1, 2, 3, and 4 are represented by the solid, dotted, dashed, and dash-dotted curves, respectively.

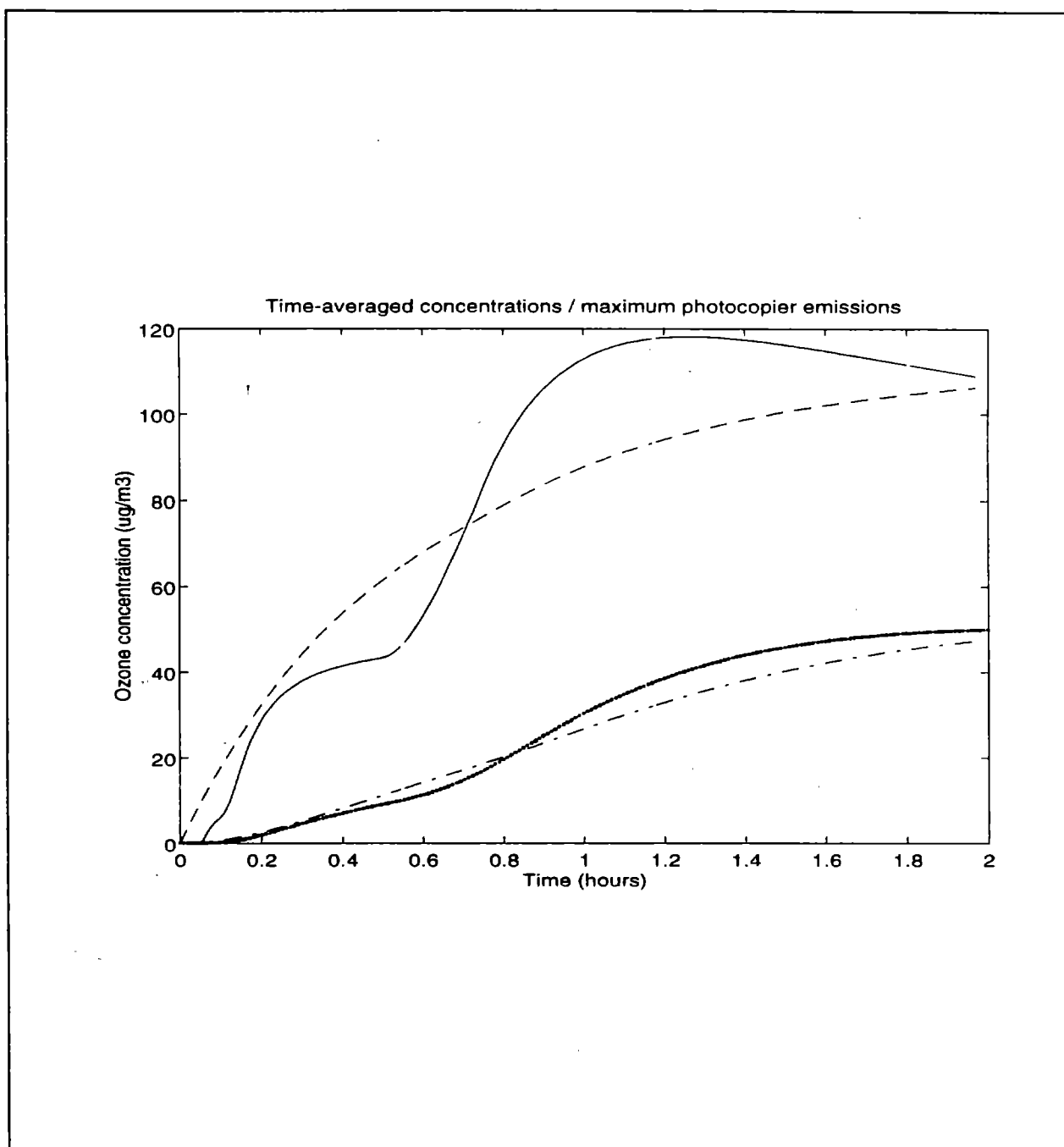


Figure 6.26 Time-averaged ozone concentrations ( $\mu\text{g}/\text{m}^3$ ) as a function of time with both internal and external sources. Time-averages are constructed from the time-dependent profiles depicted in Figure 6.26. Time-dependent ozone concentrations in Volumes 1, 2, 3, and 4 are represented by the solid, dotted, dashed, and dash-dotted curves, respectively.



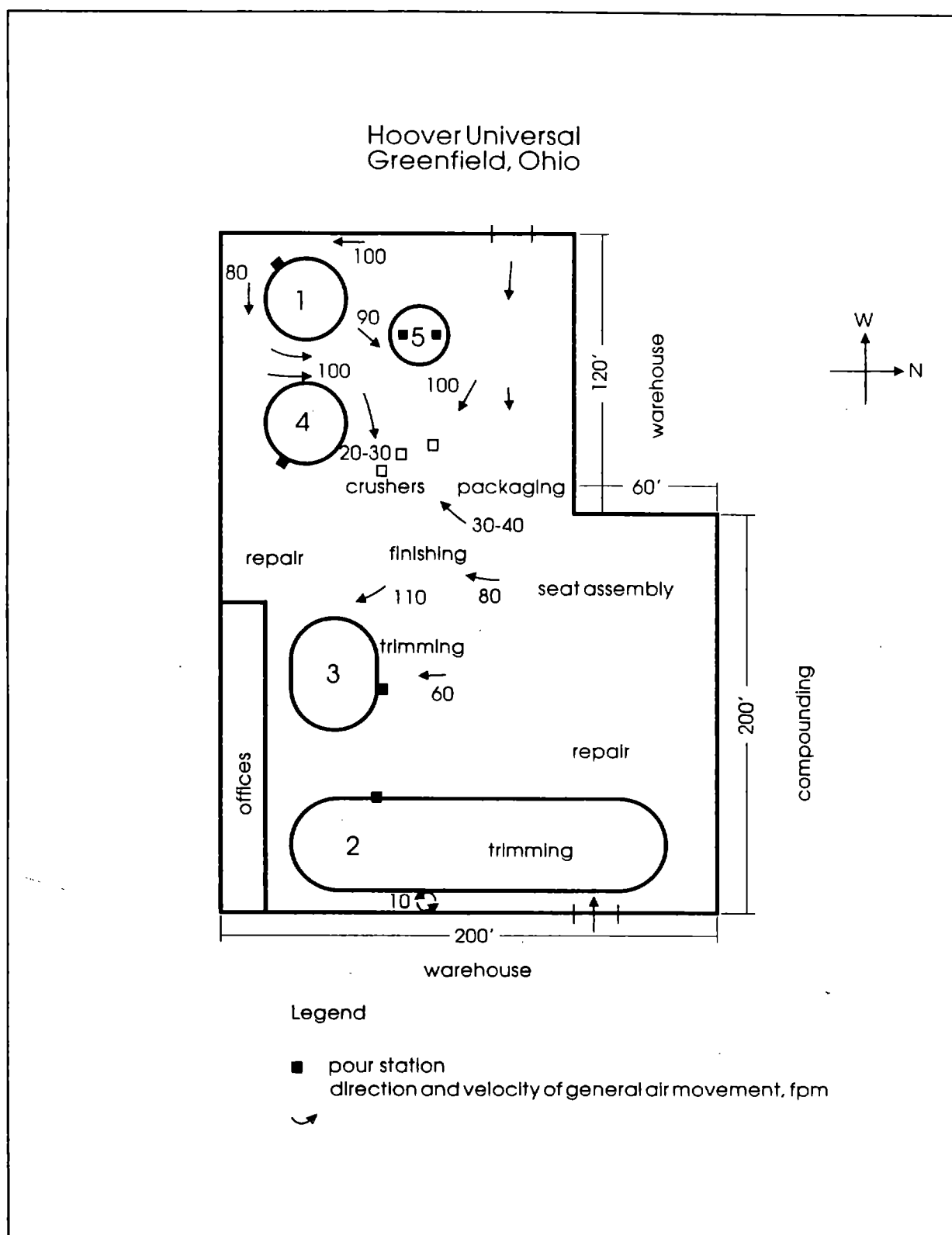


Figure 6.27 Floor plan of the Hoover Universal Plant. Adapted from Boeniger (1986).

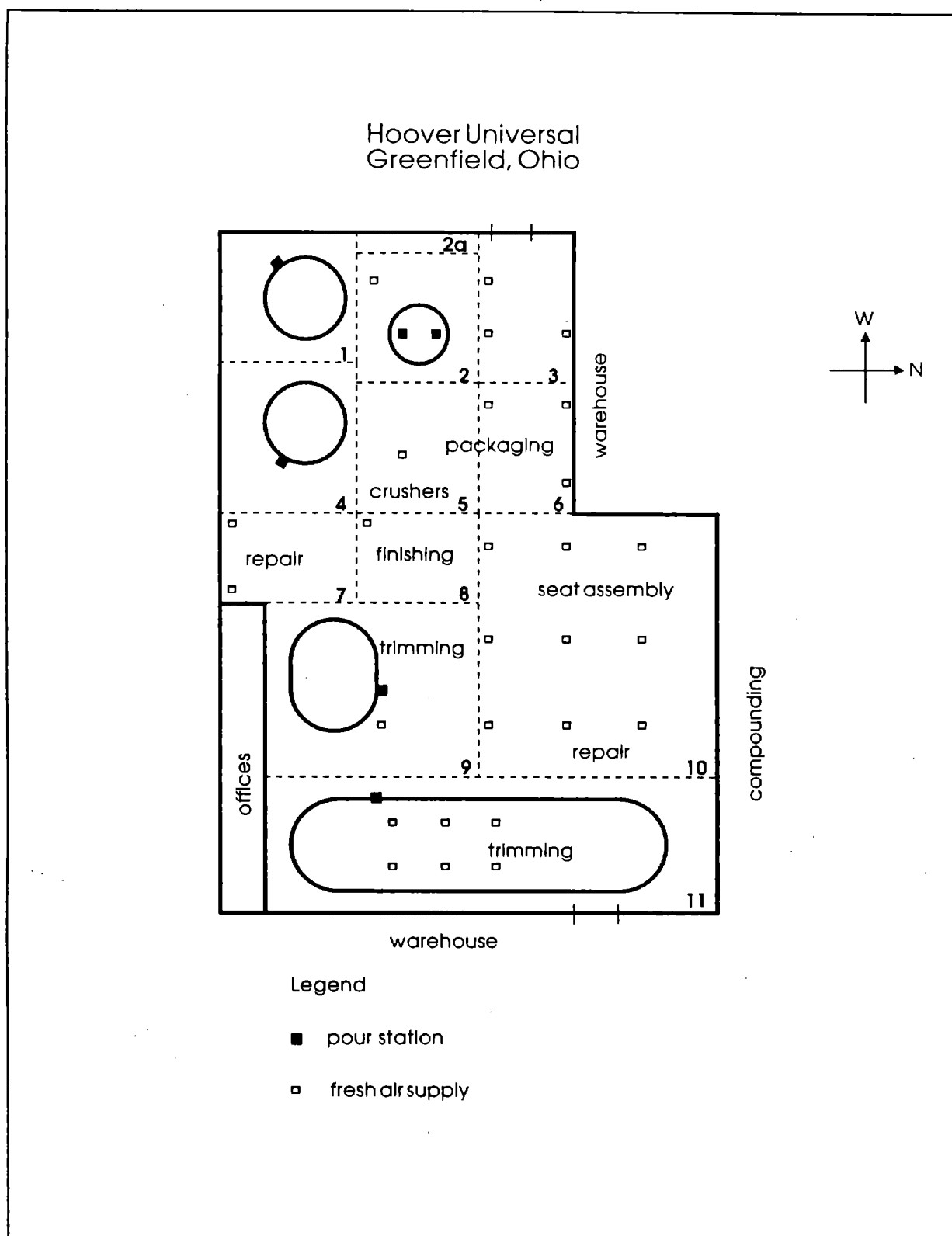


Figure 6.28 Control volumes used to model the Hoover Universal Plant

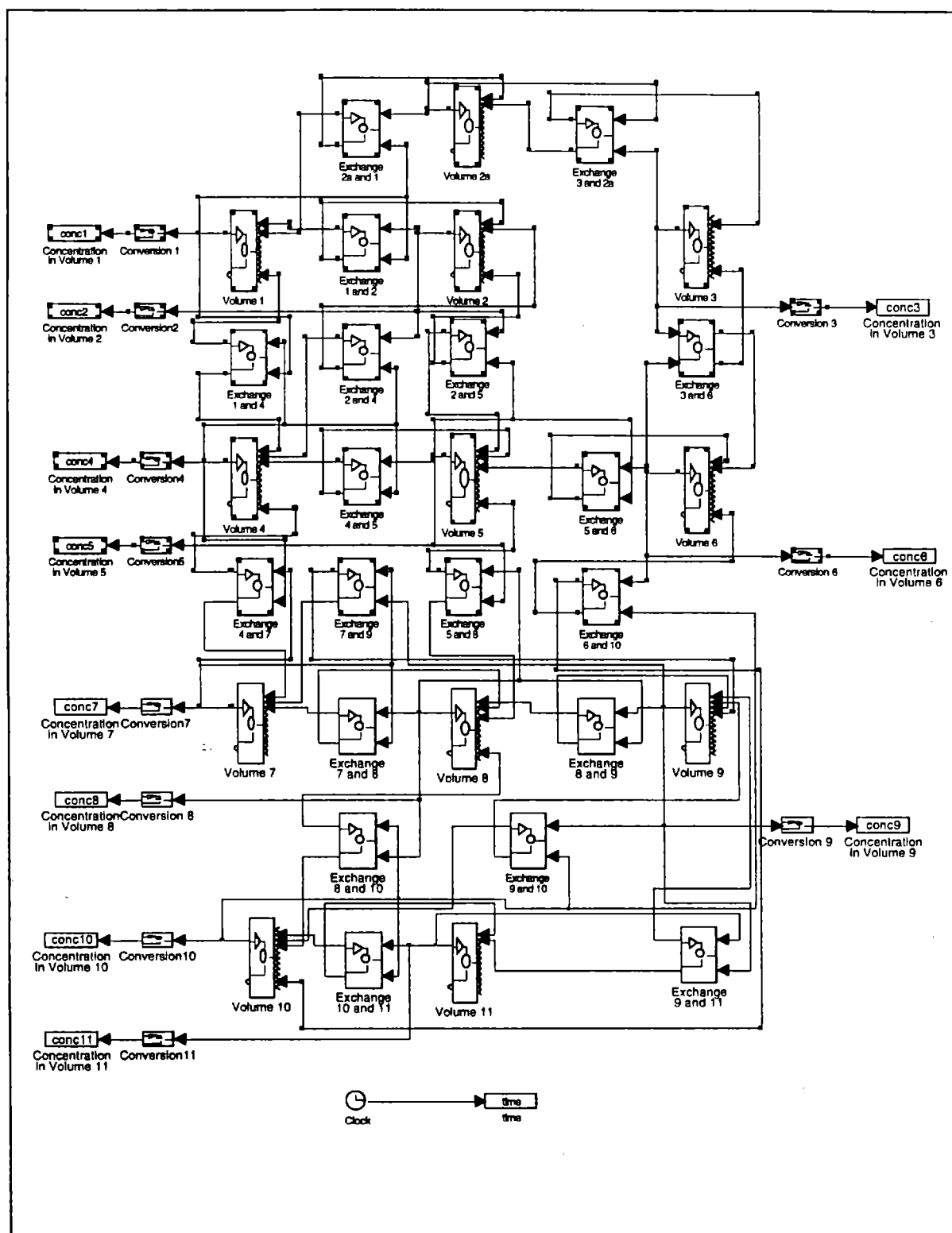


Figure 6.29 SIMULINK™ block diagram model of the Hoover Universal Plant. Volume numbers correspond to the control volumes in Figure 6.28.

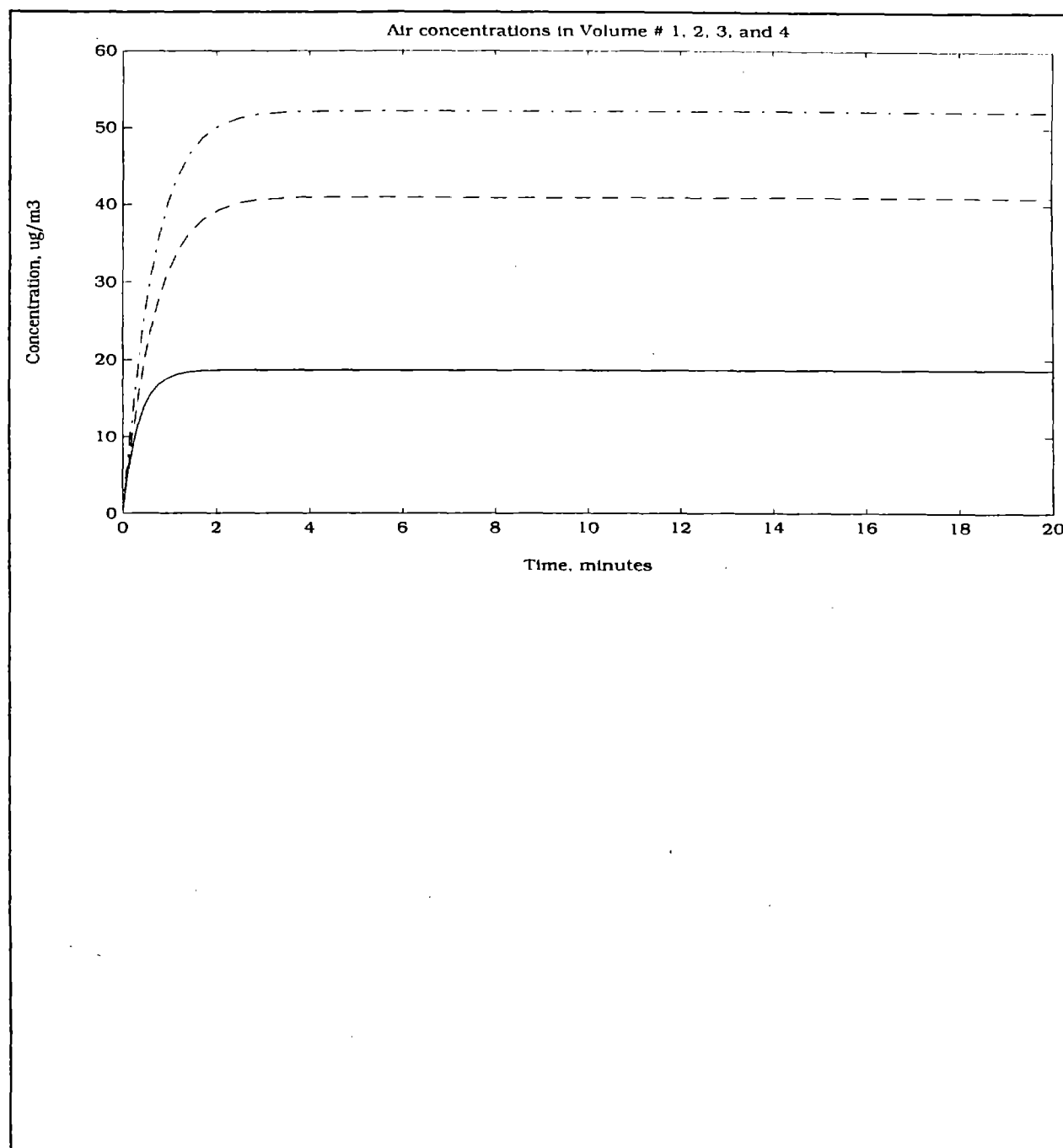


Figure 6.30 Simulation of TDI concentrations in air ( $\mu\text{g}/\text{m}^3$ ) as a function of time in Volume elements 1, 2, 2a, 3, and 4. The TDI concentration is assumed to be zero in each Volume at the beginning of the simulation. Time-dependent concentration profiles in Volumes 1, 2, and 4 are represented by the solid, dashed, and dash-dotted curves, respectively. The modeled concentrations for Volumes 2a and 3 are zero over the entire simulation.

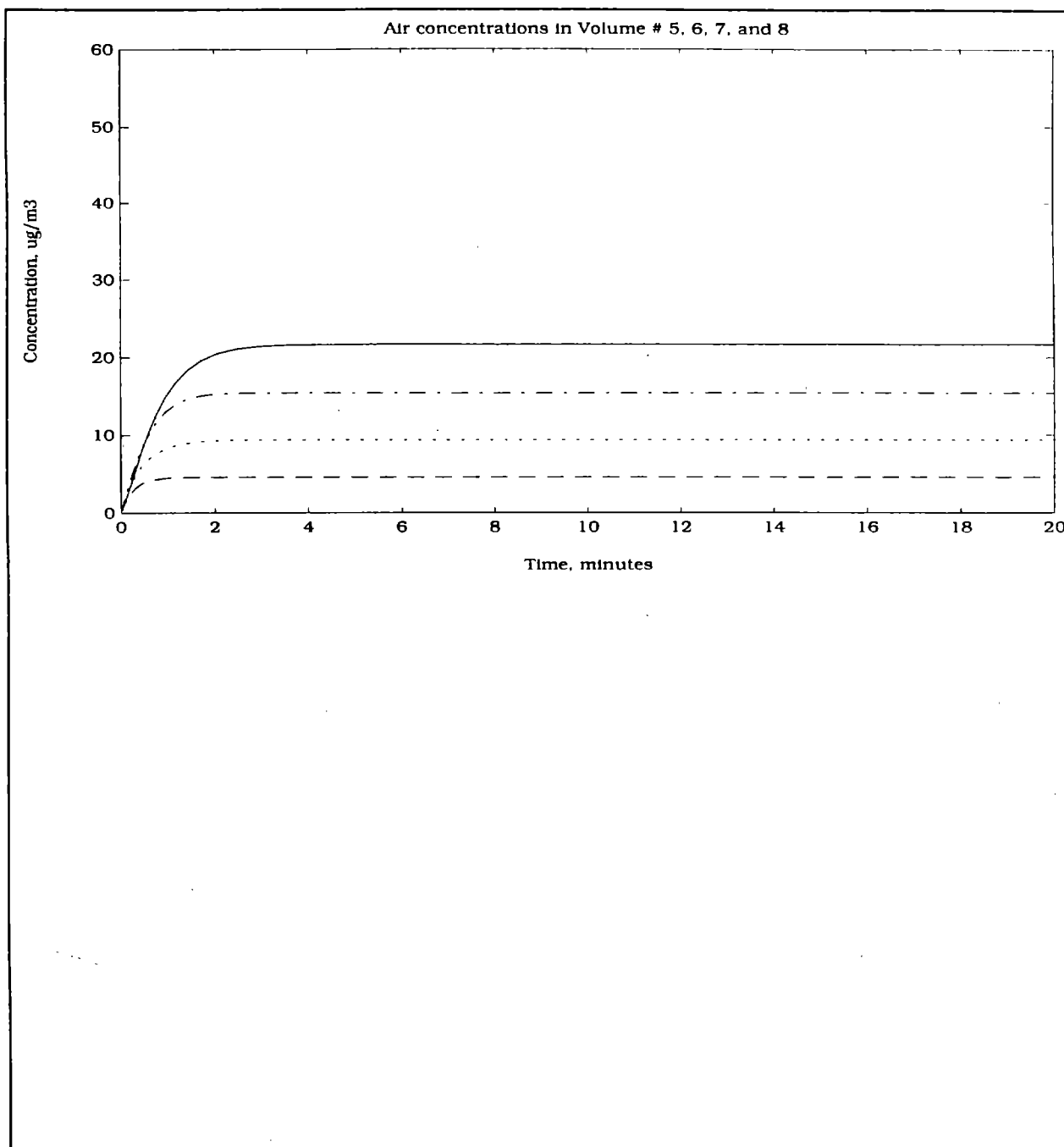


Figure 6.31 Simulation of TDI concentrations in air ( $\mu\text{g}/\text{m}^3$ ) as a function of time in Volume elements 5, 6, 7, and 8. The TDI concentration is assumed to be zero in each Volume at the beginning of the simulation. Time-dependent concentration profiles in Volumes 5, 6, 7, and 8 are represented by the solid, dashed, dotted, and dash-dotted curves, respectively.

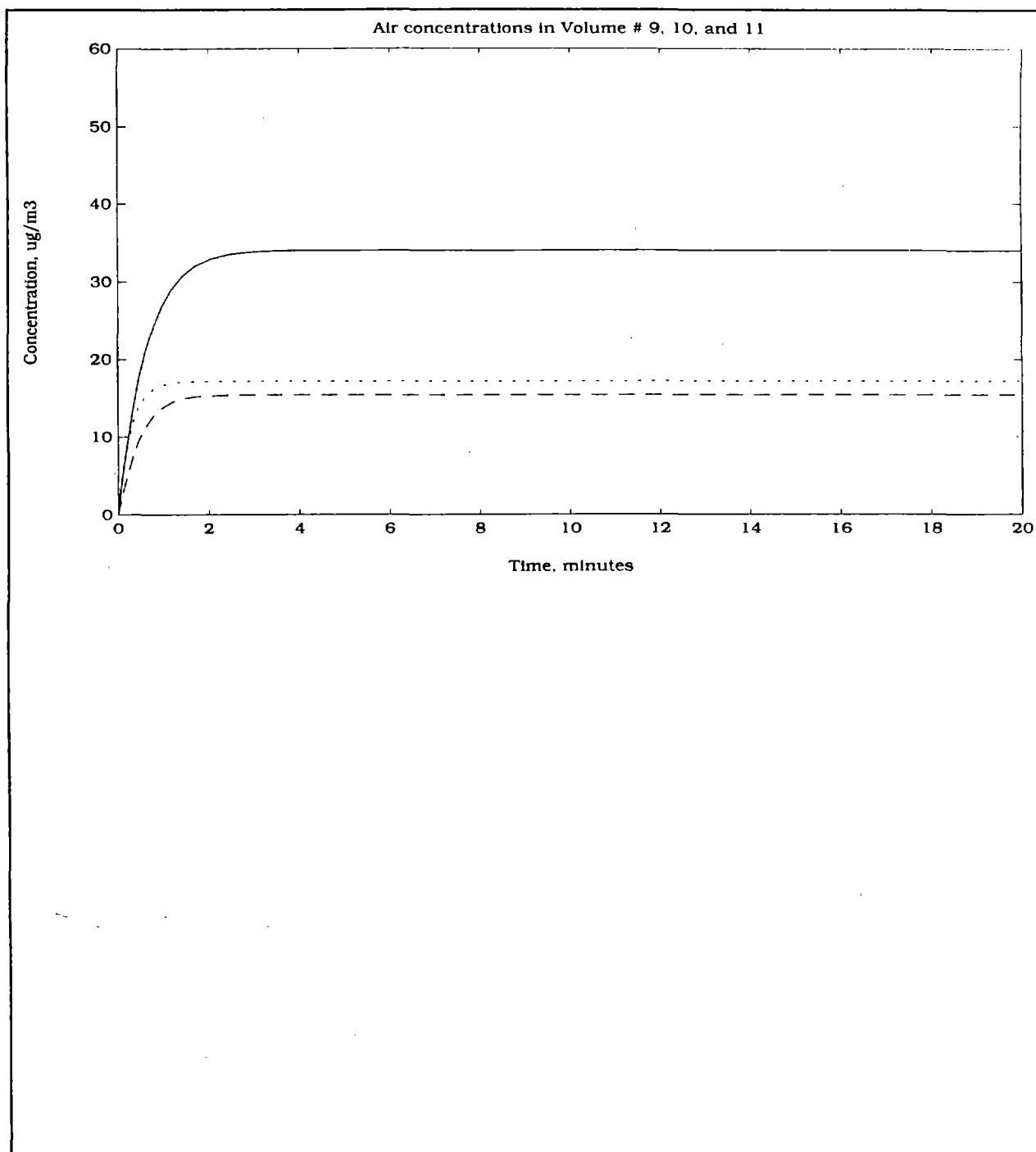


Figure 6.32 Simulation of TDI concentrations in air ( $\mu\text{g}/\text{m}^3$ ) as a function of time in Volume elements 9, 10, and 11. The TDI concentration is assumed to be zero in each Volume at the beginning of the simulation. Time-dependent concentration profiles in Volumes 9, 10, and 11 are represented by the solid, dashed, and dotted curves, respectively.

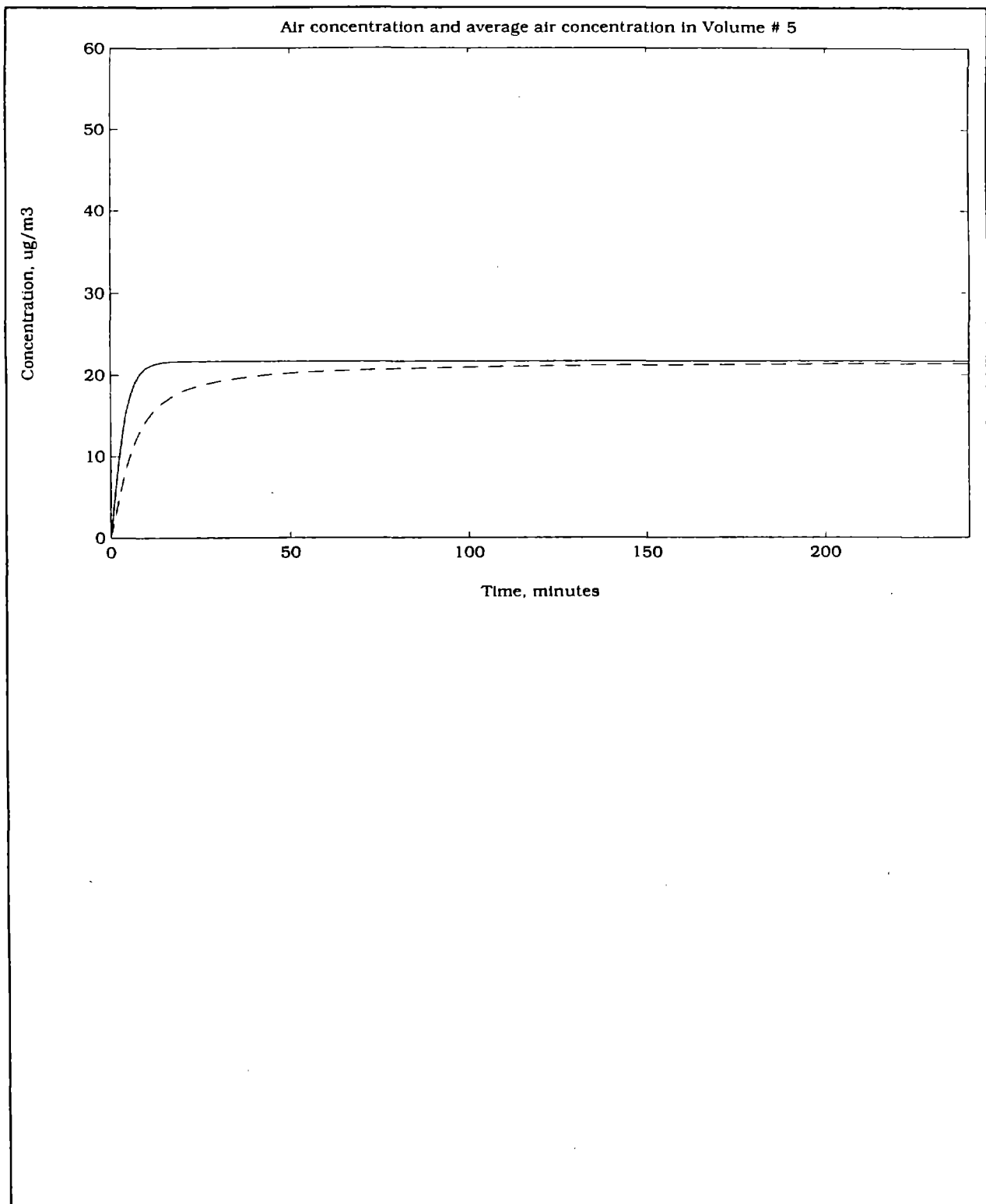


Figure 6.33 Comparison of instantaneous (solid curve) and time-averaged (dashed curve) concentration profiles predicted for Volume 5 of the Hoover Universal application.





## 7 Conclusions and Recommendations for Further Development

The objectives of this Phase I research effort were accomplished by applying SIMULINK™ software to the problem of pollutant dispersion in indoor spaces. A series of indoor air modeling elements were developed that serve as building blocks for constructing complex models of contaminant behavior in indoor settings that are not uniformly mixed. The physical processes considered are those essential to indoor air pollution: ventilation, emission, transport, and removal via chemical reaction, adsorption, and deposition. Models are constructed in an interactive Windows™ environment in which the elements represent physical processes. Applying concepts of systems dynamics, the SIMULINK™ environment integrates the mathematical equations that underlie the block diagram models. The powerful, dynamic capabilities of the approach permit the calculation of time-dependent air pollutant concentrations for arbitrary configurations, initial conditions, and time-varying parameters.

The theoretical and practical examples detailed in Chapter 6 illustrate the utility and flexibility of the modeling algorithms. Potential applications of the approach are numerous. With further development, the modeling approach could be used to simulate indoor air pollutant dispersion in more advanced studies. Model application could lead to the identification of factors responsible for unacceptable pollutant concentrations, the evaluation of control measures in existing facilities, and the design of the physical configuration and ventilation systems of new processes.

At present, however, the application of the modeling techniques is limited by the availability of input data. In general, the level of detail of indoor pollutant dispersion modeling should be consistent with the sophistication of information on pollutant emissions and air movement. Ideally, the modeling techniques such as those developed herein should be used in conjunction with data collection in a complementary approach. Approaches in which modeling techniques are applied with appropriate input data and verified by monitoring data offer a potentially powerful and cost-effective combination.

The potential for further development of these techniques is promising. A factor of critical importance is the development of the capability to predict and evaluate air movement in indoor settings that incorporates general ventilation features, local control measures, and thermal effects. Such a flow model should be founded in the theoretical concepts of fluid dynamics but should also be able to assimilate measured data. Coupled with the indoor air element approach, a generalized air flow model would provide a complete modeling tool for assessing pollutant dispersion in the indoor environment.

Finally, we note that prudent professional judgement is essential in evaluating indoor air dispersion. Such judgement is especially critical to the development and application of models. Emphasis must always be placed on the validation and verification of model predictions.



## 8 References

- Boeniger, M. (1986). Industrial Hygiene Sampling Survey Report of Hoover Universal, Inc. Greenfield, Ohio. NIOSH Report Number 83.13.
- Dyson, W.L., and Hermann, E.R. (1971). Reduction of atmospheric toluene diisocyanate by water vapor. Am. Ind. Hyg. Assoc. J. 32:741-744.
- U.S. EPA (1985). Compilation of Air Pollutant Emission Factors. Research Triangle Park, NC: U.S. Environmental Protection Agency, Office of Air Quality Planning and Standards. AP-42.
- U.S. EPA (1987). Hazardous Waste Treatment, Storage, and Disposal Facilities. Research Triangle Park, NC: U.S. Environmental Protection Agency, Office of Air Quality Planning and Standards. EPA-450/3-87-026.
- Hansen, T.B., and Andersen, B. (1986). Ozone and other air pollutants from photocopying machines. Am. Ind. Hyg. Assoc. J. 47(10):659-665.
- Holdren, M.W., Spicer, C.W., and Riggan, R.M. (1984). Gas phase reaction of toluene diisocyanate with water vapor. Am. Ind. Hyg. Assoc. J. 45:626-633.
- Incropera, F.P., and DeWitt, D.P. (1981). Fundamentals of Heat Transfer. New York: John Wiley & Sons.
- MathWorks (1991). MATLAB for Windows User's Guide. Natick, MA: The MathWorks, Inc.
- MathWorks (1992). SIMULINK for Windows User's Guide. Natick, MA: The MathWorks, Inc.
- Seinfeld, J.H. (1986). Atmospheric Physics and Chemistry of Air Pollution. New York: John Wiley & Sons.
- U.S. EPA (1985). Compilation of Air Pollutant Emission Factors. Research Triangle Park, NC: U.S. Environmental Protection Agency, Office of Air Quality Planning and Standards. AP-42.
- U.S. EPA (1987). Hazardous Waste Treatment, Storage, and Disposal Facilities. Research Triangle Park, NC: U.S. Environmental Protection Agency, Office of Air Quality Planning and Standards. EPA-450/3-87-026.

U.S. EPA (1988). Indoor Air Quality in Public Buildings: Volume 1. Project Summary. Washington, DC: U.S. Environmental Protection Agency, Office of Acid Deposition, Environmental Monitoring, and Quality Assurance. EPA/600/S6-88/009a.

Weschler, C.J., Brauer, M., and Koutrakis, P. (1992). Indoor ozone and nitrogen dioxide: A potential pathway to the generation of nitrate radicals, dinitrogen pentaoxide, and nitric acid indoors. Environmental Science and Technology 26(1):179-184.

Weschler, C.J., Hodgson, A.T., and Wooley, J.D. (1992). Indoor chemistry: Ozone, volatile organic compounds, and carpets. Environmental Science and Technology 26(12):2371-2377.

## **Appendix A: NIOSH Measurements of 2,4- and 2,6-Toluene diisocyanate (TDI)**

Boeniger (1986) conducted an extensive personal monitoring study of worker exposure to toluene diisocyanate (TDI) at the Hoover Universal Plant in Greenfield, Ohio. The study is part of a larger epidemiological/industrial hygiene survey of workers in the flexible polyurethane industry.

Samples were collected from workers in all of the major activities on the production floor; two different shifts were considered over the period of one week. Sample durations were typically 1–3 hours, and analyses were conducted for both the 2,4- and 2,6-TDI isomers.

The sampling results of the NIOSH report (Boeniger, 1986) are reproduced in this Appendix. These data are used in Section 6.3.4 to estimate exposure point concentrations of TDI in air that are appropriate to compare to indoor air modeling predictions.

Table A.1

Measurements of 2,4- and 2,6-Toluene Diisocyanate [from Boeniger (1986)]

Date	Sample Number	Sample Duration (min)	Sample Volume (m <sup>3</sup> )	Analytical Results (µg)	Air Conc. (µg/m <sup>3</sup> )	Description
Line 2 3/18 pm	IS8	210	0.220	1.1	5	operator
	IS10	204	0.218	0.9	4	operator
	IS7	203	0.207	0.6	3	operator
	IS6	160	0.160	<0.3	<2	clean and repair
	IS12	155	0.171	1.2	7	clean and repair
	IS5	173	0.178	1.6	9	trimmer
	IS3	192	0.190	<0.3	<2	packager
	IS15	blank	-	<0.3	-	-
	IS16	blank	-	<0.3	-	-
Line 1 3/18 pm	IS11	130	0.130	1.4	11	operator
	IS4	127	0.127	0.6	5	finishing, trimmed
	IS9	136	0.136	0.8	6	finishing, trimmed
	IS31	162	0.162	2.8	17	operator
	IS32	156	0.159	1.5	9	finishing
	IS25	152	0.152	0.9	6	finishing
	IS38	blank	-	<0.3	-	-
	IS39	blank	-	<0.3	-	-
3/19 am						

A-2

Table A.1 (continued) Measurements of 2,4- and 2,6-Toluene Diisocyanate [from Boeniger (1986)]

Date	Sample Number	Sample Duration (min)	Sample Volume (m <sup>3</sup> )	Analytical Results (µg)	Air Conc. (µg/m <sup>3</sup> )	Description
Line 2 3/19 am	IS28	209	0.209	1.1	5	operator
	IS27	209	0.213	1.1	5	operator
	IS33	219	0.223	2.1	9	operator
	IS30	210	0.225	1.9	8	trimmer
	IS26	210	0.214	1.8	8	inspector
	IS20	215	0.215	2.8	13	janitor
	IS41	205	0.201	0.8	4	trimmer
	IS40	205	0.211	1.2	6	trimmer
	IS51	161	0.161	0.8	5	operator, removes seats
	IS45	162	0.162	<0.3	<2	operator, bunlopper, sample faulted at 12 minutes
Line 4 3/19 pm	IS48	99	0.099	0.5	5	operator, burlapper, sample faulted at 99 minutes
	IS49	164	0.164	0.8	5	clean & repair
	IS72	BLANK	-	<0.3	-	
	IS52	130	0.130	<0.3	<2	warehouse
	IS69	208	0.280	0.8	3	packer
	IS21	189	0.189	5.8	38	operator
	IS42	152	0.147	3.9	27	operator
	IS43	156	0.156	1.9	12	operator
	IS35	158	0.158	1.5	9	operator

A-3

Table A.1 (continued) Measurements of 2,4- and 2,6-Toluene Diisocyanate [from Boeniger (1986)]

Date	Sample Number	Sample Duration (min)	Sample Volume (m <sup>3</sup> )	Analytical Results (µg)	Air Conc. (µg/m <sup>3</sup> )	Description
Line 1 3/19 pm	IS56			2,4 2,6	2,4 2,6	
	IS55	74	0.074	1.0 0.7	14 9	sabotaged operator, faulted at 74 minutes
	IS54	149	0.149	1.9 1.8	13 12	finishing operator
	IS23	145	0.145	1.1 0.6	8 4	finishing operator
	IS47	80	0.080	0.3 0.3	4 4	compounder
Integral seat 3/19 pm	IS44	160	0.160	0.5 1.2	3 8	seat assembly
	IS22	190	0.190	1.8 3.7	9 19	seat assembly
	IS24	192	0.192	1.5 2.8	8 15	seat assembly
	IS23	190	0.190	1.5 2.8	8 15	seat assembly
	IS50	201	0.201	5.4 3.4	27 17	operator, nozzle
Line 5 3/19 pm General 3/19 pm General 3/19 pm Line 1 3/20 pm	IS84	204	0.204	1.2 1.4	6 7	janitor, lines 1,4,5
	IS66	203	0.203	2.6 2.8	13 14	plant inspector
	IS67	160	0.155	0.4 0.9	3 6	finishing
	IS78	166	0.163	1.2 1.1	7 7	finishing
	IS81	165	0.163	0.7 0.8	4 5	packager

A-4



Table A.1 (continued) Measurements of 2,4- and 2,6-Toluene Diisocyanate [from Boeniger (1986)]

Date	Sample Number	Sample Duration (min)	Sample Volume (m <sup>3</sup> )	Analytical Results (µg) 2,4 2,6	Air Conc. (µg/m <sup>3</sup> ) 2,4 2,6	Description
Line 3 3/20 am	IS63	150	0.147	1.7 3.6	12 24	trimmer
	IS53	133	0.129	1.3 3.3	10 26	operator
Line 4 3/20 am	IS62	181	0.181	3.2 2.5	18 14	operator
	IS88	149	0.149	0.7 0.8	5 5	plant inspector
Integral Seat 3/20 am	IS76	169	0.169	0.6 1.0	4 6	seat assembly
	IS77	232	0.232	1.8 1.9	8 8	operator, burlapper
Line 2 3/20 am	IS57	195	0.195	0.9 1.4	5 7	operator, seat removal
	IS65	97	0.097	0.3 0.3	3 3	trimming
Integral Seat 3/20 pm	IS68	193	0.193	2.0 2.9	10 15	cold foam repair
	IS61	195	0.195	0.4 0.4	2 2	janitor
Integral Seat 3/20 pm	IS101	blank	-	<0.3 <0.3	- -	
	IS102	blank	-	<0.3 <0.3	- -	
Line 4 3/20 pm	IS86	166	0.166	0.7 1.0	4 6	seat assembly
	IS91	159	0.159	2.2 2.0	14 13	operator

A-5

Table A.1 (continued) Measurements of 2,4- and 2,6-Toluene Diisocyanate [from Boeniger (1986)]

Date	Sample Number	Sample Duration (min)	Sample Volume (m <sup>3</sup> )	Analytical Results (µg) 2,4 2,6	Air Conc. (µg/m <sup>3</sup> ) 2,4 2,6	Description
Line 1 3/20 pm	IS95	145	0.145	0.9	6	finishing
	IS79	lost			5	finishing
Line 3 3/20 pm	IS94	189	0.178	1.5	3.5	operator
	IS71	181	0.181	0.8	1.1	packager
	IS92	173	0.173	0.8	1.5	operator, sets up frames
Line 2 3/20 pm	IS46	170	0.172	1.0	1.2	operator, burlapper
	IS64	282	0.282	0.6	0.6	packager
	IS82	160	0.154	0.4	1.0	clean and repair
	IS90	90	0.090	0.3	0.5	clean and repair
	IS100	178	0.178	1.2	1.2	janitor, line 1,4,&5
3/20 pm						
Line 2 3/20 pm	IS99	195	0.195	1.6	1.9	area in operators area of line 2; hang burlap, etc. 2-3 workers
					8	
Line 4 3/20 pm	IS96	368	0.368	26	20	71
	IS74	130	0.130	2.4	2.6	18
Line 5 3/22 am	IS93	blank		0.3	0.3	20
	IS97	blank		0.3	0.3	operator

A-6

Table A.1 (continued) Measurements of 2,4- and 2,6-Toluene Diisocyanate [from Boeniger (1986)]

Date	Sample Number	Sample Duration (min)	Sample Volume (m <sup>3</sup> )	Analytical Results (µg)	Air Conc. (µg/m <sup>3</sup> )	Description
Warehouse 3/21	IS98	320	0.330	<0.3	<1	shipping warehouse
	IS60	320	0.336	<0.3	<1	shipping warehouse

A-7

 **Cambridge Environmental Inc**

58 Charles Street Cambridge, Massachusetts 02141  
617-225-0810 617-225-0813 FAX

120

## Acknowledgments

A number of individuals have provided valuable contributions to our research, and we would like to express our appreciation for their efforts. In addition to providing financial support, NIOSH personnel were extremely helpful on both administrative and technical matters. In particular, we are grateful for our interactions with Price Connor, Barbara Wedding, Vince Mortimer, Dennis O'Brien, and Mark Boeniger. Also, we would like to thank Jim Axley of M.I.T. for his advice, comments, and continued support of our efforts. In addition, we have profited from the support of our colleagues at Cambridge Environmental Inc., who continue to provide a creative and stimulating environment in which to work. We are especially thankful for Tim Lash's review of this report — his comments have been extremely useful in the production of the final document. Finally, we would like to thank Laura Green for the additional support that was necessary to complete the report.

## Present and Future Publications

As of the date of this report, no publications have resulted from this research. We do, however, intend to submit one or two manuscripts for publication that describe (1) the basic methodologies of the indoor air modeling elements and (2) the modeling applications of the Hoover Universal plant and the indoor ozone example. Depending upon the scope and content of the manuscript(s), we will attempt to publish in periodicals such as *Indoor Air* or the *American Industrial Hygiene Association Journal*. Also, portions of this research are likely to be presented at professional conferences. Currently, we are scheduled to present a talk at the annual MATLAB® conference on October 18, 1993, in Cambridge, Massachusetts, and may pursue additional presentations.

